1-1-2017

Bioreducible Layer-By-Layer Films For Gene Delivery

Lingxiao Xie
Wayne State University,

BIOREDUCIBLE LAYER-BY-LAYER FILMS FOR GENE DELIVERY

by

LINGXIAO XIE

DISSERTATION

Submitted to the Graduate School

of Wayne State University,

Detroit, Michigan

in partial fulfillment of the requirements

for the degree of

DOCTOR OF PHILOSOPHY

2017

MAJOR: MATERIALS SCIENCE AND ENGINEERING

Approved By:

_____

Advisor Date

_____

_____

_____

_____

ACKNOWLEDEMENTS

I would like to express my special thanks of gratitude to my advisor, Prof. Guangzhao Mao, for her support and guidance during my research study, for her teaching and mentoring me the knowledge, techniques, scientific thinking, and skills.

I would like to thank my dissertation committee members, Dr. Gaungzhao Mao, Dr. Haipeng Liu, Dr. Charles Manke, Dr. Olivia Merkel for the suggestion, recommendation, support, instruction, and inspiration.

I would like to thank Dr.Wei-Zen Wei lab and Dr. Heather Gibson for the help, support, and suggestion in plasmid DNA, cell culturing, and animal mold study.

I would like to thank Dr.Weiping Ren lab for the help and support in the bone cell study.

I would like to thank all the group members from Dr. Mao lab for their help, support, and advice. And, I would like to thank the group members from Dr. Ren, Dr. Liu, Dr. Cao, and Dr. Zhu labs for their help.

I would like to thank my parents, grandparents, and Fangchao Liu for all unconditional support, courage, and patience.

TABLE OF CONTENTS

LIST OF FIGURES

LIST OF TABLES

CHAPTER 1 INTRODUCTION

Gene therapy, which involves delivery of exogenous, therapeutic gene to human body aiming to treat genetic-base disease and acquired diseases, has the potential to be the next revolution in modern medicine[1]. But naked DNA molecules cannot enter cells efficiently due to their large size and hydrophilic nature[2]. Therefore, developing a suitable gene carrier is one significant step for gene therapy. In recent decades, the non-viral gene carriers have attracted lots of researcher's attention. This is because comparing with viral carrier, the non-virus vector is less toxic and less immunogenic. However, transfection efficiency, targeting specificity, vector safety, and stability are still some of the biggest challenges. One strategy to enhance the gene expression efficiency and to lower the cytotoxicity is to develop stimuli-responsive polymeric vectors. Such as the materials which would be sensitive to pH changes or redox gradients. This stimuli-responsive polymer can protect DNA during delivering process and only release DNA after reaching the targeting area. The degradable property of vector materials can also help metabolism to decrease its toxicity. In addition, developing a method to enhance DNA loading dosage onto the gene delivery vector and to have sustain releasing by simple modification is also a very promising method to improve gene delivery and transfection efficiency.

This dissertation focus on engineering novel biocompatible and biodegradable polymer--poly(amido amine)s (PAAs) as non-virus gene vector to achieve high efficiency and low toxcicty gene delivery vector. Incorporating a redox sensitive group, the disulfide bond, can protect DNA in physiological pH and deconstruct itself under reducing environment such as cell surface and early endosome by reacting with glutathione or redox-active membrane proteins through thiol-disulfide exchange reaction[3].

The type of gene vector focused on this dissertation is polyelectrolyte multilayers (PEMs) fabricated by Layer-by-layer coating method. Alternative dipping a substrate in polycation solution and DNA solution to form LbL structure film coating. This LbL film coating has potential to carry high dosage of therapeutic gene and achieve localized and sustain gene releasing.

In current gene delivery field, transfection efficiency, releasing time controlling and LbL film biocompatibility are still big barriers and therefore have large space to improve. This dissertation's goal is to provide a method to improve polymeric gene vectors efficiency, lower cytotoxicity, enhance LbL film biocompatibility and achieve sustain and sequential gene delivery.

In this dissertation, chapter 2 first presents the background information about gene delivery. Second aspect is the current barrier for LbL gene delivery. Third aspect is the most recently developing and research results of polymeric gene delivery. The fourth aspect involves the description of LbL film assemble and disassemble process.

Chapter 3 summaries how to engineer bioreducible LbL film to achieve sequential gene delivery. It describes various methods to determine the film structure, assembly and disassembly. Last, it discusses the theory back to the relation between LbL film interior structure and degradation process.

Chapter 4 describes the method to design and synthesize novel bioreducible PAA for higher transfection efficiency and lower toxicity. This chapter also describes screening of the polymers to build next generation LbL films.

Chapter 5 demonstrates the well-engineered bioreducible LbL film which can achieve sequential and sustain gene delivery. The *in vitro* transfection efficiency has been largely improved and gene releasing period has been prolonged up to 2 weeks. This chapter also describes the application of PAA/BMP-2 DNA LbL film in promoting osteoblast precursor cell differentiation

in vitro, and *in vivo* transfection study by using poly(amido amine) and luciferase-expressing plasmid pGL4 in mouse model.

Chapter 6 concludes this dissertation work in LbL film gene delivery. This chapter presents the current limitations of the application of PAAs LbL film gene vector. Prospectus and future work plans are also included.

CHAPTER 2 LITERATURE REVIEW

2.1 Gene delivery background

In recent decades, gene therapy attracted great interests in the medicine, pharmaceutical science, and biotechnology fields since it not only has the promise and potential to treat chronic diseases and genetic disorders, but also has been considered capable of replacing traditional protein therapy[4]. Instead of virus approach, non-virus gene vehicles have received significant attention in transferring therapeutic gene because of their favorable properties, such as easy reproduction, lacking immunogenicity, low cytotoxicity, and potential for target delivery. Although non-virus vectors have various advantages, the transfection efficiency is still a big barrier in gene therapy[2].

Incorporation of nanotechnology into gene delivery has made great contribution to gene vector development. This is because nanotechnology can delivery different types of gene by either localized or targeted fashion to cells or tissues of interest. Nanotechnology focuses on formulating therapeutic gene with biocompatible materials to form nanocomposites such as nanoparticles, nanocapsules, micellar systems, nano-conjugates, and nano-films. Most nanocomposites are usually made by polymeric or lipid materials and formulated in nano-meter size. By modifying these non-virus vector materials, people can lower gene vector toxicity, achieve target delivery, improve transfection efficiency, and control delivery dosage and time. The cationic polymer (polycation) or cationic lipid provided electrostatic interaction with negative charged DNA chain to form a nano-szie particle. DNA exhibits negative charge is due to the phosphate groups in its chain. The DNA/cationic lipid complex has amphiphilic bilayers and people named it as lipoplex,. Using lipoplex to delivery gene has been successfully reported[5], and the commercial lipid product has been widely used in research area such as lipofectamine[6]. Polyplex is the complex formed by polycation and DNA. The excess surface charge of polyplex can stabilized polyplex in buffer or

physiological environment. Various polycation has been reported in condensing DNA into nano-meter scale particles and transferring DNA into cell body, such as PEI[7], PLL[8], PAA, et al. Besides of nanoparticles, polyelectrolyte multilayer thin films also attracted researchers' attention in gene delivery area recently. This is because the thin film coating can achieve localized delivery which can play a significant role in tissue engineering[9, 10]. Through Layer-by-layer assembly (LbL) method one can conveniently control over the incorporation of different types of nucleic acids on the surface of a variety of implantable materials, biomedical devices, and tissue engineering scaffolds. And this method doesn't require organic solvents and allows precise control over DNA loading and releasing. It has potential to achieve programmable control of gene delivery[11-14]. However, most methods and non-virus materials developed for gene delivery have the barriers such as low transfection efficiency and high toxicity. Currently, people are making effort to overcome these obstacles to develop biocompatible gene delivery system with high transfection efficiency.

In recent decades, people start to put efforts on non-virus vector study. Because as a synthetic, the vector size and morphology is capable of being modified for transgene delivering method, the controllable molecular composition is simplified for manufacturing and analysis.[15, 16] The immunogenicity of non-virus vector is also relatively lower than that of virus vectors[17-20]. But the transfection efficiency in non-virus system is a significant problem. Typically, 10^6 plasmid copies are needed to transfect a single cell, with relative ~ 10^2-10^4 copies making it to the nucleus for transgene expression[21-23]. Developing a delivery system with high transfection efficiency, safety, stable, and programmable is the key point for next generation of gene delivery.

2.2 Current barriers for LbL film gene delivery

Numerous barriers appear in the entire gene delivery pathway resulting in low transfection efficiency. People conclude those barriers into two part: the extracellular barriers and the intracellular barriers (Figure2.1).

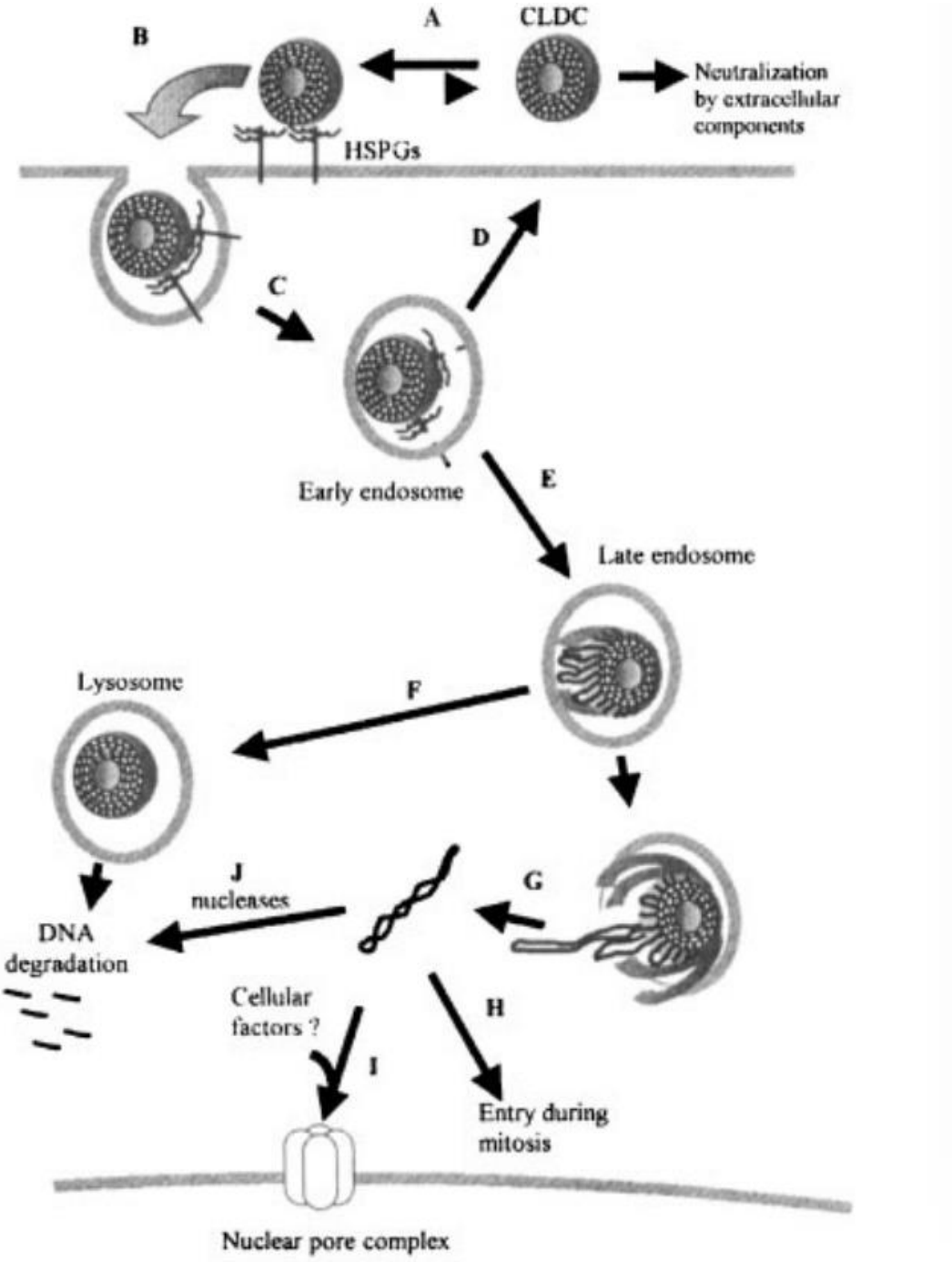

Figure 2.1. The pathway and barriers of gene delivery process. Cationic lipid/DNA complexes are used as an example here but many of the processes are presumably similar for polymeric delivery systems[24].

The first extracellular barrier is the stability of non-virus delivery system in the extracellular milieu. The instability of cationic polymer or lipid complex is frequently observed aggregating as the time passing due to the interaction with negatively charged particles encountered during the delivery process. The ionic strength introduced by the biological milieu can 1)weaken the interaction between polycation or cationic lipid and DNA; 2) shield inter-particle electrostatic repulsion force, and eventually will result in aggregation[25]. Glycosaminoglycans, serum albumin, and other extracellular protein can facilitate the aggregation of the delivery systems and effectively compete for binding DNA to the cationic delivery vehicle[26-29]. Association of DNA with the cell surface is also one of the main function of delivery agent. The association of non-virus gene delivery systems containing cationic lipids or polymer is mediated by interaction with cell surface heparin sulfate propteoglycans (HSPGs)[25]. How to increase the amount of DNA associated with the cells and induce targeting towards certain cell type should be concerned during delivery agent design. However, most of the extracellular barriers could be easily overcome by localized delivery, such as using LbL thin film coating. This method can avoid the competition of the aggregation stimuli during blood or fluid cycle and achieve targeting delivery by direct implanting.

Though LbL film gene delivery can overcome most extracellular obstacles, the intracellular barriers can still be great challenges. Potential limiting barriers for efficient transfection are endocytosis, cytoplasmic motility, transport across the nuclear membrane, and polyplex unpacking [30]. Our work is focusing on polymeric gene delivery, the following section will mainly discuss the barrier for polycation materials.

An aggregation of various cell surface proteins will occur when the non-virus gene delivery system reach the cell surface. This protein aggregation will strongly stimulus internalization of the delivery system by the cell, this process is generally referred as endocytosis. The cationic polymer/DNA complex can be phagocytosis by cells even in the cell lines that are not professional phagocytes[30-32]. Once internalized, the intracellular vesicles carrying the vector fuse with organelles collectively referred to as the endocytic compartment, also known as early endosomes. This early endosome is characterized by it peripheral location and slight acidic pH[33]. Ability of escaping from the endosome is the key step for efficient gene delivery. If the vector was unable to escape from the early endosome, the vector will traffic to the late endosomes and then to lysosomal compartments where the DNA will be eventually degraded. To polymeric vector, there are two possible mechanisms have been proposed contributing to the endosome escape. The first one is based on the physical disruption of the negatively charged endosomal membrane occurs on direct interaction with the cationic polymer, such as poly(amido amine) dendrimers, polylysine[34], and PEI[35]. However, this physical disruption is highly depending on the target membrane composition as well as the surface charge of polymer. The other hypothesis to explain the endosome escape is based on the ionizable amine groups in polymer chain, which is also named as “proton sponge” hypothesis[36]. When the polymer/DNA complex captured by endosome, the protonation of the polymer induces proton flux into the endosomal lumen and pulls chloride ions and water in because of the pH environment change. This buffering effect results in polymer swelling and, finally, osmotic lysis. This endosome escape is closely related to polymer buffer capacity. How to improve the polycation’s buffer capacity to facilitate the endosome escape is the main point to overcome the intracellular trafficking.

After endosome escape, DNA must traverse the cytosol to access the nucleus. The naked DNA exposed in cytoplasm results in significant degradation with a half-life of 50-90 min[37]. The diffusion barrier caused by cytoplasm requires the polymer and DNA released out by endosome continuing to be complexed or at least partially complexed. Researchers who used microinjection method to inject PEI/DNA complex into the cytoplasm concluded that cationic complexes are passed from proteoglycans to cytoplasmic spanning polyanions of increasing affinity, such as tubulin (microtubules) and actin (microfilaments), to the nucleic acid rich nuclear region[38]. Although whether this mechanism of cationic polymer bond DNA in cytoplasm can facilitate transgene expression is not clear. At least, enhancing the cytoplasm diffusion by condensed DNA is partially involved[25].

Ultimately, DNA should be delivered into cell nucleus for transgene. The first method for delivering DNA to nucleus is to pass the nuclear pores. Nuclear pores are located on the nucleus envelope with high density, normally 3000—4000/nucleus[39], but with very small size. The nucleus pore in close state permits the passive diffusion of molecules with diameter less than 9 nm and in open state facilitates transport of particles diameter less than 26 nm[40, 41]. Which means the particles should be smaller than 30 nm, otherwise it will be very hard to pass the nuclear pore[42-44]. This size limitation is a very restricted condition for polymer/DNA polyplex size controlling, especially for the complex released out from LbL films. The second method is to associate the DNA physically with chromatin during mitosis when the nuclear envelope break down. This association has already been observed by numerous occasions both on cationic lipid and polymer mediated gene delivery[45-48]. DNA is localized in the perinuclear region waiting for the breakdown of the nuclear membrane[49]. People also observed that polycation vector, such as polyethylenimine (PEI) and polylysine remained bond with DNA to protect it in the cytoplasm before to mitosis[50].

But cationic lipid in cytoplasm doesn't show significant enhancement of DNA uptake. This observation suggests that cationic polymers may have an additional role in the nuclear delivery of DNA[49, 50].

2.3 Polymeric gene delivery development

Cationic polymer is considered as an attractive non-viral gene vector due to their immense chemical diversity and their potential to functionalization. Polycation has shown promise as a safe, predictable, biodegradable and low toxic carrier to conjugate the targeted gene or other biological molecules. Early example for polycation gene delivery is poly(L-lysine) (PLL) and PEI. PLL is a homo-polypeptide of the basic amino acid lysine, and its ability to condense DNA has been known as early as 1960s[51, 52]. But its low transfection efficiency limits its application. Currently, various modified PLL with enhanced delivery efficiency has been reported[53], such as PLL covered hydrophilic polymer PEG to minimized nonspecific interaction with serum component[54, 55]. PEI and its variants are the most studied polymeric materials for gene delivery since it has been demonstrated with extraordinary ability in promoting gene transfection both *in vitro* and *in vivo* in 1995[36], people found that the delivery efficiency and cytotoxicity are highly depending on structural properties, such as molecular weight[56], linear or branched structure[57]. Known that PEI induces toxicity, people developed various methods to optimize PEI biocompatibility, such as inducing block co-polymers of PEG and PEI for improved stability and biocompatibility[58, 59], degradable disulfide-crosslinked PEIs for reduced toxicity[60] and alkylated PEIs for increased potency[61, 62]. To better develop polymeric delivery vector and address the delivery efficacy and toxicity problem, a lot of polymers have been investigated, such as chitosan, poly(amdio ester), poly(amdio amine), and various carbohydrate based polymers and dendrimers[13, 63-66]. One vector

has reached clinical development is a formulation that comprises the non-ionic poloxamer CRL1005 and the cationic surfactant benzalkonium chloride (Astellas Pharma Inc.)[67]

The escape of nanoparticle from the cell organelle and nanoparticle unpacking is one of the key steps influencing the final successful delivery. Another big barrier for delivery vector is the cytotoxicity, which may be caused by the poor biodegradability of polymeric materials. Therefore, bioreducible polymeric delivery vectors are needed. One type is the hydrolytically degradable polymer. The other one is the polymer contain reducible disulfide link. The Lynn group focuses on the design and incorporation of hydrolytically degradable synthetic cationic polymers. They synthesized a class of polyamines known as poly (β-amino ester)s, which are hydrolytically degradable by esters located in the polymer backbones in physiological environment[68-70]. But such hydrolytic degradation cannot be triggered *in vivo* with enough spatial accuracy. The stability in the extracellular and "unpacking" ability in the intracellular environment are very signification for delivery system. The polycations containing disulfide bonds are bioreducible through the reaction with redox agents in sub-cellular compartments such as glutathione (as well as membrane surface proteins containing thiol groups). Through the disulfide-thiol exchange reaction, the high-molecular-weight polycations could be cleaved into low molecular weight oligocations. The oligocations with low binding affinity allow the DNA being released out from the complex. Blacklock et al.[13] and Chen et al.[71] fabricated degradable cationic poly(amido amine)s (PAAs), which contains such disulfide bonds, can successfully release DNA in cell body. Cytoplasmic delivery of gene is also the major limitation for gene carry design. Gene delivery systems sensitive to intracellular stimuli mechanisms have been the subject of intensive scrutiny as they would allow formation of gene carriers stable in blood circulation that disintegrate after intracellular uptake[72]. High redox potential difference (100-1000 fold), between intracellular space and oxidizing

extracellular space enables it as potential stimuli mechanism to overcome the cytoplasm delivery[3, 72]. Therefore, the disulfide bond induced polymer provides a method to protect DNA from degradation in extracellular circulation and has a potation to achieve targeting delivery.

2.4 LbL film assemble and disassemble

LbL assembly provides compelling, thin-film platforms for the highly controlled and localized delivery of therapeutic agents such as DNA. The LbL technique is based on the adsorption of alternating polycation and polyanion layers through electrostatic force. One of the most widely used methods is alternatively immersing the substrate into polyanion and polycation solutions followed by rinsing with DI water in order to remove weakly bound molecules (figure 2.2). In LbL gene delivery systems, DNA is incorporated as the polyanion component and gene carrier is incorporated as polycation component. Films that disassemble in physiological condition or reducing environment, in particular, could create unique opportunities to sustain, trigger, or target releasing of DNA. LbL films assembly and disassembly offer numerous potential advantages compared with conventional methods for the encapsulation and controllable releasing of macromolecular therapeutics, such as friendly assembly environment, product stability, controllable dosage adjustment, tunable releasing time and location[73].

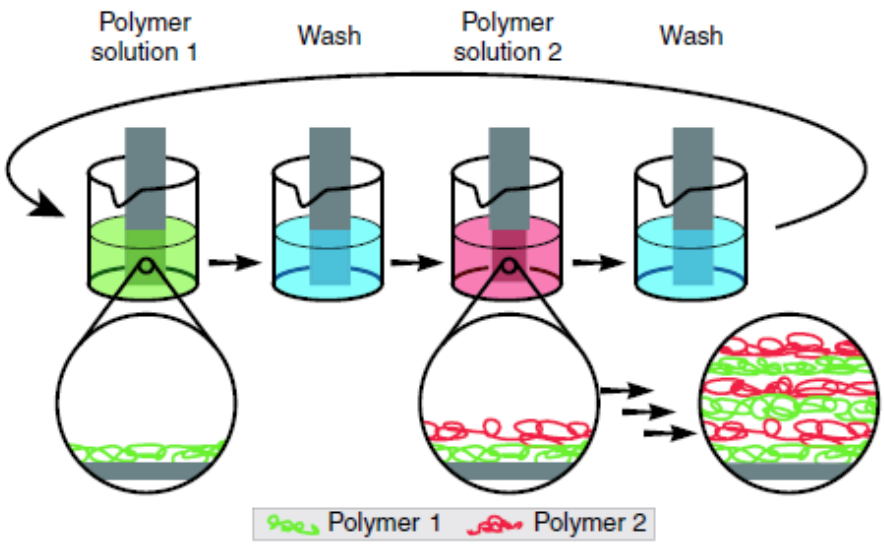

Figure 2.2. Basic principle of the layer-by-layer technique. A substrate is alternatingly immersed in solutions of two interacting polymers. The template is washed in between the immersion steps[74]

The interior structure of LbL films can influence the releasing process of therapeutic agents. People fabricated LbL films one layer followed by another layer, but they found that the perfect LbL structure is highly idealized. In reality, the polyelectrolyte components of LbL films are often not compartmentalized into discrete and neatly stack entities. Each layer at least interpenetrates to some extent with other layers surrounding it. The inherently "fuzzy" nature of these assemblies depends on a number of factors, such as molecular weight, chain structure, charge density of polyelectrolyte, and assembly environment[73].

The interlayer diffusion of polyelectrolytes during film fabrication contributes to film architecture with more homogeneous distribution of individual film components[75, 76]. The diffused layer structure can give rise to "bulk erosion" disassembly and stratified layer structure leads to "surface erosion" one (figure 2.3). The bulk film erosion would provide opportunities to release precisely defined quantities of multiple agents simultaneously however this also will cause faster releasing. In contrast, films that eroded in a manner that approximates surface type would have the potential to provide a method to control over both the releasing order and time. Therefore,

this surface type erosion might be able to obtain a sustained releasing and sequential releasing of multiple agents[73]. This type of programmable release of DNA is desirable for bone regeneration and cancer vaccine delivery applications as we are currently pursuing.

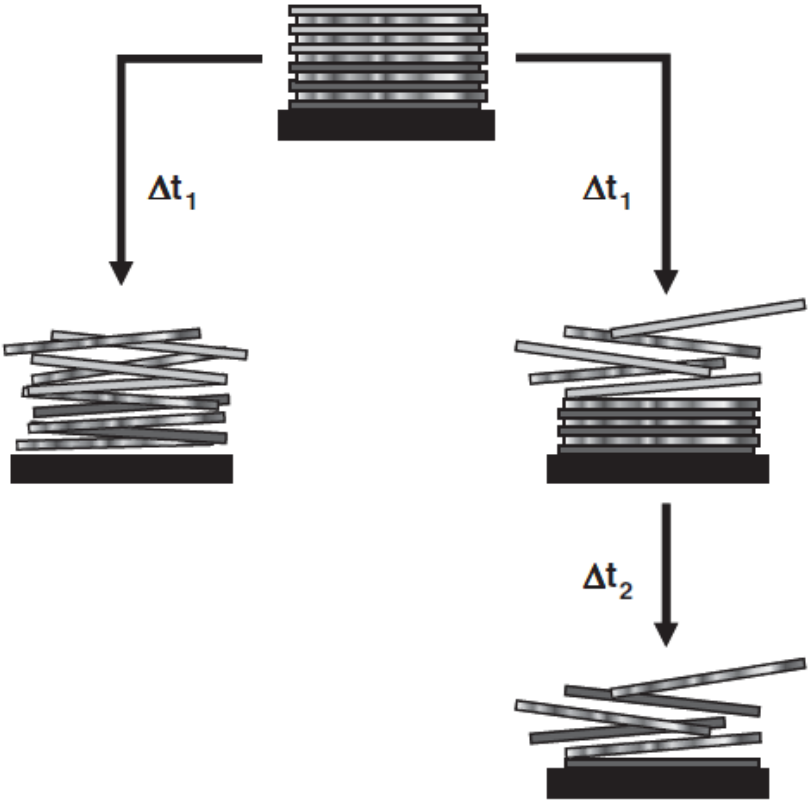

Figure 2.3. Schematic illustration of LbL film disassemble process. Either simultaneous (left) or sequential (right) release of two different components (depicted here as dark grey and light grey) upon erosion of a film fabricated from multiple different layers of two different macromolecular components by bulk-type erosion (left) or top-down erosion (right)[73].

This two types of disassemble fashions of LbL film provide a hint that by adjusting the film interlayer structure, the film releasing would be controllable. Therefore, it requires us to investigate the relationship between film assemble and disassemble, find proper polycaiton materials to build LbL film with desired interlayer structure, and then achieve our goal—sustain and sequential gene releasing.

CHAPTER 3 ENGINEERING BIOREDUCIBLE LAYER-BY-LAYER FILM STRUCTURE FOR SEQUENTIAL AND SUSTAIN GENE DELIVERY

3.1. Introduction

Layer-by-layer (LbL) deposition of polycations and polyanions to build polyelectrolyte multilayer (PEM) films is an approach to prepare tunable, biologically active surface[77]. Since DNA is anionic bioactive molecules, it can be easily fabricated into LbL films with polycation. LbL films have the ability to coated on various biomedical substrates such as silk suture, Ti[78, 79], stainless steel, stents[80-82], and microneedles[83-85]. LbL films is one of the most promising coating methods capable of mimicking cellular microenvironments and releasing therapeutic agents from the surface of biomedical devices.

Polycation selection in LbL film is the key point for high gene loading efficiency, gene protection, low vector cytotoxicity and good transfection efficiency[86]. Bioreducible polymer attracted most researcher's attention because of the reducible property, which can largely reduce gene vector cytotoxicity and has the potential to achieve target delivering[1, 87]. For example, polymer containing disulfide bond can keep stable in physiological pH and deconstructed under reducing environment such as cell surface and early endosome by reacting with glutathione or redox-active membrane proteins through thiol-disulfide exchange reaction[3]. The polycation used as delivery vector focused in this dissertation is poly(amdio amine)s (PAAs). Incorporating disulfide bond in PAAs backbone can offer PAAs biodegradable property. The molecular structure of PAAs used is shown in figure 3.1. This polymer is synthesized by Michael addition polymerization between amine group and bisacrylamide[14, 88, 89]. The structure can be adjusted to hyperbranched or linear chain by changing the feeding ratio of monomer containing different degree of amine group and bisacrylamide monomer[88, 90]. In this Michael addition polymerization, the activity of amine group in monomer is following the order of secondary amine

(original)>primary amine >>secondary amine (formed)[89]. As a result, changing the reacted ratio of triamine monomer and bisacrylamide monomer can be used to control polymer chain structure[88]. The disulfide bond content in polymer chain also can be controlled by adjusting the amount of monomer containing disulfide bond. The reason to change the disulfide bond content and polymer structure is because they can largely influence polymer degradation rate and transfection efficiency, respectively[88].

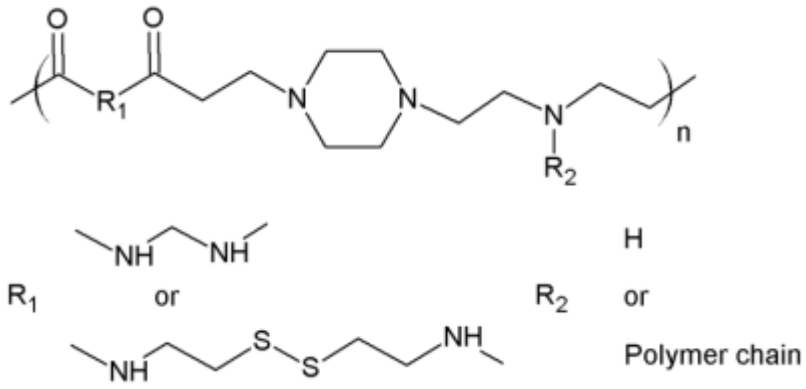

Figure3.1. Bioreducibale PAAs molecular structure.

The LbL film assemble process is based on electrostatic attraction between polycation and polyanion by dipping method. The automatic and programmable dipping is a simple, efficient, and quality coating method to assemble LbL film[14, 91]. As discussed in the literature review part, the film composite with different polyelectrolyte could have different interior structure and disassemble process. Understanding the relationship between the film assembly and disassembly can guide people to engineer the film structure to control the releasing property such as dosage and time. This chapter is aiming to explore the disassembly process of bioreducible LbL film, the nanostructure of the released species, and trying to find how to engineer the film structure to control the film releasing type. The polycation used is PAAs since this polymer with redox-sensitive behavior, reduced cytotoxicity, and enhanced transfection efficiency than most non-

bioreducible polycations[92, 93]. Two types LbL film structures studied is shown in figure 3.2. The type A film is made by PAA/DNA bilayer and type B film consists of type A bilayer film and PEI/DNA bilayer which is periodically inserting into films. The barrier layer here is used to separate the type B film into several PAA/DNA blocks. The reason of adding the non-biodegrdable PEI in type B film is to prevent the polyelectrolyte interlayer diffusion in LbL films. Fabrication of these two type LbL film with different interlayer structure can help to study the relationship between the film structure and disassemble process. The bioreducible PAAs with disulfide bond can be cleaved into short chain by endogenous reducing agents such as thiol-containing membrane proteins and glutamine. When the PAAs chain is cut into short fragment with low molecular weight through the thiol-disulfide exchange reaction, the LbL film will lose its layer-structure due to the reduced binding affinity among PAAs fragments. Then the DNA chain will be released out with full structure and activity. The main goal in this chapter is to engineer LbL film with these two different types to achieve different DNA releasing processes and so that can obtain a sequential and sustain DNA releasing.

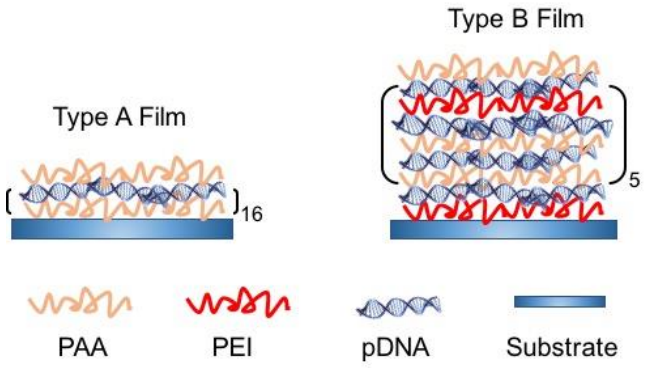

Figure 3.2. Layer composition structure of bioreducible LbL film PAA/DNA (Type A film) and PAA/DNA layer structure with bPEI barrier layer n every 3 bilayers (Type B film).

The LbL film assemble process was studied by AFM and ellipsometry. The LbL film disassemble process was monitored by AFM, fluorescence spectroscopy, and dynamic light

scattering (DLS) in reducing environment—Dithiothreito (DTT) PBS buffer solution. The results indicate that the type A film thickness growth exhibit exponential increasing as a function of the number of deposition layers, and the disassembly shows a fast and bulk releasing property. The type B film, by inserting PEI layers, has a linear growth, and it shows a sustain and sequential releasing property. The film transfection efficiency was examined by in vitro cell culturing experiment. The type B film shows successful gene expression by Human embryonic kidney 293 cell line (HEK 293). But type A film doesn't show any positive transfection in HEK293 cells. This study established connections among LbL film interior layer structure, disassembly mechanism, and gene expression efficiency. It also suggested a simple method to design and engineer sustain and sequential DNA releasing.

3.2. Experimental methods

3.2.1. Materials.

1-(2-Aminoethyl)piperazine (AEPZ, 99%), N,N′-methylenebis(acrylamide) (MBA, 99%), N,N′-Cystaminebis(acrylamide) (CBA, ≥ 98%), Dithiothreitol (DTT, 99%), Fluorescein (FITC, 90%), Tetramethylrhodamine (TRITC, 90%), Hyperbranched polyethylenimine (bPEI, Mw ~ 25 kDa, ≤1% water), Poly(2-hydroxyethyl methacrylate) (PolyHEMA, BioReagent powder), Hyaluronic acid, sodium salt from human umbilical cord (HA, 95%), and Fibronectin (from human plasmid, 0.1%) were purchased from Sigma-Aldrich and used as received. Cy5 nucleic acid labeling kit was purchased from Mirus Bio. Muscovite mica (Grade V5) and glass slides (15 mm diameter) were purchased from Ted Pella Inc. Silicon wafers (Polished, n-type, resistivity 50−75 Ω·cm) were purchased from Wafer World Inc.

Deionized water (18 MΩ·cm resistivity, Barnstead). Mica was hand cleaved into 1 × 1 cm^2 square and freshly used. Silicon wafers were cut to 1 × 1cm^2 square pieces and cleaned via standard

RCA-1 procedure[94]. The RCA-1 solution was prepared by adding 65 mL of NH_4OH (27%) into 325 mL of deionized water and heating the solution to 70 °C followed by adding 65 mL of H_2O_2 (30%). The duration of the RCA-1 process was 15 min. Glass slides were pretreated by soaking in methanol and HCl (v/v = 1:1) mixed solution for 30 minutes and then rinse with deionized water about 2 minutes. After rinse, take the glass slide immersed into 98% H_2SO_4 for another 30 min and followed by rinsing with deionized water to remove the residue acid.

Green fluorescent protein (GFP) reporter plasmid (pEGFP-N1 from Clontech, 4700 bp) was prepared by Qiagen Plasmid Giga kit (Qiagen Inc). Bacterial was cultured overnight and the plasmid was isolated from it. Anion-exchange column chromatography was used to isolate bacterial lysate followed the instruction of Giga kit. Isopropanol precipitation was used to concentrate and desalt the isolated. After removed the protein residue, the final product was dissolved and stored in PBS buffer (pH7.4).

A gift product Arginine-glycine-aspartic acid peptide-bPEI (RGD-bPEI) was from Dr. Olivia Merkel's lab, College of Pharmacy and Health Science, Wayne State University, Detroit, Michigan.

3.2.2. Synthesis and Characterization of Bioreducible PAAs.

Bioreducible PAAs is synthesized through Michael addition copolymerization by the reaction between amines and bisascrylamide under mild conditions[13, 14]. CBA (0.260g, 1.0mmol), MBA (0.308g, 2.0mmol), and AEPZ (0.193g, 1.5mmol) were added in small vial with methanol/water mixture (3mL, 7/3 v/v). The reaction with stirring and reacted under 60˚C for 2 days. Then added 0.019g, 0.15mmol AEPZ reacted 24 hours. The product PAA were fractionated using a semipermeable membrane with a cutoff molecular weight between 30kDa to 3kDa. The final products were obtained by freeze-drying and stored in -20˚C. For linear PAA, the synthesis

method is similar as the hyperbranched one. The different is the to control the reactivity of amine in AEPZ monomer. Changing the mole feeding ratio of (CBA+MBA): AEPZ=1:1 can yield the linear structure PAA. Four type of PAAs with different structure and disulfide bond content are list as table 3.1.

Varian spectrometer (400MHz) ^{1}H and ^{13}C NMR were used to characterize PAAs chemical composition.[92]. Size exclusion chromatography (SEC) (Waters Alliance 2695 HPLC) was used to determine the number average molecular weight (Mn), weight-average (Mw) molecular weight, and polydispersity index (Mw/Mn) 0.03 M sodium acetate (pH 4.5). The column used is Waters Ultrahydrogel 250 PKGD column [92]. Results are shown in table 3.1.

Polycation	(CBA+MBA):AEPZ (n:n)	CBA contents (% mole)	Mw	PDI
Hyperbranched PAA-1	2:1	33%	66,000	2.2
Hyperbranched PAA-2	2:1	67%	10,500	3.9
Hyperbranched PAA-3	2:1	100%	127,000	2.2
Linear PAA-4	1:1	100%	20,800	3.8

Table 3.1. PAAs structure composition and molecular weight.

3.2.3. Deposition of LbL films

The LbL Films fabrication were programmable Carl Zeiss HMS50 slide stainer. Glass slide or silicon wafer substrate hold by homemade Teflon substrate holder and alternatively dip in polymer or DNA solution [14]. Polycation PAAs or bPEI solution was prepared with concentration 0.5 mg/mL in 30 mM pH 5.5 acetate buffer and 0.1 M NaCl). Plasmid DNA solution was dilute to 0.25 mg/mL in 30 mM pH 5.5 acetate buffer and 0.1 M NaCl. Each dipping in these prepared solution is 150s and followed by three deionized water rinses (60s for each rinse). This dip coating

steps was repeated till a desired number of layers and then stopped. The dipping solutions were refreshed every eight dipping cycles in order to minimize concentration variation.

3.2.4. AFM imaging

All AFM images were performance and obtained by Dimension 3100 AFM (VEECO). LbL film surface morphology and thickness were measured under tapping mode in air. When measure film thickness, a razor blade used to scratch film surface to exposed part of the substrate. The height difference between substrate and film surface is the thickness. Each sample measured at least five spot and get average value. The real time LbL film degradation imaging was conducted in tapping mode in liquid environment (100μL, 20mM DTT in PBS buffer, pH7.4). After 100μL DTT solution injection, AFM imaging process start immediately and continued with an average rate of 1Hz till experiment stop. The AFM probe used in air was silicon probe with nominal frequency of 150kHz (VEECO). The probe used in liquid was silicon nitride probe with nominal radius of 0.28N/m (NP type, VEECO). Nanoscope software (5.12) was used to analyzed AFM images, including section analysis, bearing volume analysis, root mean surface roughness analysis, et al.

3.2.5. Ellipsometry

Phase-modulated ellipsometer (Beaglehole Instruments, New Zealand) was used to anlysis LbL film thickness. The LbL film deposited on silicon and then measured under fixing incidence angle near the Brewster angle ($\theta B \approx 70°$) . Each LbL film sample was measured at least in five different spots to get average result. Drude equation and the ellipticity, $\rho = Im\left(\frac{r_p}{r_s}\right) l_{\theta_B}$(r_p and r_s: complex reflection amplitudes for p and s), were used as fundamental theory to calculate film thickness.

3.2.6. Fluorescence spectroscopy

LbL film contain TRITC or FITC labeled PAA degradation process were monitored by fluorometer (SpectraMax M5 Plate Reader, Molecular Devices). TRITC and FITC labeling process was conducted as previous published paper[14]. LbL films were immersed into 20mM DTT in PBS buffer (2.5mL, pH7.4) in room temperature. The degradation solution was collected in each setting time point and freeze-dry to concentrated in 0.25mL in order to get sufficient fluorescence signal. The cumulative fluorescence intensity divided by the total fluorescence intensity, I/Itotal, was used to determine the amount of dye-labeled PAA released from the LbL film as a function of time.

3.2.7. Dynamic light scattering (DLS)

The size of degradation products released from LbL film were analyzed by zetasizer (Nanosizer ZS, Malvern Instrument) at room temperature[14]. The LbL film were cut into small pieces by 5mm×5mm to fit the microcuvette (ZEN0040, Malvern Instrument). A stainless-steel mesh was insert to microcuvette and fixed at the top part. The LbL film put on the mesh and filled the whole microcuvette of 20mM DTT solution (Ph7.4) to immersed the LbL film. Immediately start the Zeta sizer measurement to measure the releasing products hydrodynamic diameter (D_H) as function of LbL film degradation time. Stokes−Einstein equation: $D_H = (kT/3\pi\eta D)$ was used to determine the D_H by DLS. In Stokes−Einstein equation, D is diffusion coefficient, obtained from autocorrelation function via the cumulant fitting; T is temperature, 25 °C; η is viscosity; k is the Boltzmann constant. **LbL**

3.2.8. *In vitro* Transfection of LbL film and cell cultruing

24-well culture plated were coated with poly(HEMA) before using by evaporating 200 μL of 20 g/L polyHEMA in 95% ethanol solution under sterile conditions overnight. LbL film transfection were conducted by human embryonic kidney 293 (HEK 293) cells (Gift from Dr.Wei-

zen Wei lab, Barbara Ann Karmanos Cancer Institute, Detroit, Michigan). Transfection were indicated by GFP reporter plasmid. Each LbL film put into the bottom of the well of the coated tissue culture plate. LbL fim first treated with fibronectin coating with 40μL fibronectin (0.2 g/L) adding to the LbL film surface for 60min and then sterilized under UV light for 1.5 hours. Cells seeded on LbL film surface with cell number 4×104 and incubated at 37˚C with 1 mL/well DMEM culture medium. Cell medium change to fresh one for every two days. Cell morphology and fluorescence were detected every day by optical microscope and fluorescence microscope.

3.3. Results

3.3.1. Structure analysis of LbL films

LBL film fabrication is based on the electrostatic attraction between the polyanion and polycation to form the multilayer structure. This chapter focus on two types of LbL films as described in figure 3.2. The PAA used in these two films is PAA-1 which contains 32% of CBA. The reason of choosing this PAA is that from our previous study, PAA with 32% CBA has better transfection efficiency[92]. The successful PAA and DNA deposition on glass substrate can be demonstrated by fluorescence image as show in figure 3.3. 20% of the PAA-1 was labeled with TRITC and 5% DNA was labeled with Cy-5 in the fluorescence experiment (Figure 3.3c) demonstrates the co-exist of PAA and DNA in the LbL film. The structure composition and thickness data of these two films is shown in table 3.2. The film thickness was analyzed by AFM and ellipsometry as function of number of layers as shown in figure 3.4. The thickness increasing curve of type A film deviates in two part. The first 6 bi-layer shows linear growth and then changes to exponential growth. For the first 6 bi-layers, the average thickness of PAA-1 layer is 1.9 nm and that of DNA is 2.1 nm. But for following layers, along the layer number increasing, the thickness of each layer starts to increase. For the final 6.5 bi-layers, the thickness of PAA-1 is 3.9

nm and that of DNA is 4.0 nm. The average thickness for the total layer is 3.2 nm. This thickness increasing feature fits exponential growth behavior of some LbL films reported previous[75]. For type B film, with an insertion of bPEI/DNA bilayer in every 3 PAA-1/DNA bi-layers, the film thickness growth pattern changes to a linear growth one. The curve can fit a growth curve with slop of 4.6 which means the average thickness of per bi-layer is 4.6 nm. Without an exponential growth feature, the layer of final part in type B film can keep the thickness like of the first few layers. The total thickness is less than type A film. The average thickness of each layer in type B film is 2.3 nm. The data obatained from ellipsometry thickness agree with the AFM results. The stand deviation of film thickness measured by ellipsomtry is less than 5% and by AFM is less than 8%.

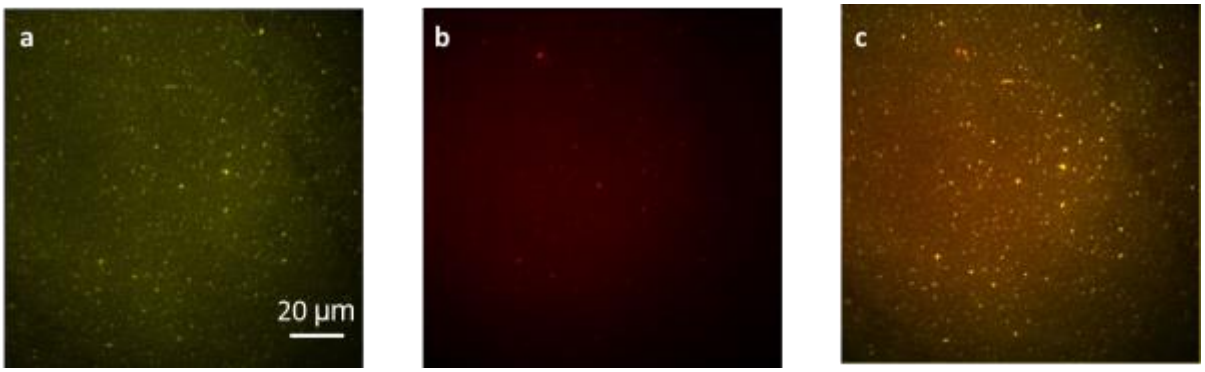

Figure 3.3. Fluorescence image of LbL type A film. (a) Type A film with 20% of TRITC labeled PAA-1 (b) Type A film contains 5% Cy-5 labeled. (c) Immersed image of image a) and image b).

LbL Film type	Polycation	Polyanion	No. of bi-layers	Thickness (nm)
Type A	PAA-1	DNA	16.5	104 ± 9
Type B	PAA-1, bPEI	DNA	16.5	75 ± 4

Table 3.2. LbL film type, composition, and thickness. Thickness was measured by AFM in tapping mode in air.

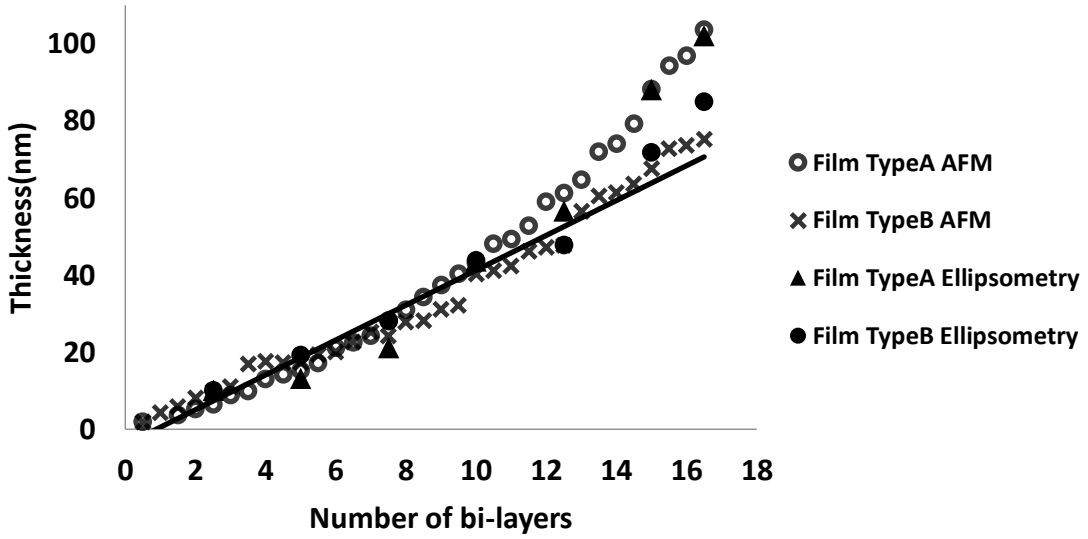

Figure 3.4. LbL film thickness as function of the number deposited layers measured by AFM and ellipsometry. A line fit for type B film shows a slop of 4.6nm per bi-layer[14].

LbL film surface feature and surface roughness were imaged and analyzed by AFM. Figure 3.5 shows the AFM height image of type A film and type B film both with 16.5 bilayers. Comparing with type B film, type A film has some larger granular and rougher surface feather. Which is closely related to the exponential thickness growth property as reported[76]. The root mean square (RMS) surface roughness is obtained by AFM height image in scan size of 20 × 20 μm^2. Figure 3.6 indicates the RMS surfaces roughness as function of each layer of type A and type B film. Both film show roughness increasing with the increasing of layer number. A smooth film surface turn to network-like appearance along with the number of layer increasing. From the type A film roughness change curve, the increasing rate starting from 6 bi-layer becomes more rapid which is similar to the trend of the thickness growth curve. Which further demonstrates the exponential increasing property of type A film.

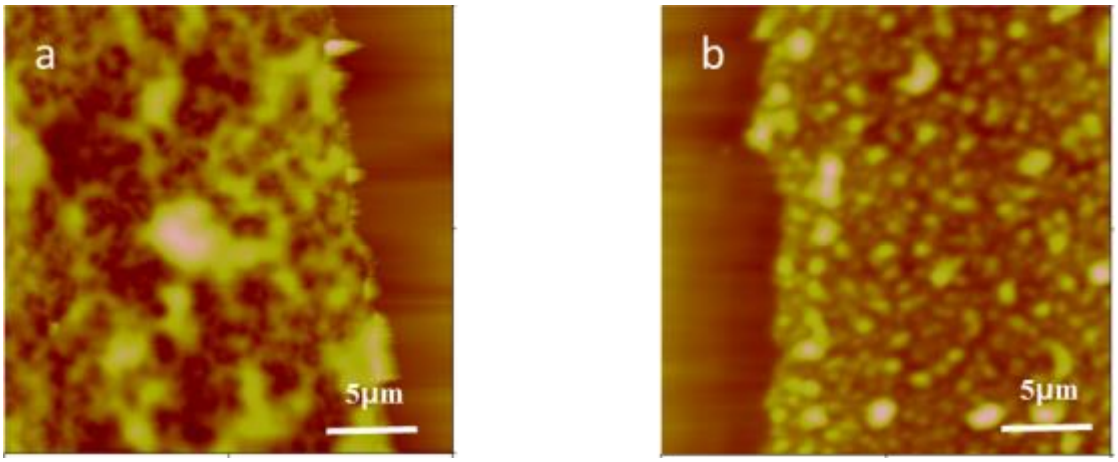

Figure 3.5. AFM height image of LbL film. a) type A film, roughness is 59.4nm, Z-range is 500 nm; b) type B film, roughness is 40.9 nm, Z-range is 450 nm.

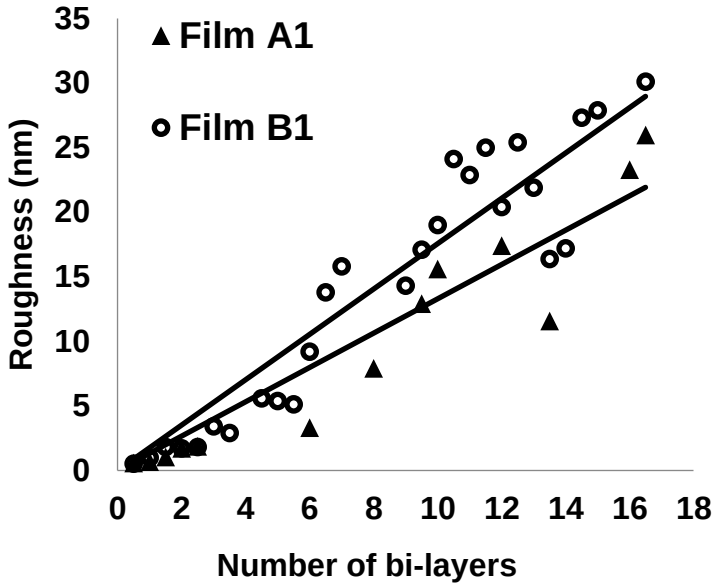

Figure 3.6. RMS roughness as function of number of bi-layers of type A and type B film measured by AFM in air. Line are linear fittings of the two sets of data[14].

The total amount of DNA loaded in LbL film was measured by fluorescence spectroscopy. Two types of film were immersed into reducing environment, 20 mM DTT solution, for 14 days letting the film totally release out. Ethidium bromide (EtBr) was used to label DNA in the degradation solution. Calibration curve was used to calculate the amount of DNA in each film.

The total DNA amount in type A film is 6.6 μg/cm^2 and type B film is 5.0 μg/cm^2. The difference of DNA content in two type of LbL film is caused by the film interior structure. The type A film shows exponential growth that can absorb larger amount of DNA in the final few layers compared with the initial layers. The total thickness of type A film is larger than type B film also can indicate the amount difference of loading DNA in LbL film.

LbL film thickness showing linear growth mode is due to the polyelectrolytes deposited on the film surface only react with the neighboring layer surfaces. This linearly grew film usually has no or only very slight degree of interlayer diffusion thus results in a well-defined layer structure. However, if the polyelectrolytes able to diffuse through it neighboring layer, such as diffusing "in" and "out" through the whole film, the film would exhibit an exponential growth mode of thickness. 25 kDa bPEI is a polycaiton with higher charge density and lower diffusion coefficient than PAA. Benefiting from the high charge density and long molecular chain, periodically incorporated bPEI barrier layer in LbL film can decrease the degree of LbL film interlayer diffusion and support the layer structure. That's why the type B film show linear growth mode.

3.3.2. Disassemble of LbL films in DTT reducing environment

The LbL film is made by biodegradable PAA which can be cleaved into short chain via thiol-disulfide exchange. The cleaved short PAA chain cannot keep enough binding affinity and then trigger the film disassembly.

LbL film disassembly process was studied by AFM and fluorescence spectroscopy. LbL film surface change can be monitored by AFM imaging in reducing enviroment, 20 mM (DTT) in PBS buffer (pH7.4). The DTT can react with the disulfide bond in PAA to degrade LbL film. Figure 3.7(A) shows the time-lapse AFM image of type A film which was immersed in 20 mM DTT solution. Those images were focused on an area of the film with partially removed film and

the exposed substrate. The height difference between substrate and film can indicate the film variation during degradation process. At time zero, type A film thickness in liquid environment was 600 nm with surface roughness of 124 nm. During the degradation process, starting from 1 hour, part of the film pieces started to peel off from the substrate. Such as 3 μm by 17 μm in 64 min; 9 μm by 15 μm in 72 min; 6 μm by 19 μm in 83 min. This microscale pieces indicate that the film has a bulk degradation instead of the expected layer-by-layer erosion. The film was completely removed from the substrate after 100 min. For type B film, which shows linearly growth, was reduced in the enviroment and imaged by AFM as shown in figure 3.7B. In this case, the film was taken out from the DTT solution in setting time point and imaged by AFM in tapping mode in air. The film degradation lasted for 38 hours, much longer than type A film. During the degradation process, there is no big pieces peeling off from the film surface or substrate. Instead, nanometer scale particles formed on the film surface and subsequently released to the solution. These particles have an average diameter ~ 300 nm and average height ~ 30 nm. This indicates that comparing with type A film, type B film has much slower degradation rate and no bulk releasing situation. The complex released from type B film is much uniform and with much smaller size. Figure 3.8 shows the thickness change obtained by AFM analyzing during film disassemble in 20 mM DTT. For type A film, there is no obvious thickness change in the first 1 hour. But a rapid thickness decreasing starting from 60 min and reached to 0 nm in 90 min. But for type B film, the film thickness decreasing rate in first 3 hours is higher than that of the following time. After 3 hours, the thickness change slowed down with gradual decreasing and lasted up to 120 hours. The AFM characterization experiment for film degradation demonstrates that periodic insertion of bPEI barrier layer greatly prolongs the film reducing period: from 1.5 hours in type A film to at least 120 hours in type B film. The LbL films surface change and released particle

morphology change indicate that type B film convert LbL film disassemble process from bulk releasing to sequential releasing.

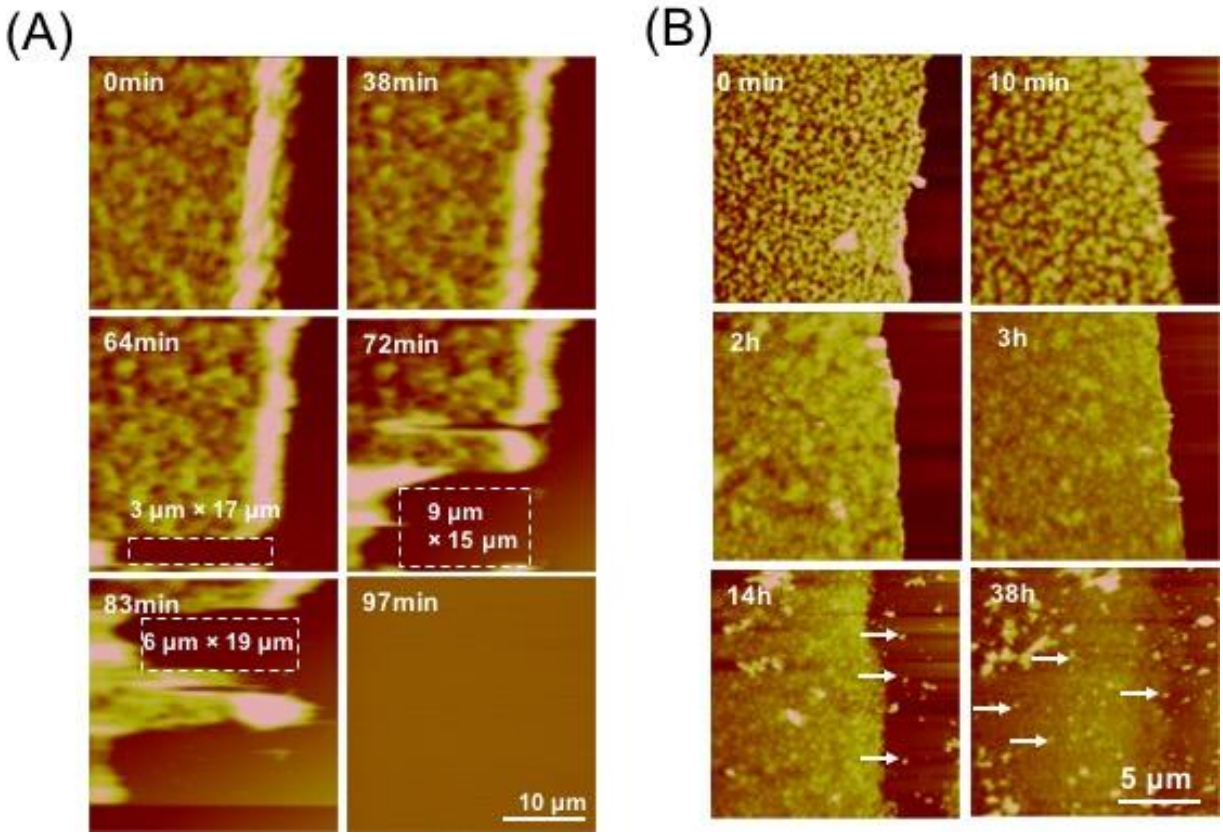

Figure 3.7. Time lapse real-time AFM height image. (A) type A film thickness and morphology change in 20 mM DTT in PBS buffer (pH7.4). Patches left by released film parts were marked in the image. Z-range: 2 μm. (B) Time lapse AFM height image of the type B film thickness and morphology change treated with 20mM DTT in PBS buffer (pH7.4). Z-range: 150 nm[14].

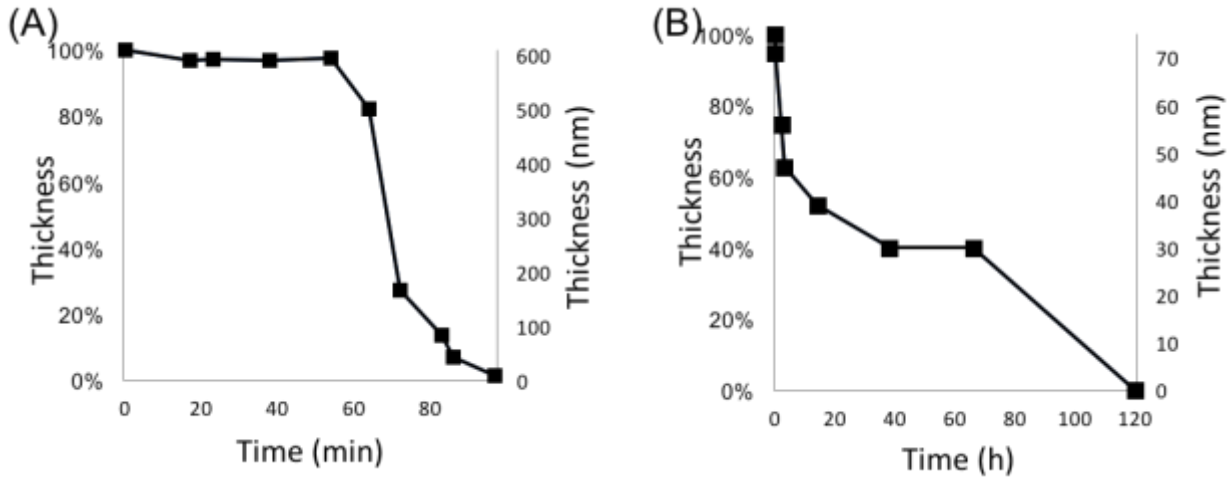

Figure 3.8. LbL film thickness change as a function of degradation time. (A) type A film and (B) type B film. Reducing environment: 20 mM DTT. Thickness were measured by AFM [14].

LbL film disassembly was further analyzed by fluorescence spectroscopy. The PAA fabricated into LbL film were labeled with fluorescence dyes, including FITC and TRITC. Through analysis of the cumulative fluorescence intensity in the degradation solution as function of degradation time can indicate film disassemble rate. As shown in figure 3.9 (A), type A film shows the increasing fluorescence intensity in the first 1 hour and then reach to the plateau indicating that the film released PAA out and completed this process in 1 hour. But for type B film (figure 3.9 B), the cumulative fluorescence intensity increased much slower than that of type A film and continued increasing for ~140 hours. PAA labeled with two fluorescence dye were used to determine the releasing sequence. The top half part of the film was labeled with FITC and bottom half part was labeled with TRITC. From figure 3.9 (C), the PAA in type A film, have been released out at the same time regardless of position. But for type B (figure 3.9 D) film, the bottom part PAA were released out followed by the top part. This fluorescence spectroscopy experiment demonstrates that by inserting PEI/DNA bilayer, LbL film changes from fast bulk releasing to slow sustained and sequential releasing.

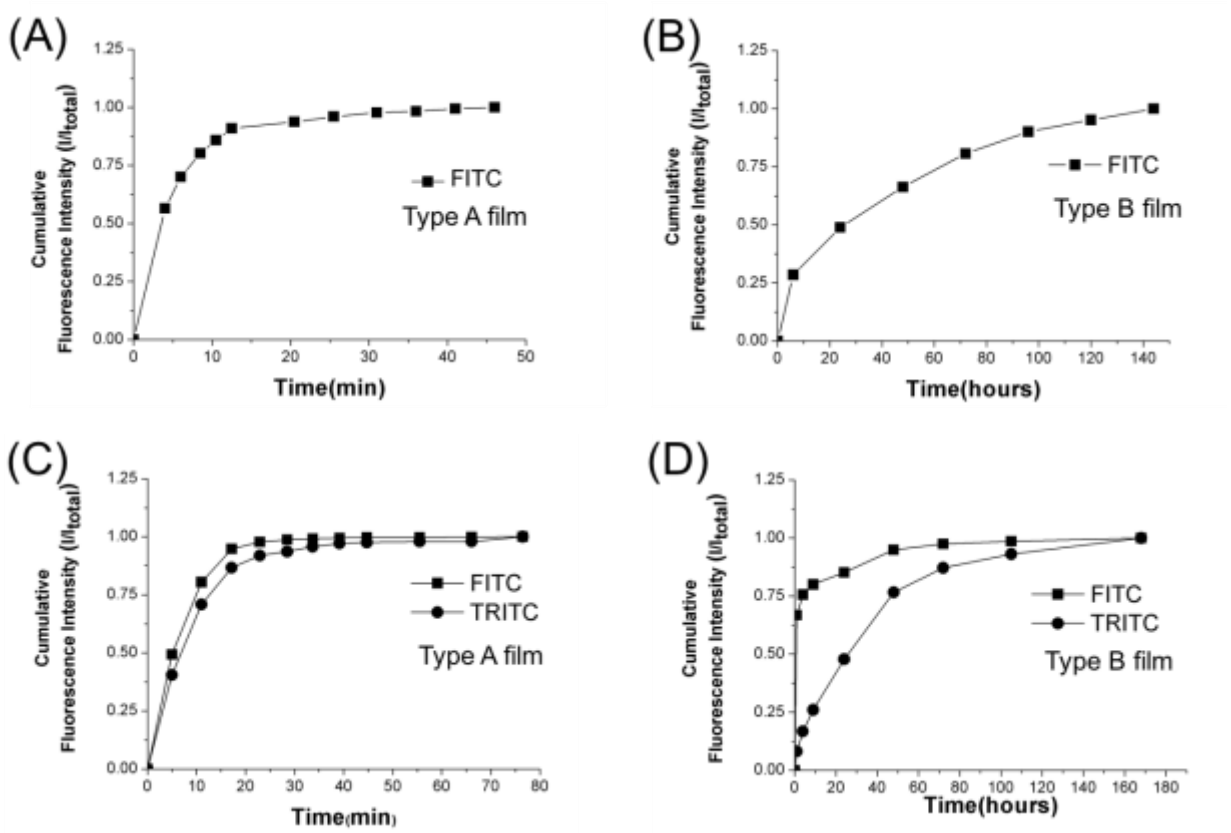

Figure 3.9. Cumulative fluorescence intensity as function of degradation time for (A)Type A film and (B)Type B film made with FITC labeled PAA. (C)Type A film and (D)Type B film made of FITC labeled PAA in top half and TRITC labeled PAA in bottom half film[14].

The size of degraded products released from LbL was analyzed by DLS. The hydrodynamic diameter (D_H) of released products in 20mM DTT is a function of degradation time as shown in figure 3.10. At the beginning of type A film degradation, the average D_H of released particles was ~700 nm and then decreased to ~100 nm after 2 hours. Since the AFM images showed the type A film finished degradation in 1.5 hours, we can assume that the small particle released after 1.5 hours is not directly from the film but the secondary degradation product from the primary released large film pieces. The D_H of released particle from type B film keeps in a constant range of diameter between 300-400 nm. This DLS data consisted the AFM image data in figure 3.7, which indicates that the released particle size can be reduced by inserting bPEI barrier layer. The

smaller sized particle can make contribution to high transfection efficiency since nanometer scale particles would have much higher opportunity to across cell membrane to get into cells.

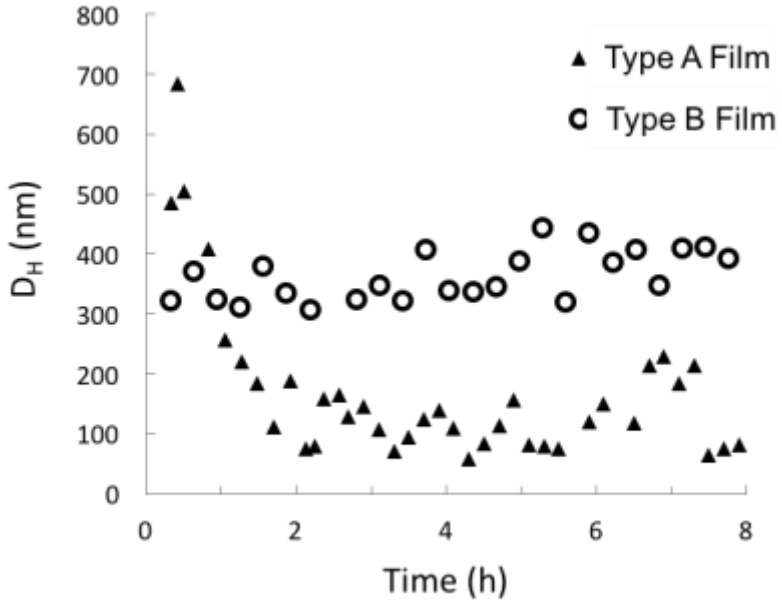

Figure 3.10. Hydrodynamic diameter of the degradation products from type A film and type B film measured by real-time DLS in 20mM DTT in PBS buffer (pH7.4)[14].

From disassemble study of two different types of LbL filmw, we can conclude that the LbL films with exponential growth such as type A film have a fast and bulk releasing property. The releasing product size is in micrometer-scale and peeling off from the film surface quickly. While films with linear growth mode like type B film show slow, sustained, and sequential releasing property. The releasing particle can keep in nanometer scale during the whole degradation process.

3.3.3. Transfection efficiency of LbL films in vitro.

The transfection efficiency of LbL film can be detected by in vitro experiment through cell culturing. HEK 293 cells were seeded on the LbL film surface and let grow naturally. The DNA used in those LbL film is pEGFP-N1 plasmid. As shown in figure 3.11 (B), the type B film with PEI barrier layer shows transfection start from day 4 and continues for about 9 days. The mean fluorescence intensity (MFI) detected by flow cytometry of the type B film in day 6 was measured

to be 2086. Which is much higher than that of the control sample (cell grown on uncoated substrate), which was 1175. But for type A film (figure 3.11 A), there is no transfection observed. This is because the film undergoing fast bulk releasing with micrometer sized product is prevents effective cell uptake. For type B film, the released product was in nanometer size which demonstrated by AFM and DLS is much easier to delivery into cells across the cell membrane. In addition, the sustain releasing can largely increasing the opportunity of endocytosis due to the longer releasing time. That's why, the transfection can last at least 9 days[14].

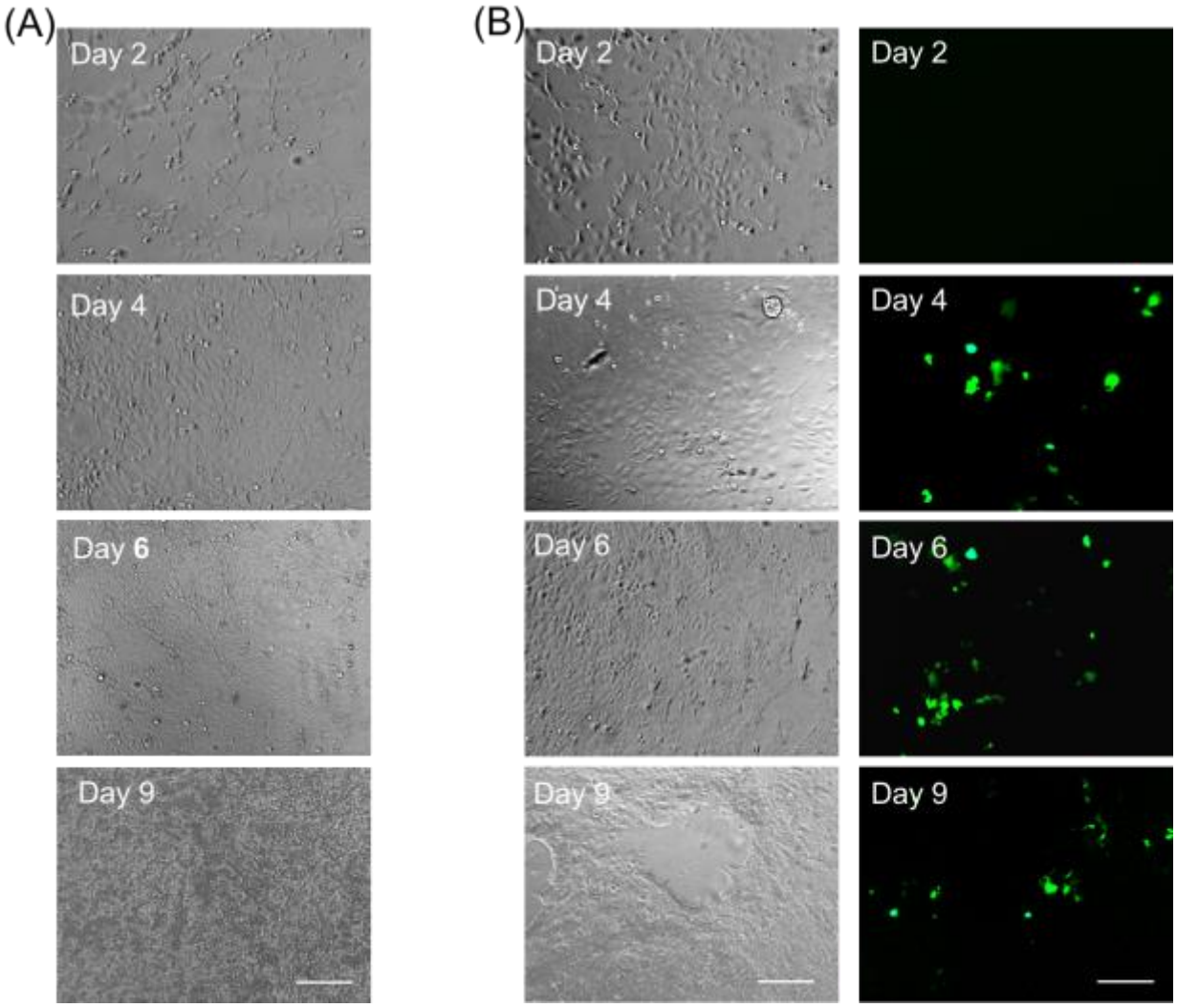

Figure 3.11. Gene express in vitro experiment of HEK 293 cells cultured on (A) type A film, bright field, and (B) type B film, bright field (right column) fluorescence microscopy images (left column). Magnification is 10× for all images; scale bar is 200μm.

3.4. Discussion

This chapter first described the polycation structure and film interior structure design. Polycation's selection and arrangement can largely influence the LbL film interlayer structure. Different interlayer structure could affect the film disassemble property. This chapter demonstrated the relationship between bioreducible LbL film interlayer structure and its degradation property. Furthermore, provided a simple method to overcome the bulk and fast DNA releasing problem and convert it to sustained and sequential releasing.

The LbL film exhibits that exponential growth, such as type A film, is due to the polymer chain interlayer diffusion. This diffused internal structure is determined by the strength of intermolecular interaction between polyelectrolyte pair[95-99]. When the polyelectrolytes deposit into the film and only interact with the neighboring species to form an organized structure, the film will show linear structure. But when the polyelectrolyte in LbL film extensively interpenetrate its adjacent layers, the film thickness growth pattern will show exponential growing. The films with interlayer diffusion do not exhibit well-defined layer structure[97]. The exponential thickness growth usually happens when more hydrophilic, weakly charged, short chain electrolytes or biologically derived molecules (e.g., polypeptides and polysaccharides) are used[75, 100]. The diffusion feature of the LbL film acts as "reserve tank". It can continue absorb the polymer chains from the outside environment till reach kinetic limitation[97-99]. The more layer deposited, the larger the "reserve tank" will be. Along continues deposition steps processing, LbL film thickness exhibits the exponential growth.

LbL film with interlayer diffusion leads the film interior structure into homogeneous distribution[75]. This diffused layer structure gives rise to "bulk erosion" behaves like our type A film. But when the film with well-defined stratified layer structure, the LbL film tends to exhibit the "surface erosion" with sustain releasing property[73]. DNA can be considered as non-diffusing polyelectrolyte due to its high charge density, long chain length, and high chain rigidity[101]. Therefore, the exponential growth feature of type A film indicates diffusing property of PAA. Moreover, PAA is biodegradable polymer due to the disulfide bond. When exposing type A film into reducing environment, the cleaved PAA fragments can amplify the interlayer diffusion since short chains have lower molecular weight and lower charge[101, 102]. The PAA fragments have higher mobility than the completely long PAA chains. After the LbL film is full of the cleaved PAA fragments, the LbL film tends to contain a high degree of mixing interior structure due to the increased chain mobility. When film starts to disassemble, all the materials with homogeneous distribution in the film will be released out together which results in bulk releasing. The AFM experimental result in figure 3.7 demonstrated this bulk releasing process. The type A film shows big species peeling off from film surface or substrate with high degradation rate.

By periodically inserting bPEI layer into LbL film, the appearance of high charge density and high molecular weight bPEI introduces barrier in LbL film. This bPEI strongly binds with its neighboring layers so that it can prevent the PAA from diffusing across itself through the whole film, and consequentially, converts the film thickness growth mode from exponential to linear. When exposing this type B film in reducing environment, the bPEI cannot be broken down due to the nondegradable property. Therefore, it can keep in a trapped status to stabilize the nearby PAA fragments and reduce the PAA chain mobility[75, 98]. The bPEI only can be released out when the entire region become soluble. By lowering the PAA mobility and introducing the nondegradable

property, the appearance of bPEI barrier layer successfully prevents the bulk erosion. Therefore, the type B film shows sustained releasing property and exhibits linear growth mode.

The appearance of bPEI layer in our LbL film somehow prevents the complete detachment of PAA and DNA in a short period of time. The releasing products are changed from large micrometer pieces to nanometer complexes. The formation of small complexes on LbL film surface in DTT solution is due to the unreducible bPEI. It can maintain high positive charge density and interact with nearby DNA. The interaction between polymer chain and DNA can reduce their mobility which might lead to release out. Therefore, the PEI, PAA, and DNA will have opportunity to rearrange into polyplex-like particles and will be desorbed from the film surface. The polyplex-like products have already been demonstrated in some hydrolysable LbL films[102]. We can assume that the low chain mobility may also contribute to the small size of releasing products

The different disassemble properties also have influence on the efficiency of gene expression. The main reason for the bare transfection in type A film is the appearance of large released species during degradation process. The particle size can strongly influence particle endocytosis process[103, 104]. For example, a 100 nm particle has 250-folder higher opportunity to be uptaken by cells than the 10 μm particles[104]. The released particle from type B film can keep in a nanometer range during the whole degradation process. This small-sized particle is one of the reasons helping type B film achieve transfection during in vitro transfection experiment.

3.5.Conclusion

This study provides a method to engineer bioreducible LbL film with a sustained and sequential gene releasing property. Inserting dPEI barrier layer in LbL film changed the LbL film interior structure, degradation process, and releasing product morphology. The degradable PAA makes LbL film coating capable of being degraded in target environment to release the therapeutic

gene. This bioreducible property improves the transfection efficiency and decreases cytotoxicity. The LbL type B film made by PAA, dPEI, and DNA shows prolonged DNA releasing period. This disassembly type has a potential to deliver multiple therapeutic genes or agents with desired sequence. This chapter establishes connections among LbL film internal structure, disassemble property, and transfection efficiency and further reveals the mechanism to guide the fabrication of sustained and sequential DNA releasing LbL film.

CHAPTER 4 DESIGNING BIOREDUCIBLE POLY(AMIDO AMINE)S FOR HIGH EFFICIENCY GENE DELIVERY VEHICLE

4.1.Introduction

Good water solubility and biodegradability of poly(amdio amine)s (PAAs) have attracted researcher's attention of the application in medical field such as drug and gene delivery. The PAAs are hydrolysable but much more stable than poly(amino ester)s, which improved the stability in extracellular environment. People found amphiprotic PAAs with carboxylic acid side group have greater transfection efficiency even when compared with 25kDa branched bPEI[105]. Adjusting the conformation of PAAs can help the endosomes or lysosome escape during the intracellular delivery[106]. Though the slow degradation rate of PAAs can protect the drug from metabolizing in extracellular environment, the amide hydrolysis cannot contribute to the intracellular DNA releasing from the polyplex. The incorporation of disulfide bond can solve this problem. This is because there is redox potential gradient between extracellular environment and various subcellular organelles. The disulfide bond can react with small redox molecules through the thiol-disulfide exchange. Designing a PAAs containing disulfide bond can make this polymer stable in the extracellular environment but quickly and easily being reduced in the intracellular environment[88, 107, 108]. The reducing is brought by small redox molecules like glutathione (GSH) or intracellular protein with thiols either alone or with the help of redox enzymes[109]. Therefore, the reducing rate of PAAs in intracellular environment can be largely enhanced to help DNA releasing. Researchers believe that the appearance of disulfide bond increased intracellular bioavailability[110-112] and decreased polycation cytotoxicity[107, 113-115] of polymeric gene delivery. Oupicky group showed that the reducible cationic polypeptides $(Cys\text{-}Lys_{10}\text{-}Cys)_n$ have 187-fold higher level of gene expression than that of nondeductible polylysine[116, 117]. Lee ta al showed that disulfide-containing PEI has considerable lower cytotoxicity than 25 kDa bPEI[118].

The chapter 3 discussed the PAAs which synthesized by monomer CBA, MBA, and AEPZ. Though the LbL films made by PAA-1 has some gene expression in HEK 293 cell during *in vitro* experiment, the efficiency still needs to be improved. Chao et al described a novel serials of poly(amido amine)s with disulfide linkage in polymer main chain and evaluated their gene delivery capacity[119]. These PAAs structures are shown in figure 4.1. This chapter will first focus on developing new type of poly(amido amine)s with high transfection efficiency based on Chao's work. We designed the polymers with similar chemical stricture of polymer pAPOL (Figure 4.1) due to the high transfection efficiency and comparably low toxicity[119]. The novel pAPOL interacted with DNA can form polymer/DNA conjugate: the polyplex. With the help of multiple characterization methods, we can find relationships among high transfection efficiency, polymer chemical and physical property. Finally, by optimizing structures of various pAPOLs we can build the next generation LbL film with improved transfection efficiency and biocompatibility.

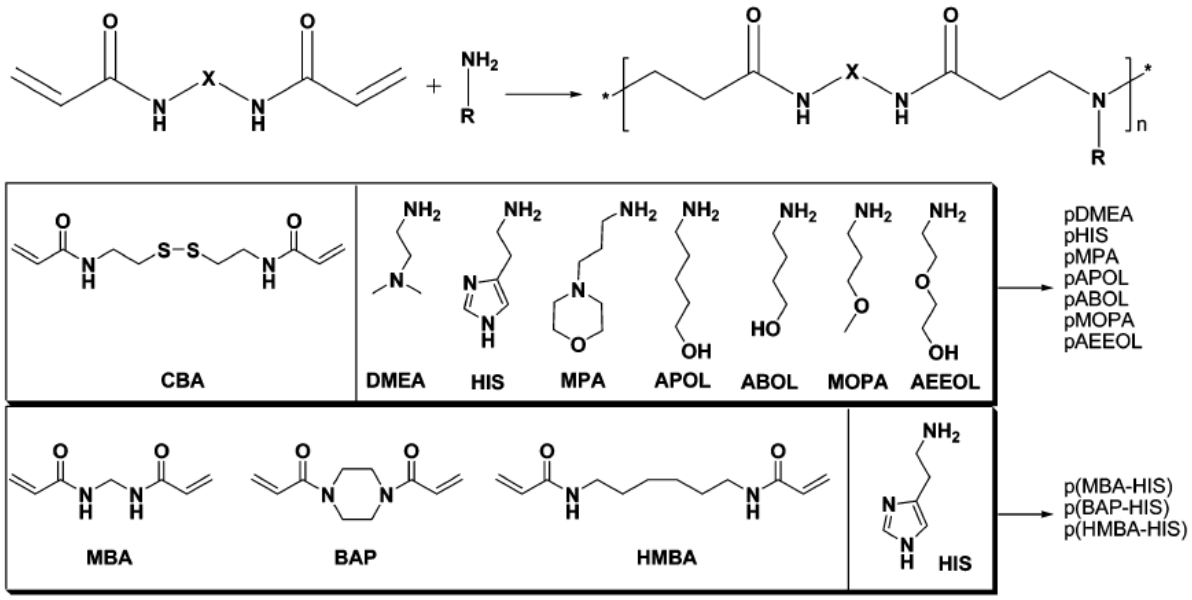

Figure 4.1. Structure component of bioreducible poly(amido amine)s and nonreducible control polymers (p(MBA-HIS), p(BAP-HIS) and p(HMBA-HIS))[119].

Polyethylenimine (PEI) is one of the most successful and widely studied gene delivery polycations due to the relatively high delivery efficiency and availability. The 25kDa branched PEI always acts as the gold standard to compare with the newly designed and synthesized gene delivery vectors. However, the toxicity in many cell lines has largely limited PEI applications. People found that after PEI treatment, the cell metabolic activity was reduced by 4-90%[120, 121]. Gosselin and his colleagues found the PEI toxicity decreases as a function of polymer size, coupled with decreased transfection capability [118].

In chapter 3, the type B film we designed contains 25kDa bPEI. The toxicity should be the major concern during the future developing. Considering the PEI with small molecular weight has lower cytotoxicity than the high molecular weight one. The reducible property can also help improve polymer biocompatibility. We developed a degradable PEI (dPEI) by crosslinking 800Da branched PEI with1,6-hexanediol diacrylate through the reaction between amino groups and diacrylates[87]. This dPEI has a highly-branched structure and a hydrolysable property. More importantly, the toxicity is much lower than that of bPEI[87]. We expect that using the dPEI instead of bPEI can improve our LbL film biocompatibility in future application.

4.2. Experimental methods

4.2.1. Materials

N,N'-Methylenebis(acrylamide) (MBA, 99%), dithiothreitol (DTT, 99%), branched poly(ethylenimine) (bPEI, Mw~25,000Da, ≤1% water), branched poly(ethylenimine) (bPEI, Mw~800Da), 1,6-hexanediol diacrylate (80%), 5-amino-1-pentanol (APOL, 95%), and bovine serum albumin (BSA, heat shock fraction, pH 7, ≥98%) were purchased from Sigma-Aldrich. N,N'-Cystaminebisacrylamide, (CBA, 98%, Electro Pure™) was purchased from Polysciences, Inc. Sodilum chloride (NaCl, BioReagent) and sodium hydroxide (NaOH, BioReagent) were

purchased from Fisher Scientific. Sodium acetate anhydrous (NaOAc, 99%) was purchased from Mallinckrodt Chemicals. Phosphate buffered saline (PBS, PH 7.4), Minimum Essential Medium α (MEM α, nucleosides), Dulbecco's Modified Eagle Medium (DMEM), fetal bovine serum (FBS, certified, Gibo™), penicillin-streptomycin (10,000 U/mL), Vybrant® MTT cell proliferation assay kit, 4-(2-hydroxyethyl)-1-piperazineethanesulfonic acid (HEPES, 1M) were purchased from Thermo Fisher Scientific, Inc. Deionized water obtained under 18 MΩ cm resistivity (Barnstead).

Green fluorescence protein (GFP) reporter plasmid (pEGFP-N1 from Clontech, 4700 bp) and E2-Crimson reporter plasmid (pEF.myc.ER-E2-Crimson from Benjamin Glick, 6263 bp) were prepared and obtained by Qiagen Plasmid Giga kit (Qiagen, Valencia, CA). The method used is same as chapter 3 described.

4.2.2. Synthesis of novel bioreducible poly(amdio amine) (pAPOL)

Bioreducible pAPOLs were synthesized by Michael addition copolymerization of equal molar ratio of monomer 5-amino-1-pentanol (APOL) and bisacrylamide monomers (CBA and MBA)[122]. Adjusting the feeding mole ratio of CBA and MBA can be used to produce the pAPOLs with different disulfide content. Typically, for PAA containing only CBA and APOL, CBA (309 mg, 3 mmol, 1 equiv.) was dissolved in CH_3OH/H_2O (4:1 v:v, 3 mL). APOL (781 mg, 3 mmol, 1 equiv.) was added followed by degassing with N_2. The vial was wrapped with foil and then placed in 50°C oil bath. This mixture was stirred for 10 days at 50°C to yield a light yellow viscous solution. Additional APOL (10 mol%) was added and the reaction continued for another 2 days in order to consume all acrylamide. After evaporating CH_3OH, the resultant solution was added dropwise into 20 mL 4°C acetone. The acetone phase was discarded while the oil phase was washed with 4°C acetone (3×5 mL). After acetone evaporation, 5 mL water was added and the pH of the solution was adjusted to 4 using 1M HCl. The polymer chloride salt was obtained as solid

foam (520 mg, 48% yield) after freeze drying. ^{1}H NMR, 400MHz, D_2O: δ1.29 (CH_2CH_2OH, 2H); δ1.45 ($CH_2CH_2CH_2OH$, 2H); δ1.64 ($CH_2CH_2CH_2CH_2OH$, 2H); δ2.67 ($NHCOCH_2$, 4H); δ2.72 ($SSCH_2CH_2$, 4H); δ3.09 ($NCH_2CH_2CH_2CH_2CH_2OH$, 2H); δ3.33 ($CH_2CH_2NCH_2CH_2$, 4H); δ3.40 ($SSCH_2CH_2$, 4H); δ3.47 (CH_2OH, 2H).

PAAs containing different feed ratios of monomer CBA and MBA were synthesized BY the same method described as above. PAA made with APOL/CBA/MBA=3/1/2 used 86 mg CBA (0.33 mmol, 1 equiv.), 103 mg MBA (0.67mmol, 2 equiv.), and 103 mg APOL (1mmol, 3 equiv.). ^{1}H NMR, 400MHz, D_2O: δ1.29 (CH_2CH_2OH, 2H); δ1.45 ($CH_2CH_2CH_2OH$, 2H); δ1.64 ($CH_2CH_2CH_2CH_2OH$, 2H); δ2.67 ($NHCOCH_2$, 4H); δ2.72 ($SSCH_2CH_2$, 4H); δ3.09 ($NCH_2CH_2CH_2CH_2CH_2OH$, 2H); δ3.33 ($CH_2CH_2NCH_2CH_2$, 4H); δ3.40 ($SSCH_2CH_2$, 4H); δ3.47 (CH_2OH, 2H); δ4.45($NHCH_2NH$, 2H). PAA made with APOL/CBA/MBA=3/2/1 used 174 mg CBA (0.67 mmol, 2 equiv.), 51 mg MBA, (0.33mmol, 2 equiv.), and 103 mg APOL, 103 (1mmol, 3 equiv.). ^{1}H NMR, 400MHz, D_2O: δ1.29 (CH_2CH_2OH, 2H); δ1.45 ($CH_2CH_2CH_2OH$, 2H); δ1.64 ($CH_2CH_2CH_2CH_2OH$, 2H); δ2.67 ($NHCOCH_2$, 4H); δ2.72 ($SSCH_2CH_2$, 4H); δ3.09 ($NCH_2CH_2CH_2CH_2CH_2OH$, 2H); δ3.33 ($CH_2CH_2NCH_2CH_2$, 4H); δ3.40 ($SSCH_2CH_2$, 4H); δ3.47 (CH_2OH, 2H); δ4.45($NHCH_2NH$, 2H).

4.2.3. Synthesis of degradable polyethylenimine (dPEI)

Degradable polyethylenimine (dPEI) was synthesized through crosslinking low molecular weight PEI (branched, 800Da) by diacrylate cross-linker[87]. One gram of 800Da PEI was add in 20mL glass vial and dissolved in 3 mL methylene chloride. An equimolar amount of cross-linker, 1,6-hexanediol diacrylate was add dropwise. Then the vial sealed with solvent-resistant cap. The reaction was carried out at 45°C with stirring for 6 hours. The polymer was then precipitated with hexanes and collected by freeze drying. Product were stored at liquid nitrogen.

4.2.4. Buffering capacity

The buffering capacity of PAA was determined by acid-base titration. PAA containing 0.1 mmol protonable amine groups was dissolved in 10 mL 150 mM NaCl aqueous solution. The pH of the solution was adjusting to 2 by 1M HCl. The solution was titrated by 100 mM NaOH. 25 kDa bPEI was used as a control. PEI containing 0.1 mmol protonable amine groups was dissolved in 10 mL 150 mM NaCl aqueous solution and titrated following the same procedure. The buffering capacity is defined as the percentage of protonable amine groups become pronated from pH 7.4 decrease to 5.1. It can be calculated from the following equation[123, 124]:

$$\text{buffer capacity}(\%) = \frac{\Delta V_{NaOH} \times 0.1M}{\text{N mol}} \times 100\%.$$

ΔV_{NaOH} is the titration volume of NaOH (100 mM) added during the pH change from 5.1 to 7.4. N is the moles of protonable amine groups in the polymer.

4.2.5. Preparation of polyplex

Polyplex were prepared by adding the pDNA aqueous solution to the polymers HEPES buffer (20mM, pH7.4) with setting N/P ratio (as show as table 4.2). Then immediately mixed well by vortex mixer 10 second. N/P ratio is defined as the number of amines (N) of the cationic polymer per DNA phosphate group (P) in the complexation solution. All the preparation process was handled in room temperature 25 ºC.

4.2.6. AFM imaging

AFM tapping mode (in air and) contact mode (in liquid) were used to characterize polyplex morphology in different environment (VEECO, Dimension 3100). When tapping mode was used in air, the AFM probe used was a silicon probe tap300-G (Budget Sensors) with a factory-specified resonant frequency of 300 kHz and a spring constant of 40 N/m. In liquid environment, the probe

used was non-conductive silicon nitride NP-20 (Veeco) with cantilever 0.4-0.7μm, resonant frequency 14-26 kHz, and spring constant 0.12 N/m.

In a polyplex sample preparation for AFM imaging, a droplet of 50 μL polyplex or LbL film degradation solution were placed on approximately 1×1 cm^2 of freshly cleaved mica. Excess solution or buffer were removed after 5 min by deionized water and the sample was rinsed 3 times by deionized water. In liquid contact mode, the probe used is non-conductive silicon nitride probe NP-20 (VEECO). PBS buffer of 100 μL was added on the sample surface to cover the sample and probe. The particle volume was analyzed by the bearing analysis command in the Nanoscope software (5.12, VEECO). The substrate was used as the threshold bearing plane. The typical error of the size measurement is 30%. And the apparent particle volume according to the AFM analysis is generally higher than the actual one due to the tip-convolution effect. It is more accurate to consider only the top half of the structure for particle volume determination[125]. However, in the case of cap-shaped objects likely adopted by the adsorbed polyplexes, this method could lead to an underestimation of the particle size[92].

4.2.7. Dynamic light scattering (DLS)

The polplex size and surface charge were analyzed by zetasizer (Nanosizer ZS, Malvern Instrument). The hydrodynamic diameter (D_H) and zeta potential measurements of polyplex proceeded immediately after the polyplex freshly made. Data were collected every 7 min and continued 1 hour. The D_H calculation was automatically finished by DLS software according to Stokes-Einstein equation, as described in chapter 3.

4.2.8. Cell culturing and Polyplex transfection *In vitro*

Transfection experiments using polyplexes were performed with HEK 293, MC 3T3, and NIH 3T3 cell line by using plasmid pEGFP-N1 as the report gene[14]. Transfection experiments of

each cell line were carried out in separate 24-well plates (ca. 80,000 cells per well). The cells were first incubated 24 h to grow and cover 80% full of each well in humidified incubator (37°C, 5% CO_2). The polyplex solutions of Different basic amino acid residue-to-DNA phosphate molar ratios (N/P ratios) from 6/1 to 24/1 were freshly prepared for transfection experiment. The regular cell medium was removed and replaced with 300 µL fresh medium which is absenting FBS in culture plate before adding polyplex solution. 50 µL polyplex solution, which containing 1 µg DNA, was added into cell medium. Then cells were incubated with polyplexes at 37°C in incubator for 3 h. Next, after 3 h, the polyplex-containing meedium was removed and replaced with freshly regular cell culture medium (1 mL/well) which is containing FBS. Incubated cells for 24 h at 37°C in cell culturing incubator with 5% CO_2. After 24 h incubation, cell morphology and growth situation were captured by fluorescence microscopy; transfection efficiency was determined by flow cytometer; and cell viability was characterized by the MTT assay. All cell culturing and transfection experiment *in vitro* were carried out in triplicate.

4.3. Results

4.3.1. pAPOL and dPEI synthesis and characterization

We employed Michael addition copolymerization of a primary amine monomer, APOL, and two bisacrylamide monomers, CBA and MBA, to prepare pAPOLs. We synthesized 3 different pAPOLs with different contents of disulfide bond by varying CBA to MBA molar ratio (figure 4.2)[126]. The synthesized pAPOLs have linear polymer structure with various CBA percentages (33, 67, and 100%). Because this addition polymerization is a stepwise process, the disulfide bond ratio can be adjusted by the feeding ratio of CBA and MBA. In the final stage of the reaction, excess amine monomer, APOL, was added to ensure that all potential toxic acrylamide has been consumed. Therefore, the final product polymer only has amino end group.

The polymers' chemical structures and compositions were characterized by ^{1}H NMR spectrometer (400 MHz, Varian). The CBA ratio in the final product can be identified by the peak δ4.45 as shown in figure 4.3. By calculating the integral area of peak δ4.45, we found that the CBA ratio in the final product agrees with the feeding ratio as shown in table 4.1. All pAPOLs final products were isolated in their HCl-salt to obtain a good solubility in aqueous buffer. According to the ^{1}H NMR spectra of these three pAPOLs, the absence of proton signal between 5 to 7ppm indicates no residual acrylamide end group.

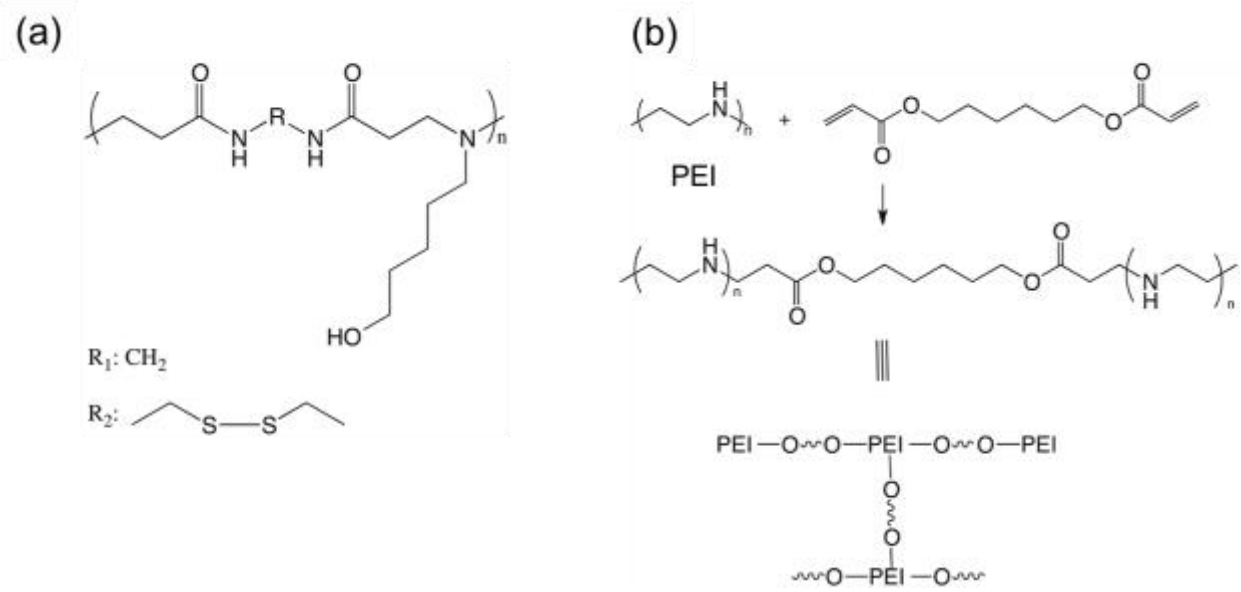

Figure 4.2. Polymer structure. (a) The molecular structure of the random copolymer pAPOL containing APOL monomer and the R group being either R_1 (non-reducible monomer) or R_2 (reducible monomer). (b) Synthesis of degradable PEI (dPEI).

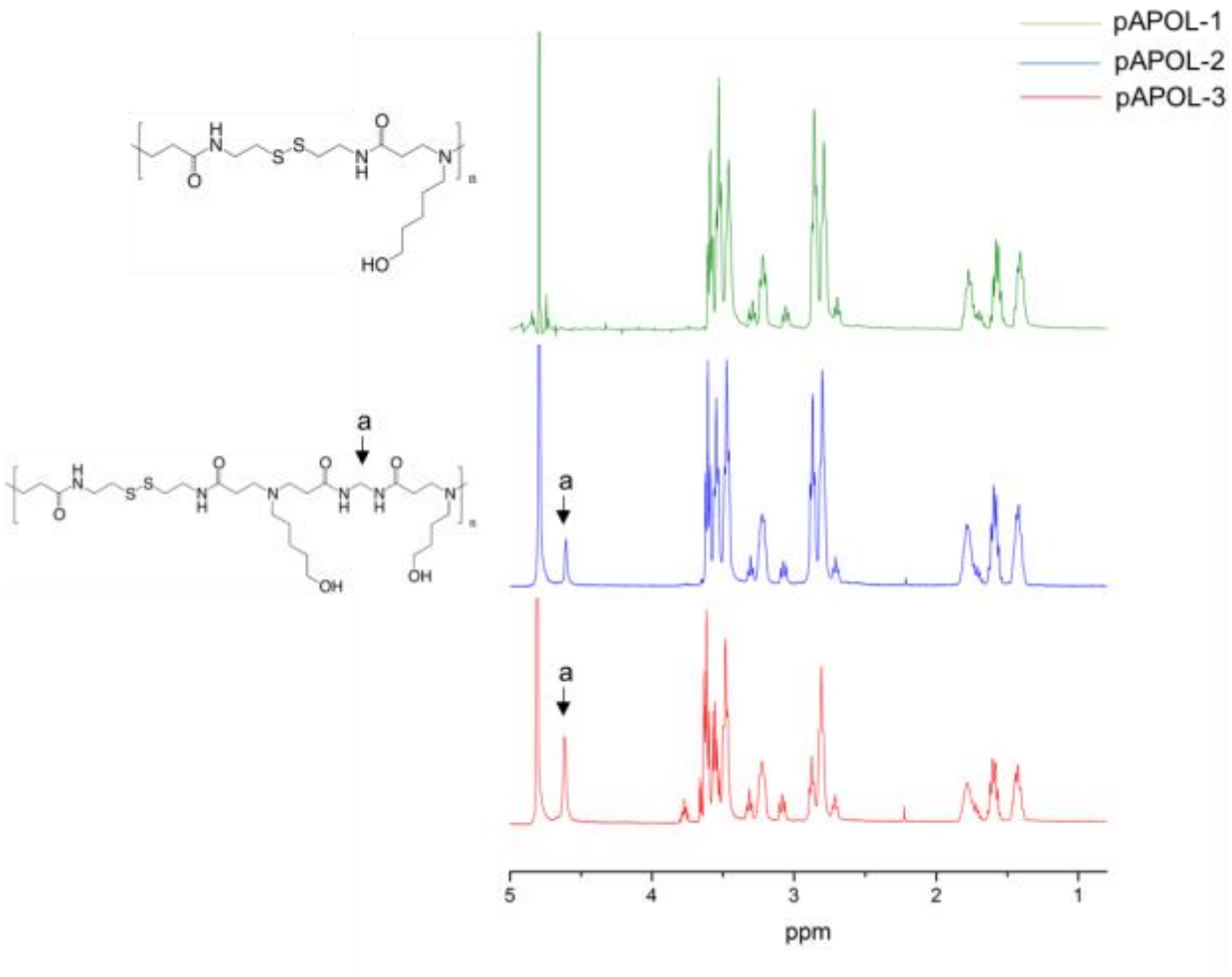

Figure 4.3. ^{1}H NMR spectra of pAPOLs.

We synthesized a biodegradable PEI (dPEI) in order to take advantage of its low cytotoxicity and high transfection efficiency[87, 127]. dPEI was synthesized by reacting branched 800Da PEI with 1,6-hexanediol diacrylate (figure 4.2 b) [128, 129]. The acrylate group reacting with either a primary amine or a secondary amine results in a highly-branched structure. The structural characterization of dPEI is reported in Table 4.1.

The weight-average molecular weight (M_w) of 3 different pAPOLs is in the range from 1,200 to 3,200 with a polydispersity index (M_w/M_n) ranging from 1.0 to 1.5. M_w of dPEI is 3,050 with M_w/M_n of 1.8 (table 4.1). M_w, M_w, and M_w/M_n were determined by size exclusion chromatography (SEC) in 0.3 sodium acetate (pH4.4)/ methanol (70/30, v/v) using Waters

Alliance 2690 Separation Module equipped with Waters Ultrahydrogel (500, 120 Angstrom) column. Poly(ethylene glycol) (PEG; Mp = 21160 to 106 Daltons) used as standard. The structure and polymer weight were characterization by NMR and GPC (table 4.1).

Polycations	R_1:R_2	CBA percentage (mol %)		M_w[a]	PDI[a]	Buffer Capacity[b] (%)
		In feed	In polymer			
pAPOL-1	0:1	100	100	1,420	1.1	82
pAPOL-2	1:2	67	67	3,080	1.6	38
pAPOL-3	2:1	33	33	2,375	1.4	39
dPEI	--	--		3,050	1.8	38
bPEI[c]	--	--		25,000		50

Table 4.1 Synthesized polycations structure and buffer capacity characterization. [a]Weight-average molecular weight(Mw) and PDI determined by SEC, [b]Buffer capacity of polycations between pH 5.1 and 7.4 in 150 mM NaCl, [c]The absolute weight-average molecular weight of branched PEI is 25KDa.

4.3.2. Buffer capacity of pAPOLs

The "proton sponge hypothesis" relates the buffer capacity of the polycations. It can indicate the ability of polyplexes endosomes or lysosomes escape[124, 130]. The "proton sponge effect" allows endosomal escape by creating an osmotic pressure to burst the endosomes. We measured the buffer capacity of our polymers in order to provide better understanding of the relationship between the polymer structure and their gene delivery efficiency[131]. Here, the buffer capacity of a cationic polymer is defined as the percentage of amine groups becoming protonated when the pH changes from 7.4 to 5.1 during acid-base titration (figure 4.4)[123, 124]. For example, the buffer capacity of pAPOL-1 was calculated to be 82% based on the volume used of 0.1 M NaOH solution to bring the pH value of the polymer pAPOL-1 solution from 5.1 to 7.4. The pH range of 7.4 to 5.1 is chosen to correspond to the range from the highest pH in the extracellular

environment to the lowest endosomal pH[106]. Of all the polymers studied, pAPOL-1 with 100% CBA displays the highest buffer capacity, 82%, followed by 25KDa branched PEI (bPEI) with 50% buffer capacity. pAPOL-2, pAPOL-3, and dPEI have the relatively low buffer capacity ranging from 38%-39% (Table 4.1). The titratable amine in polymer is the main factor determining the buffer capacity. The titratable amine in "macropinocytic" endosome can reduce acidification, increase Cl^- accumulation, and increase swelling/lysis that help DNA escape[132]. Primary amines in the polymers are predominately protonated at neutral pH[133]. PEI and pAPOLs both possess higher order amines (secondary and tertiary amine), which give rise to higher buffering capacity in the relevant pH range (pH5.1 to pH7.4)[133, 134]. The appearance of long continues ethylamine exhibits homogeneous protonation distribution over the entire endolysosomal pH range[135]. The appearance of ethylamine in bPEI and dPEI contributes to uniform buffer capacity, which lacks plateaus in pH ~ 7.0 as shown in Figure 4.4. We surmise that the high pAPOL-1 buffering capacity is due to the higher density of secondary amine groups comparing with pAPOL-2 and pAPOL-3[136]. From the molecular weight studied, pAPOL-1 has lowest molecular weight (Table 1), which means it has more end secondary amine groups. The secondary amine groups can contribute to slightly higher buffer capacity compare to tertiary amines due to lower pKa [137]. Therefore, the pAPOL-1 has higher buffer capacity than that of pAPOL-2 and pAPOL-3. The hydrolysis ability of dPEI affects the amine group protonation during acid-base titration, which results in the lower buffer capacity than bPEI. This "proton sponge" property can help polyplex overcome endosome capture barrier. Designing a polymer with high buffer capacity is one of the methods to improve delivery vector transfection efficiency [36, 132, 138].

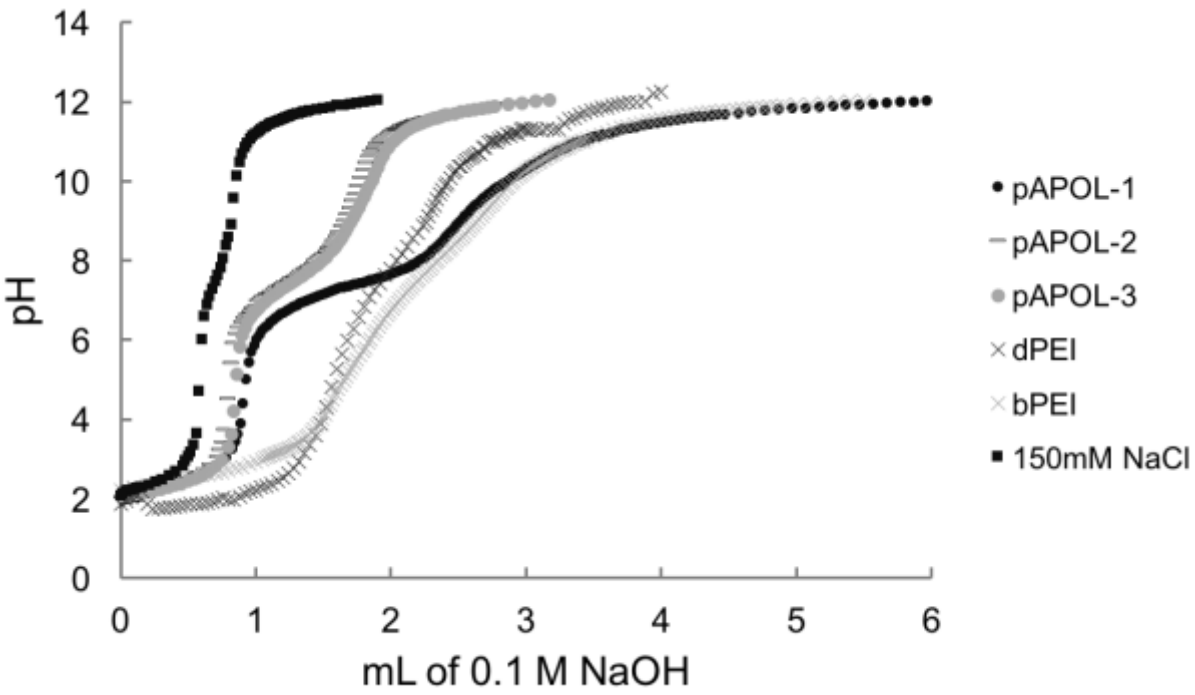

Figure 4.4. Titration curves obtained by titrating polycation solution contain 0.1 mmol protonable amine group (dissolved in 10mL 150mM NaCl aqueous solution; pH 2, adjusted by 1 M HCl) with 0.1 M NaOH.

4.3.3. pAPOLs and DNA polyplex fabrication and characterization

A main factor required for a good cationic polymer gene delivery vector is a good ability to condense DNA in a nanometer scale particle with reasonable positive surface charge. The size of polyplexes is a major factor that influences DNA delivery efficiency[139]. We studied the polyplex size and size distributions using AFM and dynamic light scattering (DLS). The particle size and surface charge of polyplexes made with pAPOLs, dPEI and bPEI in different N/P ratios are reported in Table 4.2. All the data were collected with polyplex samples incubated for 30 min after their initial formation because polyplexes change their assembly structure with time and become stable at 30 min time point[126, 140]. All the polycations studied here can condense DNA to nanometer size particles with positive surface charges. There is a significant reduction in size for pAPOL-1 and pAPOL-2 when the N/P ratio is increased from 8 to 12. However, pAPOL-3/DNA

polyplex cannot form nanoparticle as small as other pAPOLs and PEIs, which means this polymer does not condense DNA fully even at a high N/P ratio of 24/1. Polyplexes formed by dPEI and DNA show small size range from 60—80nm which are quite close to bPEI[141]. This indicates dPEI can condense DNA in a small compact particle. The stability of the polyplexes was studied as a function of polyplex incubation time. The DLS and zeta potential data were collected every 7 min (Figure 4.5). The data indicates that the sizes of pAPOL-1, pAPOL-2, and dPEI polyplexes were stable during the 1h measurement time while pAPOL-3 polyplexes size kept increasing. The variations in the zeta potential data are less significant and they do not appear to correlate with the changes in polyplex size. Generally, the polyplexes made with pAPOL-1 and pAPOL-2 can keep zeta potential higher than 20mV while for pAPOL-3, which cannot make a small size polyplex, the zeta potential is around than 15mV.

Polyplex	N/P ratio	D_H (nm)	Zeta potential (mV)
pAPOL-1/DNA	8/1	126.2	16.9
	12/1	99.1	20.5
	16/1	95.4	24.0
	24/1	95.6	23.1
pAPOL-2/DNA	8/1	122.2	21.9
	12/1	95.8	20.2
	16/1	88.5	22.1
	24/1	82.0	18.4
pAPOL-3/DNA	8/1	293.5	15.2
	12/1	253.6	15.4
	16/1	235.2	16.7
	24/1	389.0	18.5
dPEI/DNA	6/1	86.0	10.2
	12/1	65.8	10.2
	24/1	65.0	11.1
bPEI	6/1	106.1	7.01
	12/1	52.8	18.3
	24/1	78.2	23.9

Table 4.2. Average particle size and zeta potential of polyplex of different type of PAA and PEI at different polycation/DNA (N/P) ratio.

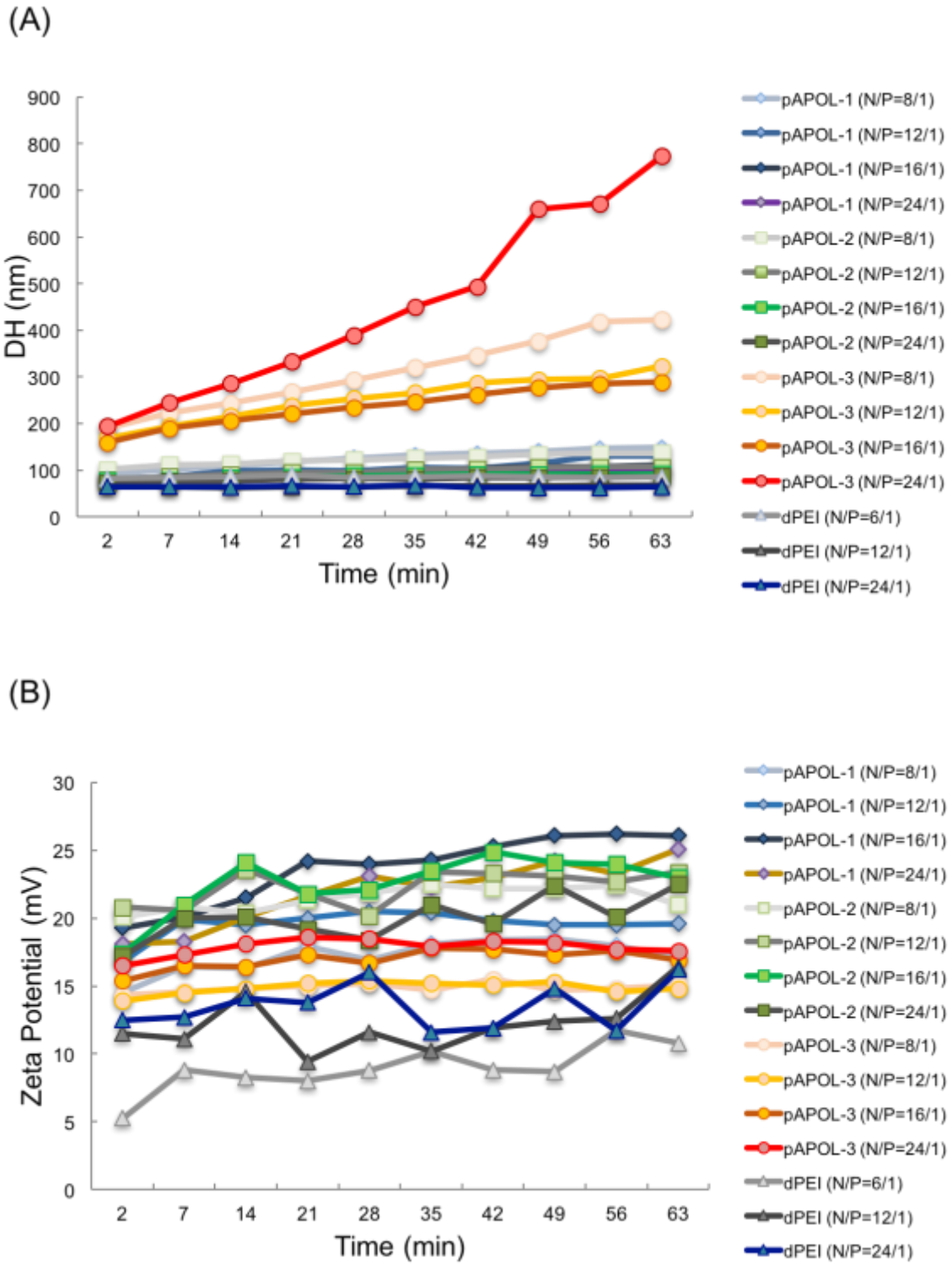

Figure 4.5. Polyplex particle size and zeta potential variation with incubation time measured by the DLS. The data were collected every 7 min for 1 h. (a) Hydrodynamic diameter vs. time. (b) Zeta potential vs. time.

AFM was used to characterize the size and shape of the polyplexes in air condition. pAPOL-1 with N/P ratio of 12 was studied at 15 min and 45 min post formation. Figure 4.6 shows compact rod shape at 15 min and lager spheroid shape at 45 min, which is consistent with our previous observations of poly(amdio amine)s and DNA polyplex showing a strong morphological dependence on incubation time[92]. The 15-minute incubation time yields the polyplex with rod structure in an average size of 164.1 ± 11.9 nm × 82.1 ±11.8 nm. The large percentage of rod shape appears near the beginning of incubation due to the more favorable formation kinetics of rod[142]. In 45 minutes, the shape tends to become spheroid with average diameter 171.9 ± 13.25 nm × 148.4 ±6.8 nm. This comparably larger size particles generation is caused by the partial condensation or polyplex aggregation[92].

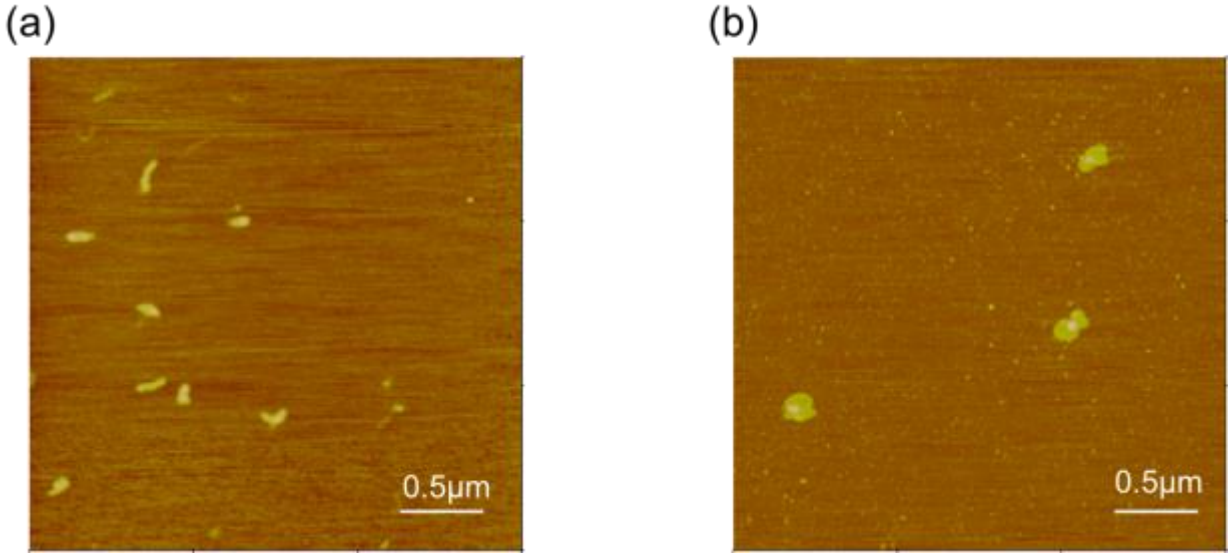

Figure 4.6. AFM height images of pAPOL-1/DNA polyplex (N/P=12/1). (a) Polyplexes incubated for 15 min. Z range: 5 nm. (b) Polyplexes incubated for 45 min. Z range:10 nm. Scan size: 3 μm for both images.

4.3.4. Transfection efficiency of pAPOLs and DNA polyplex in vitro

To evaluate the transfection capability of the pAPOLs, their polyplexes containing pEGFP-N1 plasmid DNA were incubated with HEK 293, MC 3T3, and NIH 3T3 cells. The N/P ratio of

pAPOLs/DNA polyplexes ranging from 12 to 16 were used. Here we did not include the data of N/P = 8/1 and 24/1 due to bare transfection. Poor transfection efficiency of high N/P ratio polyplex is due to excess of unbind polycations[143]. This unbinding chain can react with cell surface and trigger a competition between polyplexes[144]. Polyplex of 25KDa branched bPEI/DNA was used as control. The transfection efficiency was determined after adding polyplex into cell culture medium 24 hours by flow cytometry. Figure 4.7(a) shows the percentage of the transfected cells and figure 4.7(b) shows the relative MFI results. Both types of data can indicate the transfection efficiency. And they are almost in the same trend. pAPOL-1 has the highest transfection efficiency in all three cell lines among the pAPOLs studied. Except for pAPOL-1 and pAPOL-2 at N/P = 16, other pAPOLs polyplexes studied show little to no transfection. pAPOL-2 shows some degree of transfection but their activities are much less than pAPOL-1. pAPOL-3 shows no transfection and its data are not included. The positive control bPEI shows the highest transfection efficiency for HEK 293 cells. However, its transfection is lower than pAPOL-1for MC 3T3 and NIH 3T3. The gene expression is significantly higher for pAPOL-1 than that of bPEI in the case of the MC 3T3 cell type. dPEI at N/P = 12 shows some degree of transfection in HEK 293 but little in other cell lines.

Polycations' cytotoxicity exerts a negative impact on their transfection. Cell viability data obtained by MTT assay as reported in Figure 4.7(c). The control group consists of cells attaching and proliferating on the culture plate without polyplexes. A general observation is that HEK 293 cell line and NIH 3T3 cell line are less affected by the pAPOL polyplexes compared with the MC 3T3 cell line. Of all the pAPOLs studied, pAPOL-1 polyplexes show the lowest cytotoxicity to the three type of cells. The viability of dPEI group are still lower than that of pAPOL-1 at N/P = 12, but the dPEI data are better than 25KDa bPEI/DNA data which agrees with the reported results[145].

Forrest et al also demonstrated dPEI can improve cell metabolic activity comparing with 25KDa bPEI[141].

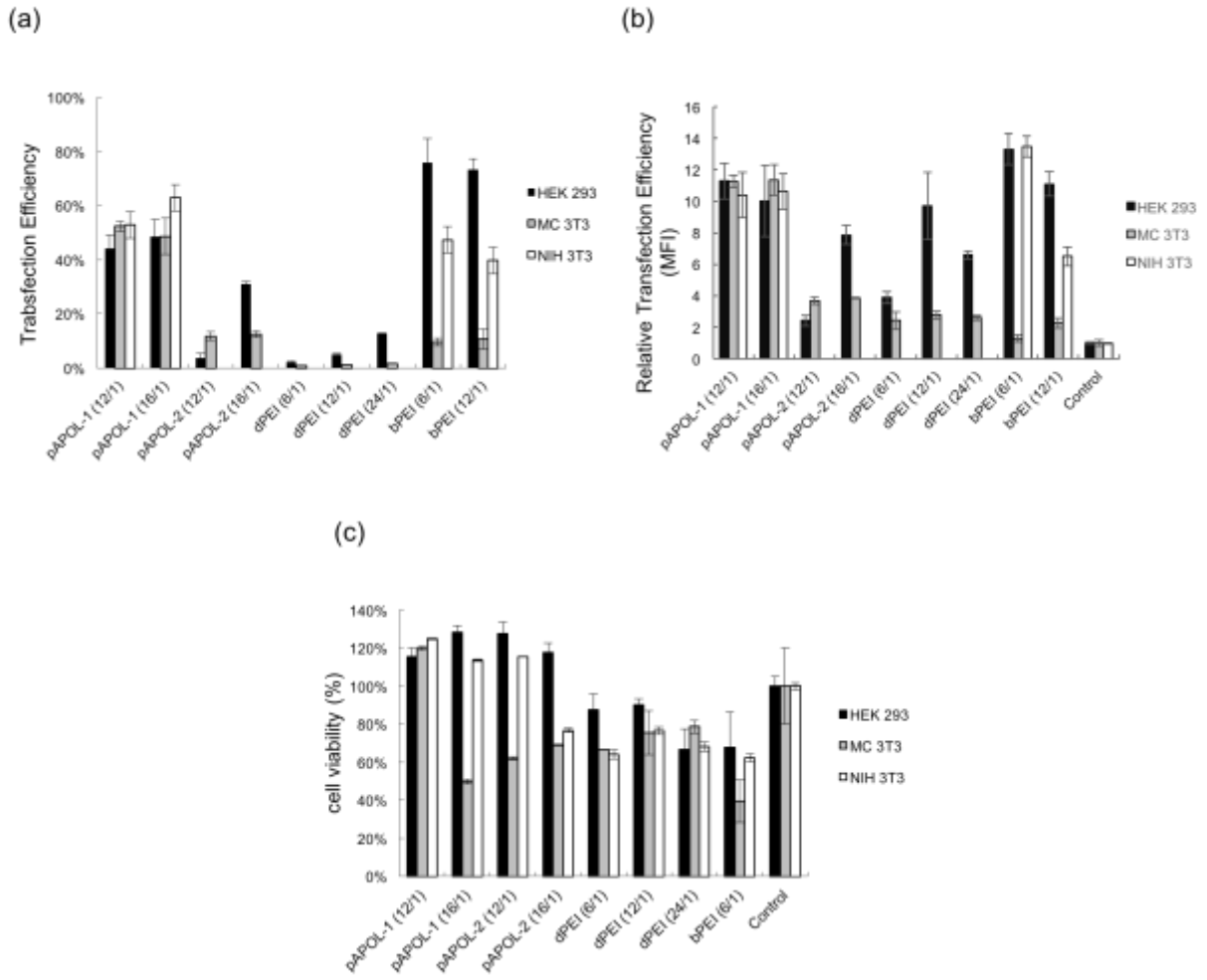

Figure 4.7. Cell transfection efficiency and cell viability. (a) Proportion of transfected cells, (b)relative MFI of transfection efficiency, (c) and corresponding cell viabilities of polyplexes of pAPOLs and PEIs in HEK293, MC 3T3, and NIH 3T3 cells as a function of different N/P ratios. Transfection efficiency was determined by flow cytometer. Cell viability was examined by MTT assay. Cultured cells without any treatment were used as control. The data were expressed as mean values (standard deviations) of three experiments.

4.4. Discussion

In this chapter, we synthesized the pAPOLs by monomer APOL, CBA, and MBA. Monomer APOL instead of the monomer AEPZ improved transfection efficiency comparing with

PAAs. By treated HEK 293 cells with PAA-1, pAPOL-1, and bPEI polyplex, we found that the number of transfected green cells has largely improved by pAPOL-1/DNA polyplex comparing with PAA-1/DNA polyplex. One of the reasons is the appearance of pendant group--hydroxalkyl group improved buffer capacity[146] resulting in improved transfection efficiency. In general, the basicity and polarity of the pendant groups in polymer structure are relevant to gene delivery transfection efficiency.

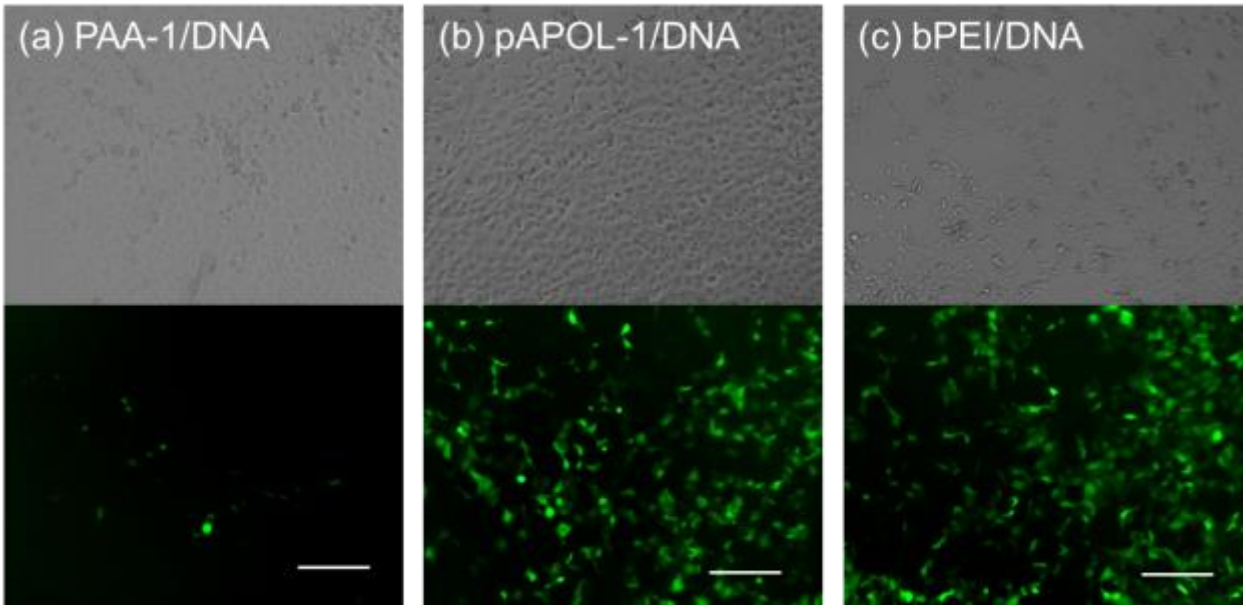

Figure 4.8. Bright field and green fluorescence image for transfected HEK 293 cell by adding polymer/DNA polyplexes. (a) PAA-1/DNA polyplex with N/P=12/1, (b) pAPOL-1/DNA polyplex with N/P=12/1, (C) bPEI/DNA polyplex with N/P=6/1. Scale bar=200μm.

Comparing the buffer capacity of pAPOLs with bPEI, pAPOL-1 has much better buffer capacity, but bPEI/DNA polyplex still shows great transfection efficiency in HEK 293 and MT3T3 cells *in vitro*. This is because bPEI can cause early endosome membrane fragment micellization by locally induced membrane curvature stress and induce pore formation in membrane. Then the osmotic pressure build-up contributes a force finally make endosome bursting[147]. But the toxicity of bPEI/DNA is much higher than pAPOL-1/DNA. This is because the bPEI alters mitochondrial function and triggers apoptosis[147]. Some researcher also mentioned that the PEI-mediated

delivery process damaged organelles, such as lysosome, endoplasmic reticulum, and Golgi and caused apoptosis[148, 149].

Generally, the polyplex made by pAPOL-1 and DNA in N/P ratio 12/1 has the best transfection efficiency and cell viability. We concluded the following reasons: first, comparing with these three types of pAPOLs, pAPOL-1 has the best buffer capacity, which indicates that pAPOL-1has great endosome or lysosome escape capability. Second, from the DLS analysis, we found pAPOL-1/DNA polyplex can keep stable in a small size diameter ~100nm. Comparing the D_H of this pAPOL-1/DNA polyplex (N/P=12/1) with dPEI/DNA (N/P=6/1), as shown in figure 4.9, pAPOL-1/DNA polyplex has a similar size variation trend comparing with bPEI/DNA polyplex during 1 hour incubation. Third, zeta potential of pAPOL-1/DNA polyplex also can keep stable at ~20 mV with small fluctuation. The stability and enough surface charge of pAPOL-1/DNA contribute to the transfection efficiency.

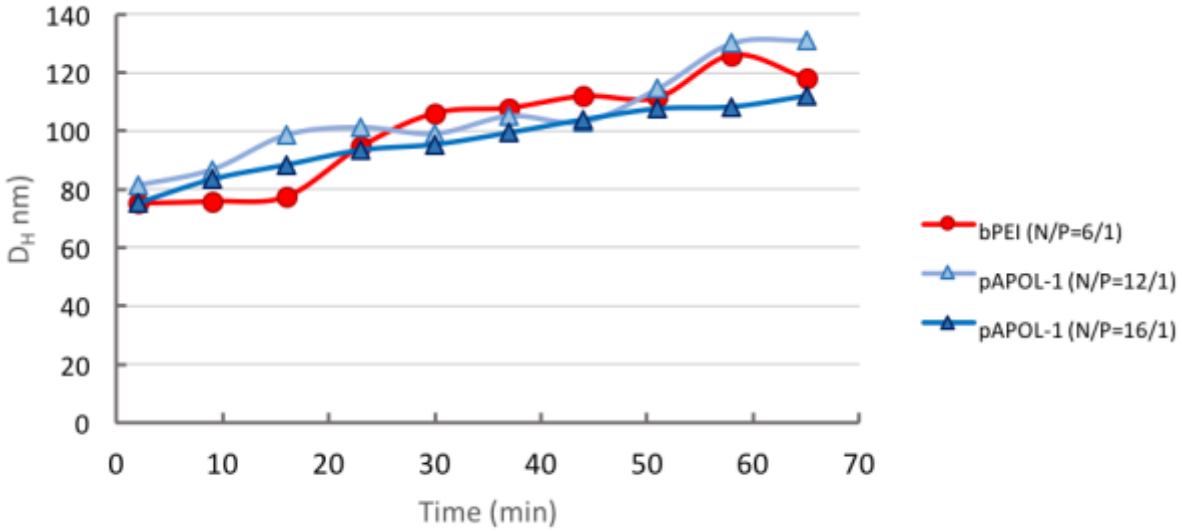

Figure 4.9. Polyplex particle Hydrodynamic diameter variation as a function of incubation time measured by DLS. The data were collected every 7 min and continued 1 hour.

The biggest barrier for obtaining successful and high transfection efficiency is to figure out the relationship between the amount of internalized DNA by cell nucleus and the level of transgene

expression after polyplex uptake[144, 150, 151]. That explained why the high buffer capacity pAPOL-1 and bPEI shows better transfection efficiency during *in vitro* study. On the other hand, the "unpacking" ability of polyplex in cell body also influences the gene expression efficiency. The excessively stable polyplex cannot release DNA efficiently due to the slow unpacking kinetics and therefore would prevent the gene expression[144]. The introduction of disulfide bond accelerates the polyplex disassembly in cell body because of the appearance of redox molecules and protein thiols in intracellular environment. The pAPOL-1 has highest disulfide bond density which equals to the highest degradation rate among pAPOLs[88]. Previous publication described a kind of poly(amdio amine) without disulfide bond displaying bare transfection efficiency in high N/P ratio polyplex[88]. In conclusion, pAPOL-1 polymer has high buffer capacity and high disulfide bond density which makes pAPOL-1 a great gene delivery vector.

One of the main reasons for low transfection efficiency of hydrolysable dPEI/DNA polyplex may relate to its low buffer capacity, only 38% as shown in table 4.1. We assumed this dPEI polymer lacks ability to escape from endosome or lysosome capture. The polyplex size of dPEI/DNA can keep stable in small size under 100nm similar to that of bPEI/DNA polyplex. But the zeta potential is lower than that of dPEI and most pAPOLs polyplexes. The lower surface charge and poor degradable property may reduce its cytotoxicity and result in relatively high cell viability in figure 4.7.

4.5. Conclusions

This chapter describes synthesis of a new type of poly(amido amine)s—pAPOLs. This new pAPOLs carries hydroxalkyl side group in polymer chain, which largely improved the polymer buffer capacity. pAPOL-1 has great buffer capacity even much higher than 25kDa bPEI. The DLS results show pAPOL-1, with highest disulfide contents, can form small polyplex less than 100nm

when the N/P ratio is higher than 8/1. Meanwhile, this polyplex can keep stable in HEPES buffer with enough positive charge. All these properties make great contribution to its high transfection efficiency. The bioreducible ability of pAPOL-1 also brings great biocompatibility. After the polymer screening, pAPOL-1 can be selected for preparing the next generation LbL film with improved transfection efficiency. Though the dPEI studied in this chapter has low transfection efficiency, its cytotoxicity has been decreased comparing with bPEI. It may still have potential to replace bPEI barrier layer during building more biocompatible LbL film. This chapter throws light upon polymer screening to find a high transfection efficiency and low cytotoxicity polymer candidate for next generation LbL film fabrication.

CHAPTER 5 IMPROVE TRANSFECTION EFFICIENCY OF BIOREDUCIBLE LAYER-BY-LAYER FILMS FOR SEQUENTIAL AND SUSTAIN GENE DELIVERY

5.1.Introduction

LbL film acts as gene or drug delivery vector which can carry different types of biomolecules and achieve localized delivery[152]. It also can easily coat on various medical devices surface such as stent, suture, porous Ti, and microneedles[13, 80, 153, 154]. And the most attractive feature is the controllable releasing property, such as the dosage and time control[14]. Since it is a localized delivery system, it can avoid the degradation and inactivation during physiological circulation before arriving the targeting cell or tissue. On the other hand, thanks to the layer structure, the loading dosage and spatial distribution of biomolecules can be easily adjusted during the LbL film assembly.

Our research goal for LbL film gene delivery study is to achieve high transfection efficiency, biocompatibility, sustained and sequential DNA releasing. In chapter 3, we analyzed the film disassemble property and found the DNA releasing mechanism is closely related to the LbL film interior structure. Biodegradable LbL film, fabricated with high diffusion coefficient polymers, has interlayer diffusion which can cause bulk and fast degradation. If the interlayer diffusion can be prevented by certain method, such as inserting high charge density and nondegradable layer, the film disassemble process could be converted into surface erosion. The size of released particle is decreased to nanometer range during the whole releasing period. Though we already successfully achieved sustained and sequential releasing property from type B film in chapter 3, the transfection efficiency is still a big problem in this LbL film. In chapter 4, we synthesized novel poly(amdio amine)s—pAPOLs and biodegradable dPEI. These high transfection efficiency and low toxicity polymers can be applied in LbL film to replace PAAs and bPEI to improve transfection efficiency and biocompatibility.

This chapter focuses on LbL film fabricated with pAPOLs and dPEI. We continue to use the dip coating method to assemble LbL film and characterize it via *in vitro* cell study. Furthermore, we incorporated therapeutic gene, Human bone morphogenetic protein 2 (BMP-2) plasmid DNA, into our LbL film and applied this film in osteoblast precursor cell line, MC3T3-E1, to promote the cell differentiation. The osteogenic potential of bone marrow stromal cells has been demonstrated by transplantation and *in vitro* culture systems[155, 156]. BMPs which are composed of at least 15 proteins, play significant roles in bone formation[157-159]. In osteoblastic MC3T3-El cell line, BMP-2 has been demonstrated to be one of the most potent stimulators to enhance ALPase activity, which can indicate the differentiation level of MC3T3-E1cells[160]. Through the therapeutic gene, BMP-2, incorporation, we want to find the potential application of our LbL films in bone regeneration.

5.2. Experimental methods

5.2.1. Materials

N,N'-Methylenebis(acrylamide) (MBA, 99%), dithiothreitol (DTT, 99%), branched poly(ethylenimine) (bPEI, Mw~25,000Da, ≤1% water), branched poly(ethylenimine) (bPEI, Mw~800Da), poly(2-hydroxyethyl methacrylate) (polyHEMA, BioReagent grade) , 1,6-hexanediol diacrylate (80%), 5-amino-1-pentanol (APOL, 95%), bovine serum albumin (BSA, heat shock fraction, pH 7, ≥98%) and fibronectin from human plasmid (0.1%) were purchased from Sigma-Aldrich. N,N'-Cystaminebisacrylamide, (CBA, 98%, Electro Pure™) was purchased from Polysciences, Inc. Sodilum chloride (NaCl, BioReagent) and sodium hydroxide (NaOH, BioReagent) were purchased from Fisher Scientific. Sodium acetate anhydrous (NaOAc, 99%) was purchased from Mallinckrodt Chemicals. Penicillin-streptomycin (10,000 U/mL), Minimum Essential Medium α, no nucleosides (MEM α, nucleosides), Dulbecco's Modified Eagle Medium

(DMEM), phosphate buffered saline, sterilized (PBS, pH 7.4), fetal bovine serum (FBS, qualified, Gibo™),), Vybrant® MTT cell proliferation assay kit, SYBR® Safe DNA gel stain (10,000× concentrate in DMSO), and 4-(2-hydroxyethyl)-1-piperazineethanesulfonic acid (HEPES, 1M) were purchased from Thermo Fisher Scientific, Inc. Alkaline phosphatase (ALP) kit was purchased from BioVision (San Francisco, CA, USA).

Glass slides of 15 mm in diameter as for LbL film substrate are same as chapter 3. The pre-treated method also same as chapter 3.

Green fluorescence protein (GFP) reporter plasmid (pEGFP-N1 from Clontech, 4700 bp) and E2-Crimson reporter plasmid (pEF.myc.ER-E2-Crimson from Benjamin Glick, 6263 bp) were prepared followed the methodology in chapter 3. Human bone morphogenetic protein 2 (BMP2) plasmid DNA (BMP2-pDNA) Glycerol Stock were purchased form Origene Technologies Inc. Plasmid preparation and purification method is same as the GFP-pDNA preparation by Qiagen plasmid Giga kit (Qiagen, Valencia, CA).

5.2.2. Deposition of the LbL film

The LbL films deposition were performance under programmable Carl Zeiss HMS50 slide stainer with a homemade substrate holder. This dip coating method is same as the method mentioned in chapter 3 following our previous work[161]. The substrate was immersed in polycation solution and DNA solution 10 minutes and followed by DI-water rinse, 5 minutes. The polycation and DNA deposition process was repeated to construct the desired number of layers. Polycation and DNA solution refreshed in every 8 circle to minimize the contamination and concentration variation.

5.2.3. AFM imaging

AFM imaging was conducted by tapping mode in air, tapping mode in liquid, and contact mode in liquid by VEECO Dimension 3100 AFM. When tapping mode was used in air to measure the film thickness, the AFM probe used was a silicon probe tap300-G (Budget Sensors) with a factory-specified resonant frequency of 300 kHz and a spring constant of 40 N/m. In order to measure the LbL film thickness, the film was scratched with a razor blade to expose a part of the glass substrate. Film thickness was determined by the step height between the substrate and the film surface using the sectional height analysis under Nanoscope software (version 5.12, VEECO). The film thickness was measured at least in 5 different spot to get average data.

AFM *in situ real-time* imaging were performance in contact mode in liquid environment. LbL films was degradation process was monitored under the *real-time* imaging in 100 µL DTT (10 mM DTT in PBS buffer, pH 7.4) at room temperature. The probe used is non-conductive silicon nitride probe NP-20 (VEECO) with 20 nm nominal radius and 0.32N/m nominal cantilever spring constant. AFM image scanning was start immediately after 100 µL DTT solution injected between AFM probe and film surface. The image scanning continued at an average rate of 1Hz for 6 hours[14].

Polyplex and released particle morphology study was done by AFM contact in liquid mode and tapping in air mode. In a typical sample preparation, a droplet of 50 µL polyplex solution or LbL degradation solution were placed on the ~1×1 cm^2 freshly cleaved surface of mica. After 5 min deposition, excess solution was removed from mica surface. Then the sample were rinsed 3 times by deionized water. The imaging method and analytical method of the released particle were conducted in the same method as mentioned in chapter 4 for polyplex sample.

5.2.4. Fluorescence spectroscopy

The amount of DNA released from the LbL films was determined by fluorescence microplate reader. The LbL films were immersed into 40 mM DTT solution (PH 7.4) in room temperature. After 2 weeks' degradation, the LbL films were fully degraded, the degradation solution was concentrated to 250 μL. The contacted solution was labeled with 10,000×SYBR® safe DNA stain (Invitrogen). In a typical experiment, SYBR® safe DNA stain was first diluted in TAE buffer. Then 100 μL of this diluted SYBR® safe DNA stain was added into 250 μL concentrated degradation solution. Then 150 μL labeled sample was pipetted into 96-well plates. Prepared plasmid DNA solution with known concentration 0, 5, 10, 15, 20, 25, 30, 35, and 40 μL/mL by the same procedure acting as standard curve. The standard curve shows a linear variation as a function of DNA concentration. The fitting equation was used to determine the DNA amount in the degradation solution.

5.2.5. Dynamic light scattering (DLS)

The size of LbL film released particle was monitored and analyzed by dynamic light scattering from Malvern Instrument, Inc (Nanosizer ZS). In order to monitor the size of the particles released from the LbL films during reductive degradation in 10 mM DTT in PBS buffer (pH 7.4), the glass slide coated with the LbL films was cut into small pieces, about 5 mm in diameter, to fit the ZEN0040 microcuvette (Malvern Instrument). We use 3D printing technology produced a nylon microcuvette insert to hold the LbL film in the top portion of the microcuvette. The microcuvette was filled with the 10 mM DTT solution till full submerging the LbL films. The size measurement start immediately after film been submerged. The measurement of the released products hydrodynamic diameter (D_H) won't stopped until whole experiment finished. Film degradation is under 25 ºC. Data were collected every 15 min in the first 24 h and every 30 min

start form day 2. The DTT solution was refreshed every 24 h. The film degradation was continuously monitored for 14 days.

5.2.6. In vitro cell transfection

Human embryonic kidney cells, HEK 293, were purchased from American Type Culture Collection (ATCC). NIH 3T3 (organism: mouse musculus) was provided by Dr. Wei-Zen Wei's lab, Barbara Ann Karmanos Cancer Institute, Wayne State University. Osteoblast precursor MC 3T3 cell line (from mouse calvaria) was provided by Dr. Weiping Ren's lab, Department of Biomedical Engineering, College of Engineering, Wayne State University. HEK 293 cell line and NIH 3T3 cell line were cultured and maintained in Dulbecco's Modified Eagle's Medium (DMEM), which with 10% fetal bovine serum (FBS), 1% penicillin-streptomycin under 37°C, 5% CO_2 in humidified incubator. MC 3T3 cell cultured and maintained in Minimum Essential Medium α medium (MEM α) with 10% fetal bovine serum (FBS) and 1% penicillin-streptomycin under 37°C, 5% CO_2 in humidified incubator. All the culture medium was replaced every 2 days during regular cell maintenance.

In order to limit nonspecific cell attachments on the culture plates, they were coated with poly-HEMA. To apply the Poly-HEMA coating, 100 mg Poly-HEMA powder was dissolved in 5 mL ethanol and water mixture (v/v=95:1) by heating while stirring at 40°C. The 100 µL well-dissolved and filtered poly-HEMA solution were added in each well of culture plate. The plate will keep in sterile conditions and dried overnight.

Transfection experiments on the LbL films were performed with HEK 293 and MC 3T3 cell lines using plasmid pEGFP-N1 and pEF.myc.ER-E2-Crimson as the reporter genes. LbL films deposited on 15 mm diameter glass coverslips were placed at the bottom of 24-well polyHEMA-coated plates. The LbL films were sterilized under UV light for 1.5 h before use. 40 µL Fibronectin

was added on the top of each film and let dry in sterilized environment for 2 h. Then, 1.5×10^4 cells were seeded on LbL film surface with DMEM culture medium or MEM α medium. Cells were grown in humidified incubator (37°C, 5% CO_2). The culture medium was refreshed every 2 days. Cell attachment and proliferation were imaged daily with inverted microscopy. The fluorescence microscopy was used to image the fluorescence protein expression in every two days.

5.2.7. Cell differentiation

MC 3T3 cell differentiation after treated with BMP2-pDNA was characterized with an alkaline phosphatase (ALP) kit (Bio Vision, San Francisco, CA, USA). 24 hours later after cell treated with polyplex, change the culture medium to differentiation medium and culture cells for 14 days. The differentiation medium is the regular MEM α medium which containing b-glycerophosphate (10mM) and L-ascorbic acid (50 μg/mL). Then the cell grown on each culture plate well were lysed by mixing with 250 μL ALP buffer overnight at 4 ºC. The ALP activity in the cell lysate was measured utilizing the conversion of a colorless p-nitrophenyl phosphate to a colored p-nitrophenol. The absorbance was then measured with a microplate reader at 405 nm. We converted the OD value to protein concentration based on a standard curve to report the final ALP activity.

5.3. Results

5.3.1. pAPOLs/DNA LbL film Assembly

The polycation screening in chapter 4 is based on polyplexes experiment has identified pAPOL-1 to be a suitable polycation with low cytotoxicity and high transfection efficiency for the subsequent LbL film study. Following our previous work[14, 82, 93, 162], we prepared 16.5 bi-layers of LbL films containing pAPOL-1 and DNA. In addition, bPEI or dPEI was inserted periodically to act as a barrier against interlayer diffusion (LbL Film 1 in figure 5.1). The LbL film assembly

was performed using an automated slide stainer[161]. A second type of LbL films was made by replacing bPEI with the less toxic dPEI [87] (LbL Film 2 in figure 5.1) in order to further decrease the cytotoxicity of the film to cells.

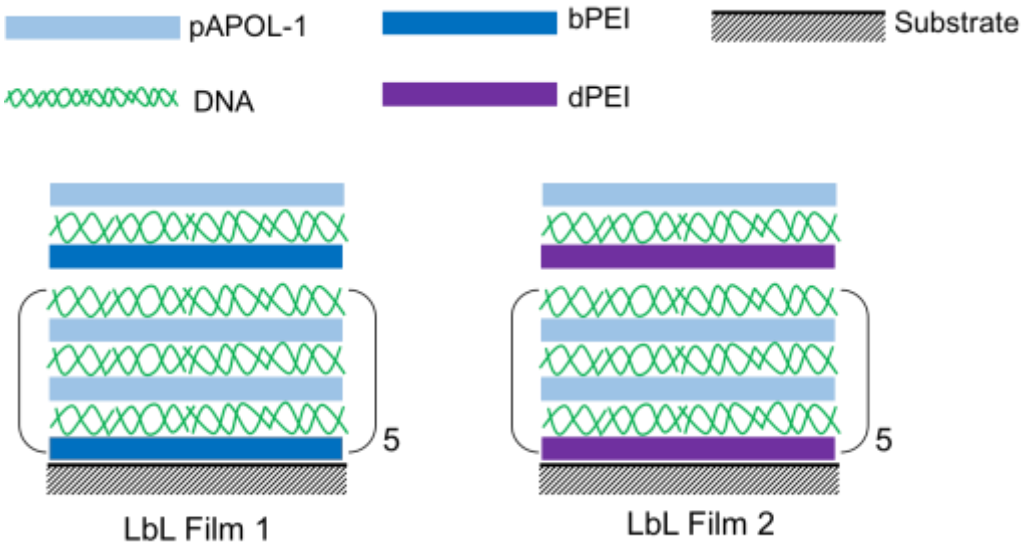

Figure 5.1. Layer composition of LbL film 1 and LbL film 2 made by pAPOL-1, DNA, bPEI, and dPEI.

In order to follow the film deposition process, we employed AFM to measure the film thickness (tapping mode, in air) as a function of the deposited bi-layer number. The LbL film thickness was measured by scratching away a part of the film to expose the substrate and measuring the height difference between the film and the exposed substrate [161]. Figure 5.2 shows the film growth feature for LbL Film 1 (Figure 5.2 a) and LbL Film 2 (Figure 5.2 b). Figure 5.2 c-d show a part of the film being removed to expose the substrate imaged in PBS buffer. The two types of LbL films do not display significant difference in film morphology. LbL Film 1 thickness growth pattern fit the linear fitting line with coefficient of determination R^2 is 0.9924 which very close to 1 (Figure 5.2 (a)). This linear likeness growing behavior indicates a film with well—defined layered structure without significant interlayer diffusion[97-99]. The total thickness for LbL Film 1 is 77.5 ± 1.9 nm and the average single polycation/DNA bi-layer thickness is 4.6 nm. The film

total thickness for LbL Film 2 is 70.1 ± 3.0 nm and the average single bi-layer thickness is 4.2 nm. The film thickness growth trend fit the linear growth curve with R^2=0.9865. Though the fitting is not as perfect as LbL film 1, it still close to the linear increasing behavior. This non-exponential thickness increasing pattern means the dPEI also can screen the residue charge in the film as barrier layer to maintain film with layer structure. The comparing more linear close growing of LbL film 1 depends the high molecular weight of bPEI comparing with dPEI[163, 164]. When immersed in the PBS buffer, the film swells significantly to 103.7 ± 3.9 nm for Film 1 (Figure 5.2 c) and 111.8 ± 2.9 nm for Film 2 (Figure 5.2 d).

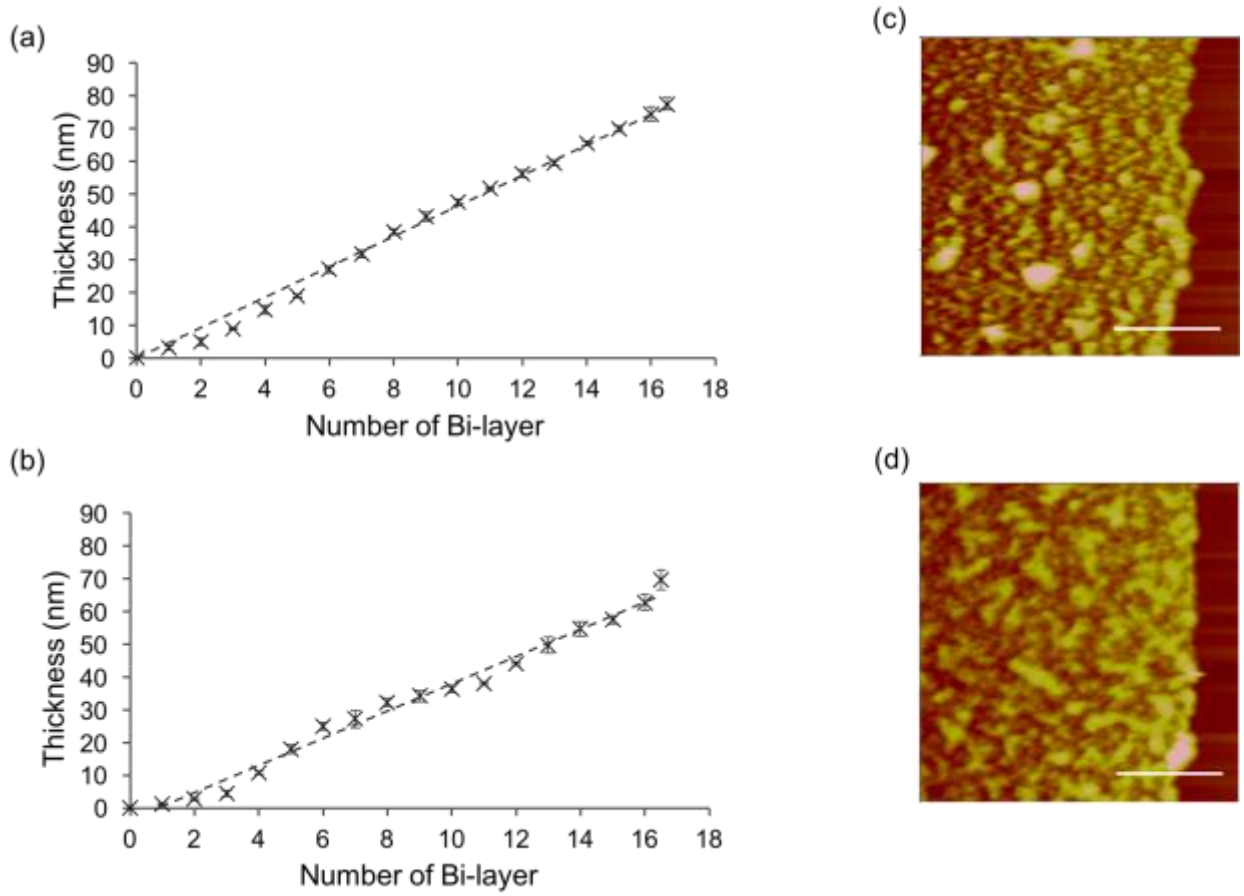

Figure 5.2. LbL film 1 (a) and LbL film 2 (b) thickness growing curve as the function of deposited bi-layer numbers measured by AFM. AFM image of LbL film 1 (c) and LbL film 2 (d) surface morphology captured in PBS buffer contact mode. Z range: 400nm, scale bar: 5 μm.

5.3.2. pAPOLs/DNA LbL film Disassembly

We studied LbL film degradation kinetics in 10 mM DTT solution using AFM, fluorescence spectroscopy, and DLS.

For the AFM study, the films immersed in reductive 10mM DTT solution were periodically taken out and imaged by AFM in air. Figure 5.3 (a) contains the AFM images captured during LbL Film 1 degradation. The film (dry) thickness and surface roughness variation with degradation time are plotted in Figure 5.3 (b) and Figure 5.3 (c), respectively. At t = 0 the film thickness is around 80 nm and the root mean square (RMS) roughness is around 15 nm, and both decreased in values during the degradation period monitored up to 225 h. The film thickness decreased more rapidly during the first 24 h indicating an initial burst release behavior and then decreased more slowly toward the limiting film thickness of 9.7±0.4 nm at 225 h. The initial film roughness is 15.1±0.6 nm, increased slightly to 19 nm in the first 4 h, and followed by a gradual decrease to ~ 15 nm at 50 h and ~ 10 nm until the end of the observation period. The initial roughness increase is due to many particles being released from the LbL film during this initial period. We did not observe micrometer size film pieces missing from the film, which is an indication that the insertion of bPEI is effective in preventing bulk degradation of the film. The Film 2 disassemble process use the AFM study method same as LbL film 1. During 8 days' degradation study, the LbL 2 film thickness gradually decreased to 10.3±0.4 nm (in air) without obvious micrometer size film pieces peel off from film surface.

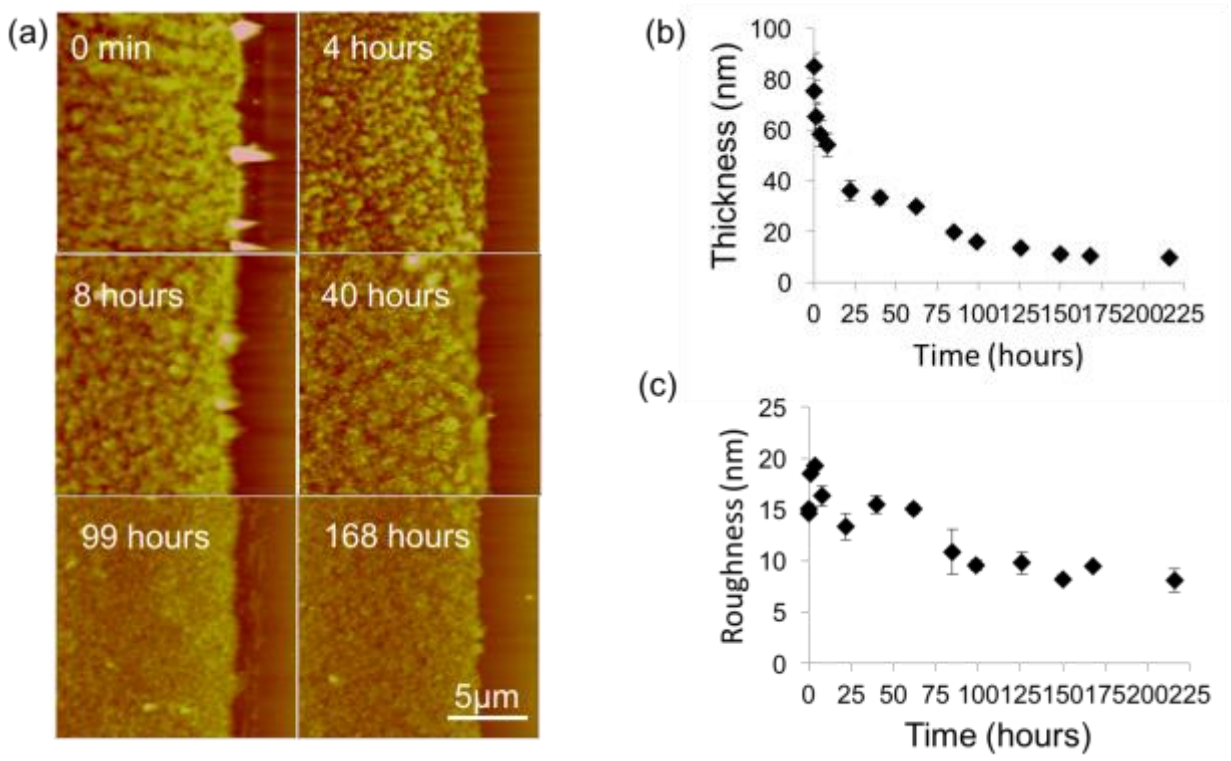

Figure 5.3. (a)Time-lapse AFM height images capture the changes in film thickness and morphology of LbL film 1 treated by 10 mM DTT. Scan size: 15μm, Z-range: 250nm. (b)thickness change and (c) RMS roughness change as function of time in 10mM DTT solution measured by AFM.

Film degradation was also studied using real-time AFM imaging in DTT solution. We monitored Film 2 disassembly in 10 mM DTT solution for 6 h in order to capture the initial disassembly process in real time. We focused our imaging on an area where part of the film was removed prior to the real-time experiment, by a razor blade, in order to monitor the film thickness change during film degradation in DTT solution. The starting film thickness is 104 ± 4 nm with surface roughness of 33.9 nm measured in PBS solution (Figure 5.2 d). The LbL film thickness is reduced much more rapidly in the first 150 min, by about 50%. After 150 min, the film degradation rate starts to slow down (figure 5.4). After 8 days of degradation, the thickness of Film 2 in PBS is 30±11 nm. Figure 5.4 a Shows the film surface morphological change in the reducing

environment. We did not observe micrometer patches in the film, again indicating sequential release of DNA.

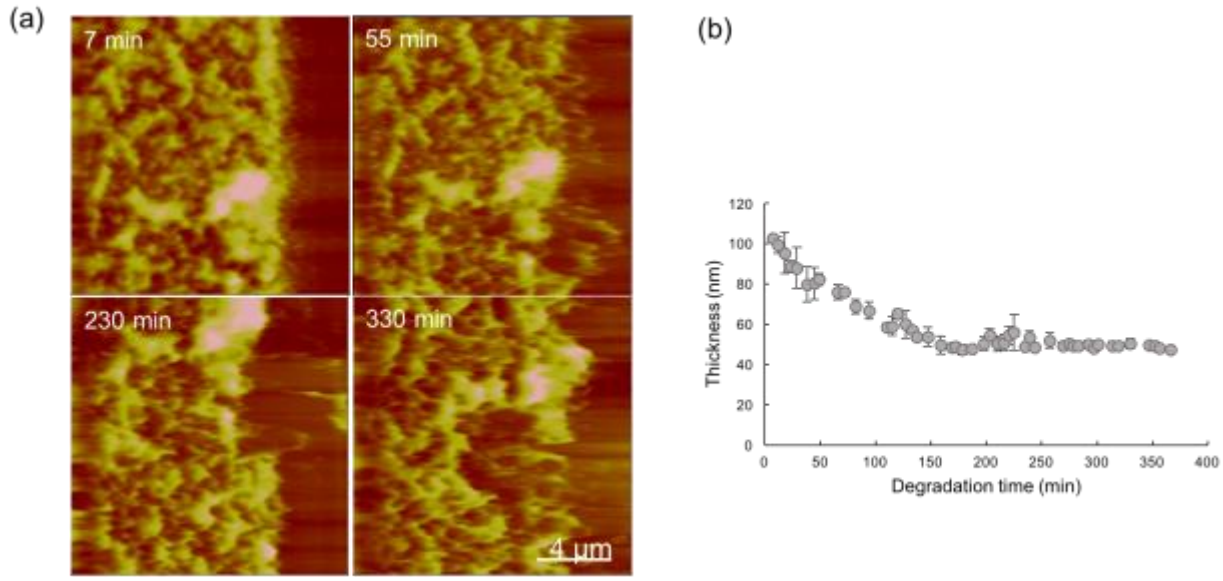

Figure 5.4. (a)Time-lapse height images obtained by real-time AFM capturing the changes in film thickness and morphology of LbL film-2 in 10 mM DTT. Images captured under contact mode in liquid. The scan size: 20 µm. The Z-range: 450 nm. Scale bar is 4 µm. (b) LbL film-2 thickness change as function of degradation time.

DNA delivery efficiency is also impacted by the particle morphology released from the LbL films upon the reductive degradation. Therefore we characterized the particles released from the LbL films by DLS. The hydrodynamic diameter (D_H) of the particles collected in the incubation solution during LbL film degradation was continuously monitored as a function of degradation time. We averaged the D_H values in one 24 h period and reported the averages every 24 h as a function of the film reducing time as shown in Figure 5.5(a). LbL Film 1 which containing bPEI releases particles with a D_H size range of 200-400 nm (PDI less than 0.5) throughout the observation period of 360 h. Note: the large error bar in the first 24 h is due to the high concentration of particles released during this period, which led to a significant degree of particle

aggregation (Figure 5.6). LbL Film 2 containing dPEI releases larger particles in the range of 350-600 nm (PDI less than 0.5). After 9 days, the number of particles released from LbL Film 2 was insufficient for DLS detection. AFM thickness analysis also shows that Film 2 is fully degraded after 9 days with the remaining 8.9% of the film accounted for by the irreversibly adsorbed anchoring layer. To study the particle morphology, the released particles were collected, deposited on mica, and imaged by AFM tapping mode in PBS buffer (Figure 5.5 b-c): figure b1 shows the particle released at 6 h from LbL Film 1 (256 nm ± 48 nm × 210 ± 49nm), figure b2 is the released particle at 6 days from LbL Film 1 (230nm ± 68nm × 202 ± 42nm), figure c1 is the particle released at 6 h from LbL Film 2 (248 nm ± 30 nm × 207 ± 10nm), and figure c2 shows the paticle released at 6 days from LbL Film 2 (363 nm ± 66nm × 428 ± 73nm). Further analysis by AFM of the released particle volume in air shows that most particles are 2-5□104nm3 in particle volume, which corresponds to 2-3 plasmid DNA molecules per particle (Figure 9). Particles released in the first 6 h are in rod or spheroid shape with a volume of 2-3 × $10^4$$nm^3$ (Figure 5.7). Particles collected on day 7 (Figure 9 c) have similar morphology as those collected at 6 h. Approximately 13% of the particles exhibit much larger particle volume equivalent to containing 10-12 DNA plasmids per particle (Figure 5.7 d), which is due to particle aggregation. The AFM and DLS data suggest that LbL Film 1 releases smaller particles for a longer period of time than Film 2. While dPEI is less toxic than bPEI because of its biodegradable property; on the other side, our data suggest that dPEI's biodegradable property also limits its ability to maintain a compact polyplex shape during a prolonged delivery process.

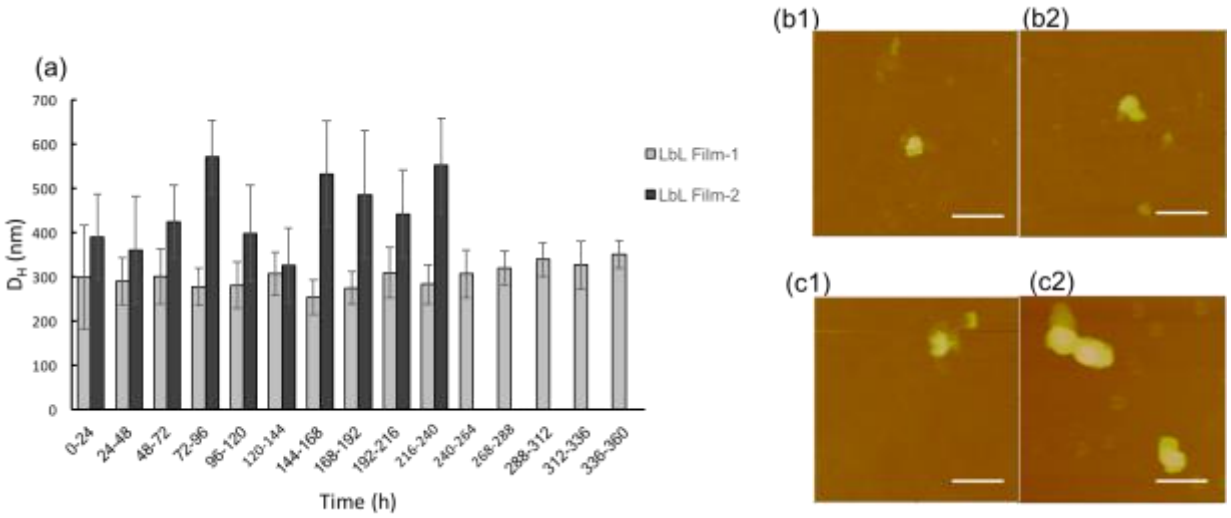

Figure 5.5. (a)Average hydrodynamic diameter of the degradation products from LbL film-1 (gray column) and LbL film-2 (black column); AFM image of particle releasing out from LbL film-1 in 6 hours, z-range 50 nm (b1) and 6 days, z-range 50 nm (b). AFM image of particle releasing out from LbL film-2 in 6 hours, z-range 50 nm (c1) and 6 days, z-range 120 nm (c2), contact mode in PBS buffer, scale bar=0.5 µm.

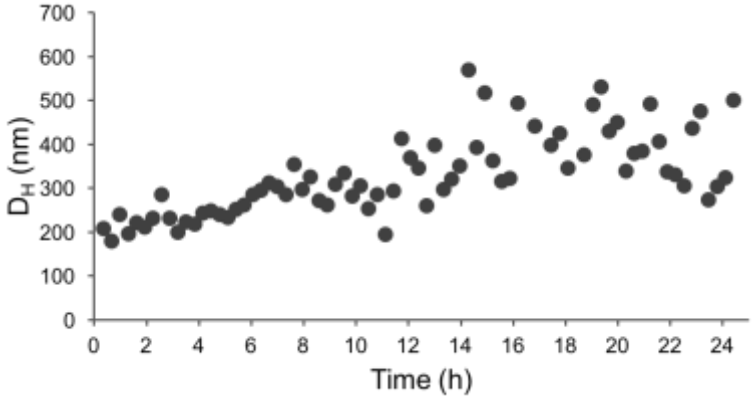

Figure 5.6. Hydrodynamic diameter of the degradation products from LbL film 1 in first 24 hours.

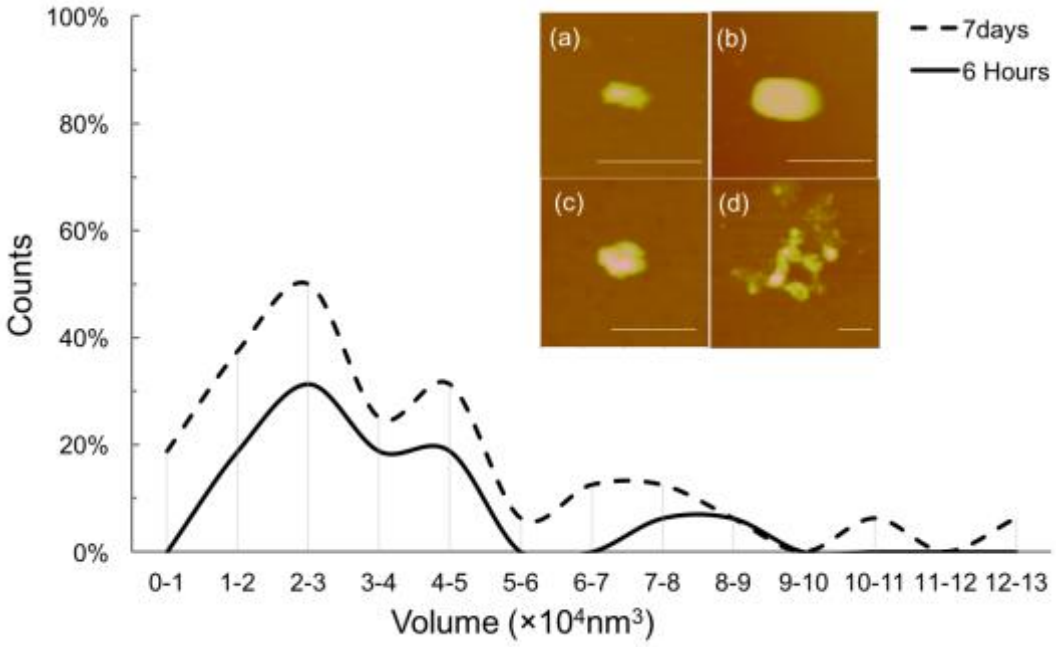

Figure 5.7. The LbL film 1 released pAPOL-1/DNA complex bearing volume distribution curve analysized by AFM. (a-d) The representative AFM height images of the released complex (Tapping mode, in air). The typical error of AFM bearing volume analysis is ~30%[92]. (a) and (b) are the complexes collected in 6 hours LbL film 1 degradation. Z range for (a) is 80 nm, for (b) is 180 nm. (c) and (d) are the complexes released out from LbL Film 1, collected in day 7. Z range for (c) and (d) are 40 nm. Scale bar in all 4 images are 500nm.

The degradation kinetics was further analyzed by fluorescence spectroscopy. The DNA amount released from the LbL film due to DTT was determined by fluorescent labeling of DNA with SYBR® safe DNA stain. The fluorescence data were calibrated using known amount of DNA as described in Experimental section. Figure 5.8 shows the continuous release of DNA from the LbL film during the 300 h observation period. The film exhibited a comparing fast releasing behavior in the first 24 h consistent with the film thickness data measured by AFM. This is probably due to polyelectrolytes quickly coming out of the film at the beginning of film degradation [165]. However, the appearance of bPEI barrier layer in the LbL film, screen the residue charge[166], slow down pAPOL-1 chain mobility[75, 98], and its own non-biodegrdable property

arrests the bulk release of the overall film [167]. In summary we have achieved sequential DNA release of the pAPOL-1/DNA films by the insertion of diffusion barrier layers of bPEI and dPEI.

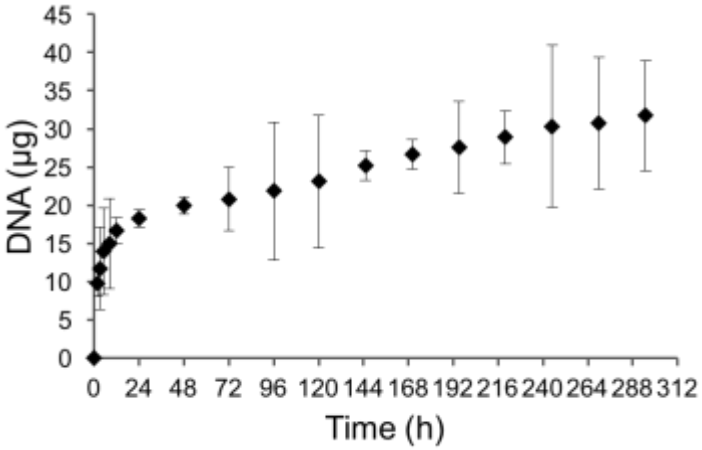

Figure 5.8. Amount of DNA releasing out from LbL film-1 vs degradation time.

5.3.3. Transfection efficiency of pAPOL/DNA LbL film

The transfection study was carried out by culturing HEK 293 cell and MC 3T3 cells directly on the LbL film surface. A layer of fibronectin was applied to the films prior to cell culture because fibronectin was found to improve cell attachment and proliferation [168]. Figure 5.9 (a) exhibits the bright field (left colum) and fluorescence image (right colume) of proliferation HEK 293 cells (left panel) and MC 3T3 cells (right pannel) on LbL Film 1 (a) and LbL Film 2 (b). When cell cultured on LbL film 1 (a), they attach and grow well on the films throughout the observation period of 6 days. GFP fluorescence images indicate transfection of pEGFP-N1plasmid DNA from day 2 till the end of the cell culturing period. We observed a significant increase in number of green fluorescence in day 4. This is attributed to the increased number of cells as well as the abundant of DNA released from the film at this time point. HEK 293 and MC 3T3 cells do not attach and grow well on LbL Film 2. Cells were observed to detach and aggregate starting day 2 (MC 3T3) and day 4 (HEK 293). On day 6, most cells appear unhealthy and aggregated. Although the HEK

293 cells can be transfected when cultured on LbL film 2 (b, left panel), the transfection efficiency is significantly reduced due to poor cell attachment and growth.

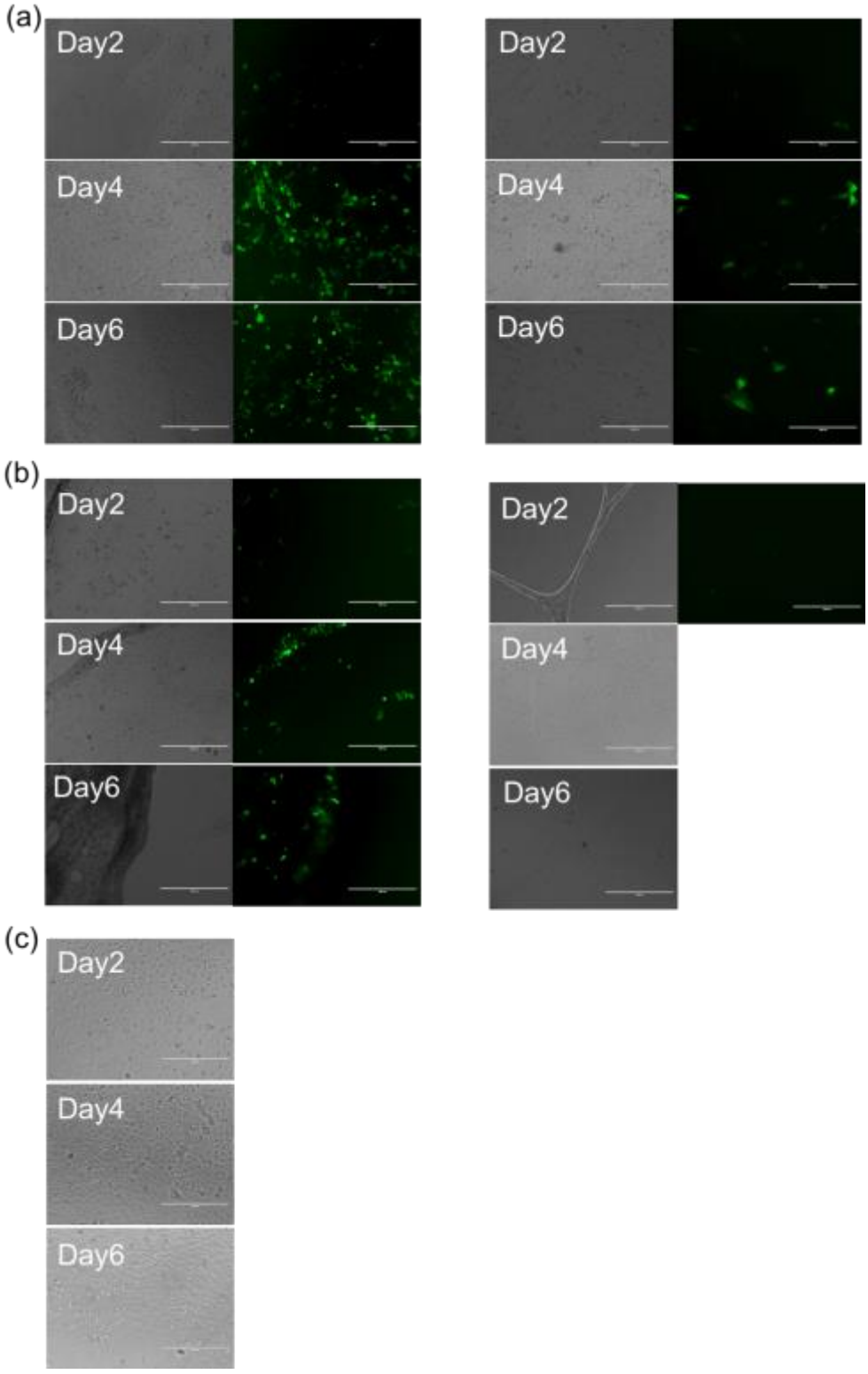

Figure 5.9. Bright field (left columon) and fluoresene microscopic image (right coloum) of gene expression cultured on LbL film 1 (a), LbL film 2 (b) and culture plate as control group (c) by HEK 293 cell line (left panel) and MC 3T3 cell line (right panel). Magnification is 10× for all images; scale bar is 400 µm.

Flow cytometry were used to characterize cell transfection efficiency in day 6. The reason to choose day 6 is because of the maximum fluorescence signal observed (figure 5.9). The percentage of transfected cells and mean fluorescence intensity (MFI) are used here to quantify the transfection efficiency. The total event measured is 10,000 for each sample. Cells grow on 24-well culture plate without any transfection agents were used as a negative control. Figure 5.10 a-b show percentage of transfected cell and relative MFI for each experimental group. HEK 293 cells grows on LbL film 1 has 9.9% cell has showed green fluorescence (figure 5.10a), and the corresponding MFI value is 4.6-fold than that of control group (figure 11b). The MFI value of MC 3T3 cells on LbL Film 1 is only 2.5-fold higher than that of the control. For LbL Film 2, HEK 293 has much lower percentage of transfected cells, ~ 0.9% (figure 5.10a). The relative MFI shows 4.0-fold higher than the control (figure 5.10b). The MC 3T3 cells grown on LbL Film 2 show lower than 0.5% transfection percentage (figure 5.10a). The relative MFI is 1.2-fold higher than the control (figure 5.10b), which means there are very bare green fluorescence has been detected in cell body.

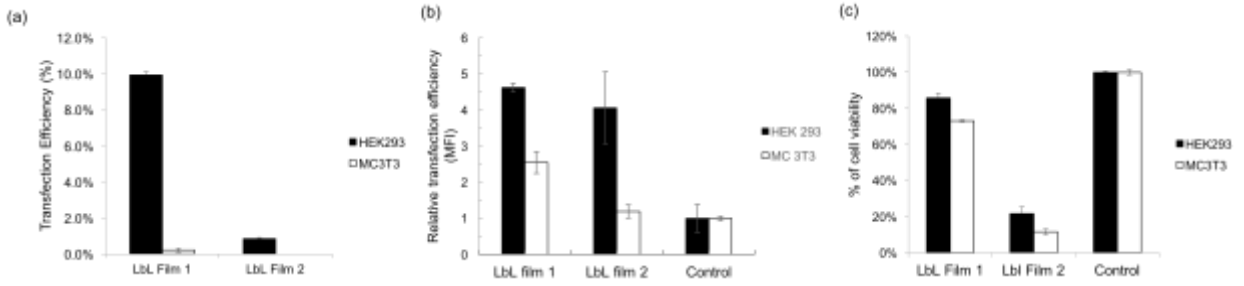

Figure 5.10. (a) proportion of transfected cells and (b) relative MFI of transfection cells of LbL films in HEK 293 and MC 3T3 cells in day 6. (c) Cell viability of HEK 293 cells and MC 3T3 cells cultured on LbL films in day 6 determined by MTT assay. All experiments were displayed by mean values (standard deviations) of three experiments.

Figure 5.10 (c) 12c plot the cell viability data cultured on the LbL films by the MTT assay. For HEK 293 cells, the cell viability of film 1 is 85.8% and for LbL film 2 is 21.6%. MC 3T3 cells showed 73.1% cell viability on film 1 and 11.6% on film 2. Our data suggest that LbL film 1 is more biocompatible than film 2, and HEK 293 cell line is less adversely affected than MC 3T3 cell line.

After 14 days culturing, the LbL film 1 was took out from the culture plate and removed cell by vigorous rinsing. Figure 5.11 shows the AFM image of film surface morphology. The thickness of LbL film 1 is decreased to 19.2 nm after HEK 293 cell culturing, only 25% of film original thickness. And for MC3T3 cells line, the film 1 thickness decreased to 38.5 nm, 50% of the original film. This thickness change indicates that the cellular film degradation occurs with a much slower rate than DTT degradation. The degradation rate is cell type dependent due to the thiol redox activity on the cell surface is different between cell type. Based on the difference reaming film thickness between two cell type, we can conclude that HEK 293 cell line can degrade LbL film 1 faster than MC 3T3 cell line. Which indicates more amount of gene can be released out form LbL film1 in the same time. The opportunity for cell to uptake DNA is higher in HEK 293 cells than MC 3T3 cells due to released DNA density. This is also one reason why HEK 293 cell line has higher transfection efficiency than MC 3T3 cell line in LbL film 1 transfection experiment.

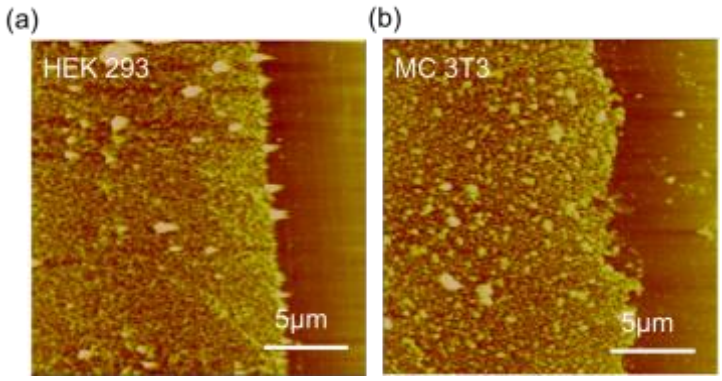

Figure 5.11. AFM image of LbL film 1 after culturing with (a) HEK 293 cells and (b) MC 3T3 cell line for 14 days. Scale bar is 5 μm, z range for (a) is 150 nm, for (b) is 120 nm.

Lastly, to demonstrate the ability of LbL Film 1 for sequential gene delivery, two different DNA plasmids were incorporated into the film as shown by figure 5.12. The bottom 9 bi-layers were constructed using the pEF.myc.ER-E2-Crimson plasmid and its transfection will give red fluorescence. The top 7.5 bi-layer contains the green fluorescent pEGFP-N1plasmid. HEK 293 cells were culture on this LbL film for 10 days. Figure 5.13 shows that the dominance of the green fluorescence on day 4 and the appearance of red fluorescence start on day 6. It shows the persistence of green fluorescence from day 4 to day 8 and that delayed expression of the Crimson plasmid from day 6 to day 10. The data demonstrate the promise of such LbL films for controlled and sequential gene delivery for biomedical applications.

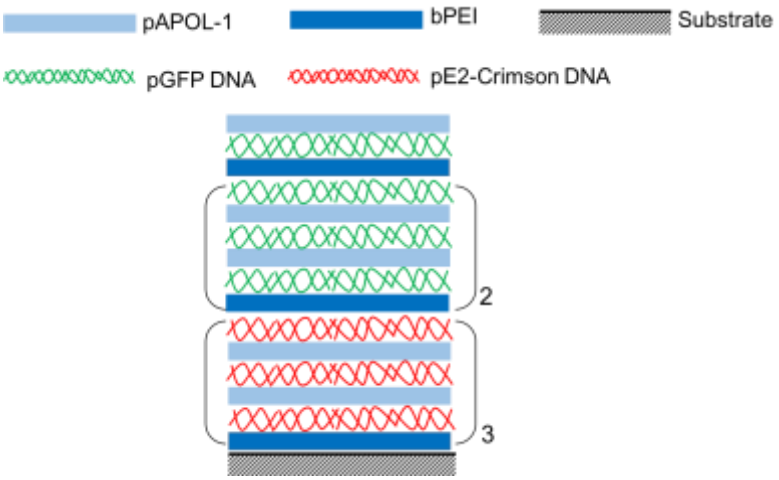

Figure 5.12. Layer composition of LbL film 1 made by two different DNA plasmids.

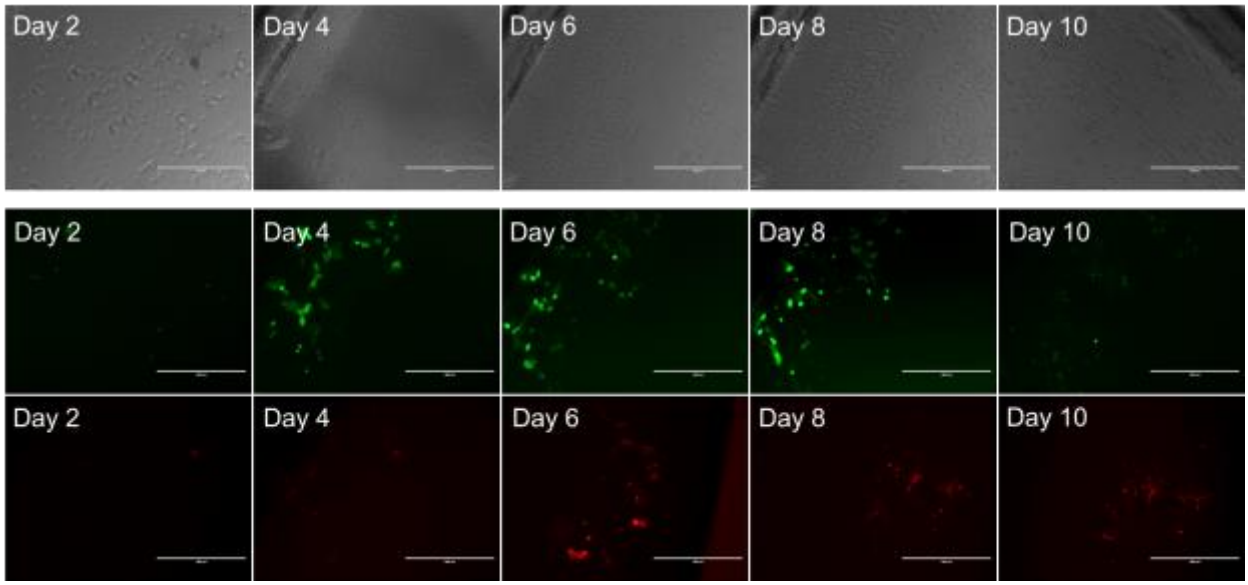

Figure 5.13. Bright field (first row), green fluorescence microscopic image (second row), red fluorescence microscopic image (Third row) of gene expression cultured on LbL film by HEK 293 cells. Magnification is 10× for all images; scale bar is 400 µm.

5.3.4. Differentiation of MC 3T3 cell line

Incorporating therapeutic gene to replace indicator gene is a significant step in the development of gene therapy. Researchers already demonstrated that BMP-2 has ability to stimulate and elevate ALP activity[169]. Promoting MC 3T3 cell differentiation is the first step to develop bone regeneration. Therefore, we treated MC 3T3 cells with pAPOL-1/BMP2-pDNA (N/P=12/1) polyplex to examine the gene therapeutic effect. The ALP activity level detected by ALP kit can indicate the degree of MC 3T3 cell differentiation. After adding polyplex into cell medium, cells were cultured in MEM α medium for 24 hours and then the medium was replaced by differentiation medium. After 14 days, the ALP activity was examined and the result was reported in figure 5.14. The result indicated that the ALP concentration was increased after treated with pAPOL-1/BMP2-pDNA polyplex. Comparing with control group, the concentration of ALP was improved by 17.5%, which is also higher than bPEI/ BMP2-pDNA polyplex group. In addition,

we designed another experiment in which added polyplex into cells every 3 days, 4 times in total, during the cell differentiation period. This is because that we want to improve the concentration of BMP2- pDNA in the entire cell differentiation period but the degree of improved ALP activity is not as good as the one-time polyplex adding experiment. Especially when adding bPEI/BMP2-pDNA polplex continuously, most cells died during the culturing. As a result, of course, there was no ALP activity detected. The result indicated that the high concentration of bPEI severely affected the viability of MC 3T3 cells and triggered apoptosis. This result agrees with the cell viability result of bPEI/GFP-pDNA polyplex (N/P=6/1) in section 4.3.4, in which the cell viability decreased 50% comparing with the control group.

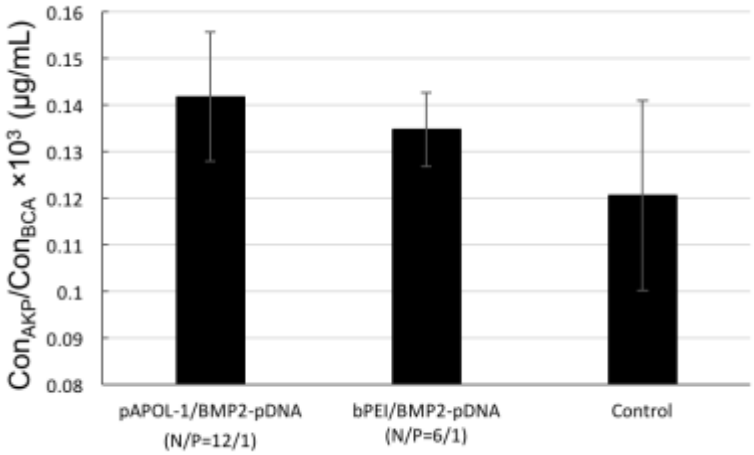

Figure 5.14. MC 3T3 cell differentiation was determine with alkaline phosphatase (ALP) kit after 14 days differentiated culture.

We fabricated a LbL film containing BMP2-pDNA with the LbL film 1 structure and characterized the film with MC 3T3 cells. The result did not show obvious ALP activity level improvement comparing with control group. The first reason is transfection efficiency of LbL film 1 to MC 3T3 cell line is not high enough. As we showed in section 5.3.3, the transfection efficiency of LbL film 1 in MC3T3 cells was lower than that of in HEK 293 cells. The second reason is the

high cytotoxicity of bPEI to MC 3T3 cell line, which can influence the level of BMP2-pDNA expression.

5.3.5. In vivo transfection

Transfection experiment *in vivo* was tried in mouse model by implanting LbL film coated silk suture. The suture was coated with type A film which fabricated by PAA-1 and luciferase-expressing plasmid pGL4. The control group is the silk suture coated with the film made by bPEI and pGL4. The total layers of film are 16.5 bilayers. The DNA content in the LbL films is ~1μg/cm of the coated suture measured by real time PCR. Electroporation was used for comparison. The transfection result was examined in day 10 after implantation. As shown in Figure 5.15, both films failed to induce luciferase activity in the mice, while electroporation showed positive result. The suture was taken out from mice and characterized with the real-time PCR analysis which showed the implanted suture surface only remained ~1/10,000 of original DNA quantity. The decreased DNA amount demonstrated the successful DNA releasing from LbL films. But the low transfection efficiency indicated that the type A films lacked the capability to transfect cells. The reason is the type A film disassembly is in the fast and bulk releasing type which lacks small-sized particles released. However, this experiment demonstrated that the PAA/DNA film can be reduced and released out from the suture surface *in vivo*.

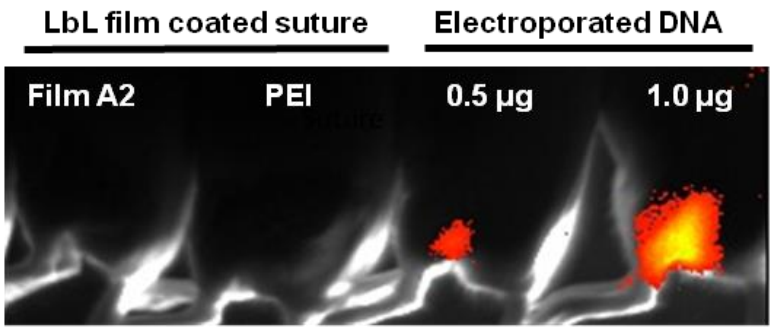

Figure 5.15. luciferase activity result in mouse by using type A film coated silk suture and electroporation. luciferase activity was detected in days 10 after materials implantation. The

luminescence image overlays a white light image to identify signal location. Intensity of light detection ranges from red (low) to blue (high).

5.4. Discussion

The work in this chapter is building on the polymer screening results described in chapter 4. We selected the pAPOL-1 to assemble LbL film. These new films, LbL film 1 and LbL film 2, have similar surface features, growth patterns, disassemble processes, and DNA releasing periods as that of type B film in chapter 3. Though the PAA-1 used in type B film has larger molecular weight than that of pAPOL-1, after switching pAPOL-1 to fabricate LbL film, the film thickness and surface feature do not have much difference. The dPEI barrier layer inside the film 2 still can act as a significant role to screen the residue charge and bind strongly with the neighboring polymers to stabilized the film interior structure and support the linear growth mode[14]. The transfection efficiency of LbL film 1 has been largely improved comparing to previous LbL films. In chapter 3, MFI of expressed gene in day 6 in type B film, which is made by PAA-1, transfected HEK 293 cells is 2086, which is 2-fold higher than the control group (MFI 1175). But for the LbL film 1 which is made by pAPOL-1 in this chapter, the MFI, comparing with control group, has been improved by 4.5-fold. This transfection enhancement is similar to the polyplex experiment results in chapter 4. Therefore, the polymer screening work via polyplex experiment efficiently helped selecting a polymer with high transfection efficiency and biocompatibility for the LbL film fabrication.

The LbL film provides a method for localized gene delivery. This method can concentrate the dosage to release in the target area. After applied disulfide bond reduction reaction in the bioconjugate to release DNA, the location and concentration of redox agents in tissue or cells should be first concerned. In cell body, the cytosolic space, cytosolic enzyme, and redox protein, such as thioredoxin, glutaredoxin[170] and glutathione[171] are playing significant roles in disulfide

bond reduction, oxidation, and isomerization. And they are abundant in most cells[3, 172, 173]. But in the extracellular environment, the glutathione concentrations are much lower than cytosol[174]. The protein disulfide isomerase (PDI) on the cell surface can maintain the disulfide bond reduction but it is cell type-dependent[175]. PDI has been identified in human B lymphocytes[176], platelets[177], rat hepatocytes [178], and rat pancreatic cells[179]. Therefore, insufficient redox agent in cell surface may cause dosage loss and poor transfection efficiency. But a "cell-favorable" surface in LbL film can overcome this problem. Because cell or tissue can directly attach or contact on the film for long time by implantation. It can largely improve the chance for cell surface redox agents to react with the disulfide bond in polymer chain to dissemble films. People already demonstrated the disulfide bond reduction begins at the cell surface[3]. The localized gene delivery can improve the biodegradation efficiency with large contact area and long contact period for the reaction between disulfide linkage-employing drug/gene conjugate and cell surface redox agents.

In this chapter, our LbL film made by pAPOL-1, bPEI, and DNA not only improved the transfection efficiency but also achieved sustained and sequential delivery. The releasing particle from LbL film 1 can keep in a relative small size, around 300 nm. When changing bPEI to degradable dPEI, the degradation rate in first 2.5 hours increased and the film thickness decreased 50%. The released particle size become larger (~400 nm) than the film 1. This is because the dPEI has smaller molecular weight (section 4.3.1) and lower surface charge in polyplex mode (section 4.3.3) comparing with bPEI. The relatively short chain length and weak charge may lead to less ability of binding with neighboring layer and screening the residue charge acting as barrier layer. After the film exposes to the reducing environment, the weekly interacted chain will be released out first. That is why in the first 2.5 hours, the film degradation rate is higher than the following time. The bPEI can be hydrolyzed under physiological condition to form the diol linker and amino

acid. And the half-life of the bPEI is 30 h[87]. As a barrier layer, before the molecular chain is fully reduced into short fragments, it still can interact with neighboring polymers to decrease its chain mobility. That is why the LbL film 2 didn't present fast and bulk degradation as type A film in chapter 3. On the other side, the shorter degradation cycle of LbL film 2 (9 days) compared with LbL 1 is due to the degradable property of dPEI barrier layer. The releasing mechanism of bPEI in LbL film is based on the entire region becoming soluble[14]. But for the hydrolysable dPEI, the hydrolyzed short chain accelerates the barrier layer releasing. Therefore, the LbL film 2 has a shorter degradation period than film 1.

The transfection efficiency of LbL film in HEK293 cell line is higher than the MC 3T3 cell line. One of the reasons is that MC 3T3 cells are much more sensitive in bPEI and dPEI than HEK293 cells, which has been demonstrated in section 4.3.4. In LbL film 2, HEK 293 and MC 3T3 cells both exhibited poor attachment. Although, people demonstrated that dPEI has better biocompatibility than bPEI in polyplex experiment[87], it did not show any improvement in LbL film application. This is because of the fast releasing rate at the beginning of LbL film 2 degradation. The high rate leads to large amount of materials released out. Therefore, the high concentration of released materials attached to cell surface may influence cell attachment and growth. And even triggered cell apoptosis. The reason is still needed to be explored and discussed in future work.

MC 3T3 cells differentiation result demonstrated the application potential of gene delivery in bone regeneration. Though the MC 3T3 cells differentiation has been improved by treating with pAPOL-1/GFP-pDNA polyplex, the differentiation degree is still needed to be enhanced for future medical application. It requires an even higher transfection efficiency of our gene delivery system. The main reason is the improvement of ALP activity needs very high dosage of BMPs. Based on

previous research work, researchers found that 3ng/mL BMP-2 only can improve 20% MC 3T3 cell differentiation. It required more than 10ng/mL BMP-2 to improve 60% differentiation. And people found that a large improvement of new bone formation *in vivo* needs ~10-fold higher BMP-2 than nature occurring[160]. This required a large amount of BMP-2 produced by gene expression. The transfection efficiency should be extremely high that can improve the bone tissue regeneration in gene therapy. On the other hand, as mentioned in chapter 4, the successful gene expression required the polymer "unpacking" ability which is closely related to the cell capability to reduce the disulfide bond. The number of redox agents in cell body such as glutathione and glutathione disulfide has been largely influenced by cell cycle. The redox activity in cell body will be greatly increased in cell M phase compared to quiescent cells and cell S phase[180, 181]. But when MC 3T3 cells cultured in differentiation medium, their proliferation rate will become much slower than undifferentiated status[182]. This slow proliferation rate largely decreases the polymer degradation rate and lowers the chance for DNA nucleus transferring via cell deviation. As a result, the transfection efficiency and the BMP-2 gene expression has been greatly limited. Therefore, the ALP activity improvement in our experiment is not high enough as prospected. In future, the transfection efficiency of LbL film is still needed to be continuously improved.

5.5. Conclusion

This chapter combined previous two chapter results, using pAPOL-1 and PEI barrier layer build a high transfection efficiency, sustained, and sequential DNA releasing LbL film. Optimized the LbL film system and built the relationship between polyplex and LbL film via polymer screening. LbL film 1 made by pAPOL-1 can continue releasing polymer/DNA conjugate over 2 weeks in a constant size around 300 nm. The transfection efficiency improved by 2.5-fold comparing to previous LbL type B film. Especially in MC 3T3 cell line, in previous work, there

was almost no transfection observed. In this chapter, we successfully transfected the MC 3T3 cells and showed the gene expression. Applied two different fluorescence protein encoded indicator gene in one LbL film, we demonstrated the sequential delivery capability of LbL film 1. Provided a method to delivery multiple therapeutic genee in a desired and controllable sequence. Biocompatibility of LbL film is closely related to the own property of polycation and cell type. The dPEI incorporation caused cell attaching problem in our LbL films. The PEI cytotoxicity is related to its structure, molecular weight, degradation rate, and cell type[141]. In the future, the PEI should be modified or redesigned it structure to improve their biocompatibility, and then to applied in our LbL film system.

CHAPTER 6 CONCLUSIONS AND FUTURE WORK

6.1.Conclusion

This dissertation described a bioreducible, biocompatible, and efficient LbL film coating for sustained and sequential gene delivery. Explored the relationship between LbL film interior structure and disassemble process. Explained the interlayer diffusion property in LbL film and demonstrated the influence of film interlayer structure. The LbL film composited with high diffusion coefficient polyelectrolyte lacks perfect layer structure. The weakly interacted polymer chain with relatively high mobility can diffuse throughout its neighboring layers to deeper layers. This diffused LbL film has fast and bulk disassemble property in reducing environment. This dissertation provides a method of inserting high charge density and long molecular weight polymer—PEI as barrier layer to screen the residue charge and stabilize the interlayer structure in LbL film. This barrier layer successfully prevents the fast and bulk releasing property, changes the LbL film to sustained and sequential disassembling. And, our work demonstrated the interlayer structure type of LbL film can be indicated by film growth pattern. The linear thickness growth considered as a function of deposited layer indicates film without interlayer diffusion and with sustained surface erosion. The film has exponential thickness growth mold indicating film with interlayer diffusion and fast bulk erosion.

This dissertation also described high efficiency and low toxicity polycation gene carry development. Synthesized novel poly(amdio amine)s—pAPOLs which contains the disulfide bond and a hydrolysable dPEI. The incorporation of disulfide bond provides pAPOLs biodegradable property through the reaction with redox agent which contained in cell body. By screening this pAPOLs by polymer buffer capacity and its polyplex chemical, physical, and biological property, we found a highest transfection efficiency and lowest toxicity polymer-- pAPOL-1. By adjusting

and modifying LbL film structure and surface property with pAPOL-1, we made the LbL film with cell favorable surface, biodegradable property, sequential releasing type, high gene expression efficiency, and localized delivery property.

In conclusion, this dissertation explained the LbL film disassemble mechanism in bulk and sustained releasing. Found the relationship between LbL film assembly and disassembly. Provided a method to screen polymer in gene delivery and related it between polyplex vehicle and LbL film coating. And, described a method to build a LbL film with biodegradable, biocompatible, and improved transfection efficiency. The well-engineered LbL film has a potential for future long period therapy and multiply therapeutic agent sequential delivery.

6.2.Future work

Currently, our LbL film with non-diffusible layer structure could delivery gene in a sustained and sequential releasing mode, but they are still containing the 25KDa bPEI. Though the bPEI content is small but it may limit future application, especially for the cell lines which are sensitive to PEI, such as MC 3T3 cells. We replaced bPEI in LbL films with dPEI to decrease toxicity, but the hydrolysable ability of dPEI prevented it from being an effective barrier layer. In order to find a barrier layer with low toxicity and small diffusion coefficient, in future, bPEI modification can be considered as a method to improve our LbL system, for example, modifying bPEI by using pendant palmitic acid chains, or PEGylation [183], or RGD peptide [14, 96, 184, 185].

Though we already improved the transfection efficiency of LbL film, it still has space to improved, especially for the application in a wide range of cell types and the *in vivo* experiment. The first method is to improve the polycation's transfection efficiency. Zhou and Gao et al demonstrated that changing the poly(ß-amino ester)s structure from linear to branched can improve the transfection efficiency and biocompatibility[186, 187]. And, the higher molecular weight of their

branched poly(ß-amino ester)s, the more efficiency the polymer would be[188]. In our poly(amido amine), we can find a monomer with triamine group and hydroxalkyl side group to react with bisacrylamide in CBA or MBA by Michael addition polymerization to form hyperbranched pAPOLs. The hyperbranched structure in poly(amido amine) may also have potential to improve the transfection efficiency[88]. In the meantime, we can produce various molecular weight and branched degree poly(amdio amine)s and screen by polymer buffer capacity and polyplex experiment to find the best polymer in next LbL film assembly.

As mentioned in chapter 5, the disulfide bond reduction potential is depending on cell types, cell proliferation rate, and the location of redox reaction. Since LbL film application requires film degradation starting at cell surface while cell attached. And, the cell surface redox protein or enzyme's type and concentration are lower than cytosol[3, 189]. To better apply LbL film system in specific cell line, cell surface redox agents such as protein disulfide isomerase (PDI), NADH-oxidase (NOX), thiroredoxin, et al, should be studied first. For example, PDI has been demonstrated in human B kymphocytes[190], platelets[191], rat hepatocytes[192], and rat pancreatic cells[193]; NOX appears on cancerous cells such as HeLa and hepatoma[194]; Thioredoxin also localized to surface of human white cell lines such as human B and T lymphocytes, monocytes and granulocytes[195].

The trafficking of the released polymer/DNA complex from LbL film in extracellular and intracellular environment needs to be studied in future by fluorescence labeling. Since our pAPOLs lack sufficient primary amine groups in their polymer chains, the fluorescence dye TRITC and FITC is not efficient enough to label our polymers. In future, finding a suitable fluorescence dye to label our LbL film to determine the releasing particle composition could be helpful to understand

the film releasing mechanism. This method also can be used to analyze the interaction between releasing particle and cell surface.

Moreover, the *in vivo* study is very necessary and important for our LbL film gene delivery study. Now, the improvement in the transfection efficiency of our LbL film should help the *in vivo* study. In future, we can try to coat our LbL film in various medical devices, such as suture and stent, to implant in animal mold so that we can investigate how the LbL film would work in physiological environment.

REFERENCES

[1] S. Y. Wong, J. M. Pelet, D. Putnam, *Prog Polym Sci* **2007**, *32*, 799.

[2] M. S. Al-Dosari, X. Gao, *Aaps J* **2009**, *11*, 671.

[3] G. Saito, J. A. Swanson, K. D. Lee, *Adv Drug Deliver Rev* **2003**, *55*, 199.

[4] F. D. Ledley, *Pharmaceutical Research* **1996**, *13*, 1595.

[5] L. Wasungu, D. Hoekstra, *J Control Release* **2006**, *116*, 255.

[6] C. Magin-Lachmann, G. Kotzamanis, L. D'Aiuto, H. Cooke, C. Huxley, E. Wagner, *J Gene Med* **2004**, *6*, 195.

[7] W. T. Godbey, K. K. Ku, G. J. Hirasaki, A. G. Mikos, *Gene Ther* **1999**, *6*, 1380.

[8] W. Zauner, M. Ogris, E. Wagner, *Adv Drug Deliver Rev* **1998**, *30*, 97.

[9] L. De Laporte, L. D. Shea, *Adv Drug Deliver Rev* **2007**, *59*, 292.

[10] H. J. Chung, T. G. Park, *Adv Drug Deliver Rev* **2007**, *59*, 249.

[11] C. M. Jewell, D. M. Lynn, *Adv Drug Deliver Rev* **2008**, *60*, 979.

[12] N. Jessel, M. Oulad-Abdeighani, F. Meyer, P. Lavalle, Y. Haikel, P. Schaaf, J. C. Voegel, *P Natl Acad Sci USA* **2006**, *103*, 8618.

[13] J. Blacklock, Y.-Z. You, Q.-H. Zhou, G. Mao, D. Oupický, *Biomaterials* **2009**, *30*, 939.

[14] Y. Zou, L. Xie, S. Carroll, M. Muniz, H. Gibson, W.-Z. Wei, H. Liu, G. Mao, *Biomacromolecules* **2014**, *15*, 3965.

[15] G. de Jong, A. Telenius, S. Vanderbyl, A. Meitz, J. Drayer, *Chromosome Res* **2001**, *9*, 475.

[16] P. Kreiss, B. Cameron, R. Rangara, P. Mailhe, O. Aguerre-Charriol, M. Airiau, D. Scherman, J. Crouzet, B. Pitard, *Nucleic Acids Res* **1999**, *27*, 3792.

[17] M. Whitmore, S. Li, L. Huang, *Gene Ther* **1999**, *6*, 1867.

[18] S. W. Dow, L. G. Fradkin, D. H. Liggitt, A. P. Willson, T. D. Heath, T. A. Potter, *J Immunol* **1999**, *163*, 1552.

[19] F. E. Ruiz, J. P. Clancy, M. A. Perricone, Z. Bebok, J. S. Hong, S. H. Cheng, D. P. Meeker, K. R. Young, R. A. Schoumacher, M. R. Weatherly, L. Wing, J. E. Morris, L. Sindel, M. Rosenberg, F. W. van Ginkel, J. R. McGhee, D. Kelly, R. K. Lyrene, E. J. Sorscher, *Hum Gene Ther* **2001**, *12*, 751.

[20] M. M. Whitmore, S. Li, L. Falo, L. Huang, *Cancer Immunol Immun* **2001**, *50*, 503.

[21] R. Tachibana, H. Harashima, N. Ide, S. Ukitsu, Y. Ohta, N. Suzuki, H. Kikuchi, Y. Shinohara, H. Kiwada, *Pharmaceutical Research* **2002**, *19*, 377.

[22] P. L. Felgner, G. M. Ringold, *Nature* **1989**, *337*, 387.

[23] M. B. James, T. D. Giorgio, *Mol Ther* **2000**, *1*, 339.

[24] C. M. Wiethoff, C. R. Middaugh, *J Pharm Sci* **2003**, *92*, 203.

[25] C. M. Wiethoff, C. R. Middaugh, *J Pharm Sci* **2003**, *92*, 203.

[26] C. M. Wiethoff, J. G. Smith, G. S. Koe, C. R. Middaugh, *Journal of Biological Chemistry* **2001**, *276*, 32806.

[27] S. Li, W. C. Tseng, D. B. Stolz, S. P. Wu, S. C. Watkins, L. Huang, *Gene Ther* **1999**, *6*, 585.

[28] D. Oupicky, C. Konak, P. R. Dash, L. W. Seymour, K. Ulbrich, *Bioconjugate Chemistry* **1999**, *10*, 764.

[29] M. Ruponen, S. Yla-Herttuala, A. Urtti, *Bba-Biomembranes* **1999**, *1415*, 331.

[30] H. Matsui, L. G. Johnson, S. H. Randell, R. C. Boucher, *Journal of Biological Chemistry* **1997**, *272*, 1117.

[31] F. LabatMoleur, A. M. Steffan, C. Brisson, H. Perron, O. Feugeas, P. Furstenberger, F. Oberling, E. Brambilla, J. P. Behr, *Gene Ther* **1996**, *3*, 1010.

[32] R. P. Harbottle, R. G. Cooper, S. L. Hart, A. Ladhoff, T. McKay, A. M. Knight, E. Wagner, A. D. Miller, C. Coutelle, *Hum Gene Ther* **1998**, *9*, 1037.

[33] M. J. Clague, S. Urbe, *J Cell Sci* **2001**, *114*, 3075.

[34] Z. Y. Zhang, B. D. Smith, *Bioconjugate Chemistry* **2000**, *11*, 805.

[35] A. R. Klemm, D. Young, J. B. Lloyd, *Biochem Pharmacol* **1998**, *56*, 41.

[36] O. Boussif, F. Lezoualch, M. A. Zanta, M. D. Mergny, D. Scherman, B. Demeneix, J. P. Behr, *P Natl Acad Sci USA* **1995**, *92*, 7297.

[37] H. Pollard, G. Toumaniantz, J. L. Amos, H. Avet-Loiseau, G. Guihard, J. P. Behr, D. Escande, *J Gene Med* **2001**, *3*, 153.

[38] H. Pollard, J. S. Remy, G. Loussouarn, S. Demolombe, J. P. Behr, D. Escande, *Journal of Biological Chemistry* **1998**, *273*, 7507.

[39] P. Walter, *Molecular biology of the cell New York: Garland Publishing* **1999**, 561.

[40] K. J. Ryan, S. R. Wente, *Curr Opin Cell Biol* **2000**, *12*, 361.

[41] I. W. Mattaj, L. Englmeier, *Annu Rev Biochem* **1998**, *67*, 265.

[42] G. R. Whittaker, M. Kann, A. Helenius, *Annu Rev Cell Dev Bi* **2000**, *16*, 627.

[43] J. C. Perales, T. Ferkol, H. Beegen, O. D. Ratnoff, R. W. Hanson, *P Natl Acad Sci USA* **1994**, *91*, 4086.

[44] D. L. McKenzie, K. Y. Kwok, K. G. Rice, *Journal of Biological Chemistry* **2000**, *275*, 9970.

[45] M. Wilke, E. Fortunati, M. vandenBroek, A. T. Hoogeveen, B. J. Scholte, *Gene Ther* **1996**, *3*, 1133.

[46] W. C. Tseng, F. R. Haselton, T. D. Giorgio, *Bba-Gene Struct Expr* **1999**, *1445*, 53.

[47] M. Brisson, W. C. Tseng, C. Almonte, S. Watkins, L. Huang, *Hum Gene Ther* **1999**, *10*, 2601.

[48] S. Brunner, T. Sauer, S. Carotta, M. Cotten, M. Saltik, E. Wagner, *Gene Ther* **2000**, *7*, 401.

[49] J. Zabner, A. J. Fasbender, T. Moninger, K. A. Poellinger, M. J. Welsh, *Journal of Biological Chemistry* **1995**, *270*, 18997.

[50] H. Pollard, J.-S. Remy, G. Loussouarn, S. Demolombe, J.-P. Behr, D. Escande, *Journal of Biological Chemistry* **1998**, *273*, 7507.

[51] D. E. Olins, A. L. Olins, P. H. von Hippel, *Journal of molecular biology* **1967**, *24*, 157.

[52] U. K. Laemmli, *P Natl Acad Sci USA* **1975**, *72*, 4288.

[53] S. W. Kim, *Cold Spring Harbor Protocols* **2012**, *2012*, pdb. ip068619.

[54] F. Alexis, E. Pridgen, L. K. Molnar, O. C. Farokhzad, *Mol Pharmaceut* **2008**, *5*, 505.

[55] D. Bazile, C. Prudhomme, M. T. Bassoullet, M. Marlard, G. Spenlehauer, M. Veillard, *J Pharm Sci* **1995**, *84*, 493.

[56] W. Godbey, K. K. Wu, A. G. Mikos, *Journal of biomedical materials research* **1999**, *45*, 268.

[57] L. Wightman, R. Kircheis, V. Rossler, S. Carotta, R. Ruzicka, M. Kursa, E. Wagner, *J Gene Med* **2001**, *3*, 362.

[58] H. Nguyen, P. Lemieux, S. Vinogradov, C. Gebhart, N. Guerin, G. Paradis, T. Bronich, V. Alakhov, A. Kabanov, *Gene Ther* **2000**, *7*, 126.

[59] H. Petersen, P. M. Fechner, A. L. Martin, K. Kunath, S. Stolnik, C. J. Roberts, D. Fischer, M. C. Davies, T. Kissel, *Bioconjugate chemistry* **2002**, *13*, 845.

[60] M. Breunig, U. Lungwitz, R. Liebl, A. Goepferich, *Proceedings of the National Academy of Sciences* **2007**, *104*, 14454.

[61] M. Thomas, A. M. Klibanov, *P Natl Acad Sci USA* **2002**, *99*, 14640.

[62] J. A. Fortune, T. I. Novobrantseva, A. M. Klibanov, *Journal of drug delivery* **2011**, *2011*.

[63] W.-B. Li, W. Yuan, F.-J. Xu, C. Zhao, J. Ma, Q.-M. Zhan, *Journal of biomaterials applications* **2013**, *28*, 125.

[64] J. B. Zhou, J. Liu, C. J. Cheng, T. R. Patel, C. E. Weller, J. M. Piepmeier, Z. Z. Jiang, W. M. Saltzman, *Nature Materials* **2012**, *11*, 82.

[65] D. W. Pack, A. S. Hoffman, S. Pun, P. S. Stayton, *Nat Rev Drug Discov* **2005**, *4*, 581.

[66] M. A. Mintzer, E. E. Simanek, *Chem Rev* **2009**, *109*, 259.

[67] H. Yin, R. L. Kanasty, A. A. Eltoukhy, A. J. Vegas, J. R. Dorkin, D. G. Anderson, *Nat Rev Genet* **2014**, *15*, 541.

[68] E. Vázquez, D. M. Dewitt, P. T. Hammond, D. M. Lynn, *J Am Chem Soc* **2002**, *124*, 13992.

[69] J. T. Zhang, N. J. Fredin, J. F. Janz, B. Sun, D. M. Lynn, *Langmuir* **2006**, *22*, 239.

[70] J. Zhang, S. I. Montañez, C. M. Jewell, D. M. Lynn, *Langmuir* **2007**, *23*, 11139.

[71] J. Chen, S. W. Huang, W. H. Lin, R. X. Zhuo, *Small* **2007**, *3*, 636.

[72] D. Oupicky, R. C. Carlisle, L. W. Seymour, *Gene Ther* **2001**, *8*, 713.

[73] D. M. Lynn, *Advanced Materials* **2007**, *19*, 4118.

[74] B. M. Wohl, J. F. Engbersen, *J Control Release* **2012**, *158*, 2.

[75] C. Picart, J. Mutterer, L. Richert, Y. Luo, G. D. Prestwich, P. Schaaf, J. C. Voegel, P. Lavalle, *P Natl Acad Sci USA* **2002**, *99*, 12531.

[76] P. Lavalle, C. Gergely, F. J. G. Cuisinier, G. Decher, P. Schaaf, J. C. Voegel, C. Picart, *Macromolecules* **2002**, *35*, 4458.

[77] G. Decher, *Science* **1997**, *277*, 1232.

[78] S. Werner, O. Huck, B. Frisch, D. Vautier, R. Elkaim, J. C. Voegel, G. Brunel, H. Tenenbaum, *Biomaterials* **2009**, *30*, 2291.

[79] P. H. Chua, K. G. Neoh, E. T. Kang, W. Wang, *Biomaterials* **2008**, *29*, 1412.

[80] F. Yamauchi, Y. Koyamatsu, K. Kato, H. Iwata, *Biomaterials* **2006**, *27*, 3497.

[81] C. M. Jewell, J. T. Zhang, N. J. Fredin, M. R. Wolff, T. A. Hacker, D. M. Lynn, *Biomacromolecules* **2006**, *7*, 2483.

[82] J. Blacklock, Y. Z. You, Q. H. Zhou, G. Z. Mao, D. Oupicky, *Biomaterials* **2009**, *30*, 939.

[83] P. C. DeMuth, Y. J. Min, B. Huang, J. A. Kramer, A. D. Miller, D. H. Barouch, P. T. Hammond, D. J. Irvine, *Nature Materials* **2013**, *12*, 367.

[84] P. C. DeMuth, A. V. Li, P. Abbink, J. Y. Liu, H. L. Li, K. A. Stanley, K. M. Smith, C. L. Lavine, M. S. Seaman, J. A. Kramer, A. D. Miller, W. Abraham, H. Suh, J. Elkhader, P. T. Hammond, D. H. Barouch, D. J. Irvine, *Nat Biotechnol* **2013**, *31*, 1082.

[85] P. C. DeMuth, J. J. Moon, H. Suh, P. T. Hammond, D. J. Irvine, *Acs Nano* **2012**, *6*, 8041.

[86] O. C. Farokhzad, R. Langer, *Acs Nano* **2009**, *3*, 16.

[87] M. L. Forrest, J. T. Koerber, D. W. Pack, *Bioconjugate Chemistry* **2003**, *14*, 934.

[88] J. Chen, C. Wu, D. Oupicky, *Biomacromolecules* **2009**, *10*, 2921.

[89] D. C. Wu, Y. Liu, L. Chen, C. B. He, T. S. Chung, S. H. Goh, *Macromolecules* **2005**, *38*, 5519.

[90] C. Lin, Z. Y. Zhong, M. C. Lok, X. L. Jiang, W. E. Hennink, J. Feijen, J. F. J. Engbersen, *J Control Release* **2006**, *116*, 130.

[91] A. L. Becker, A. P. R. Johnston, F. Caruso, *Small* **2010**, *6*, 1836.

[92] L. Wan, Y. You, Y. Zou, D. Oupicky, G. Mao, *J Phys Chem B* **2009**, *113*, 13735.

[93] J. Blacklock, T. K. Sievers, H. Handa, Y. Z. You, D. Oupicky, G. Z. Mao, H. Mohwald, *Journal of Physical Chemistry B* **2010**, *114*, 5283.

[94] W. Kern, *J Electrochem Soc* **1990**, *137*, 1887.

[95] G. Hungerford, J. Benesch, J. F. Mano, R. L. Reis, *Photoch Photobio Sci* **2007**, *6*, 152.

[96] U. Hersel, C. Dahmen, H. Kessler, *Biomaterials* **2003**, *24*, 4385.

[97] M. Losche, J. Schmitt, G. Decher, W. G. Bouwman, K. Kjaer, *Macromolecules* **1998**, *31*, 8893.

[98] E. Hubsch, V. Ball, B. Senger, G. Decher, J. C. Voegel, P. Schaaf, *Langmuir* **2004**, *20*, 1980.

[99] C. Porcel, P. Lavalle, V. Ball, G. Decher, B. Senger, J. C. Voegel, P. Schaaf, *Langmuir* **2006**, *22*, 4376.

[100] K. C. Wood, H. F. Chuang, R. D. Batten, D. M. Lynn, P. T. Hammond, *P Natl Acad Sci USA* **2006**, *103*, 10207.

[101] P. P. Lavalle, C. Picart, F. J. G. Cuisinier, G. Decher, P. Schaaf, J. C. Voegel, *Biophys J* **2002**, *82*, 53a.

[102] L. Xu, D. Pristinski, A. Zhuk, C. Stoddart, J. F. Ankner, S. A. Sukhishvili, *Macromolecules* **2012**, *45*, 3892.

[103] R. Cortivo, P. Brun, A. Rastrelli, G. Abatangelo, *Biomaterials* **1991**, *12*, 727.

[104] M. P. Desai, V. Labhasetwar, G. L. Amidon, R. J. Levy, *Pharm Res* **1996**, *13*, 1838.

[105] S. C. W. Richardson, N. G. Pattrick, Y. K. S. Man, P. Ferruti, R. Duncan, *Biomacromolecules* **2001**, *2*, 1023.

[106] P. Ferruti, S. Manzoni, S. C. W. Richardson, R. Duncan, N. G. Pattrick, R. Mendichi, M. Casolaro, *Macromolecules* **2000**, *33*, 7793.

[107] Z. Zhong, Y. Song, J. F. Engbersen, M. C. Lok, W. E. Hennink, J. Feijen, *J Control Release* **2005**, *109*, 317.

[108] Y. Kakizawa, A. Harada, K. Kataoka, *Biomacromolecules* **2001**, *2*, 491.

[109] J. E. Biaglow, J. Donahue, S. Tuttle, K. Held, C. Chrestensen, J. Mieyal, *Anal Biochem* **2000**, *281*, 77.

[110] T. Bettinger, R. C. Carlisle, M. L. Read, M. Ogris, L. W. Seymour, *Nucleic Acids Res* **2001**, *29*, 3882.

[111] D. V. Schaffer, N. A. Fidelman, N. Dan, D. A. Lauffenburger, *Biotechnol Bioeng* **2000**, *67*, 598.

[112] D. Soundara Manickam, D. Oupicky, *J Drug Target* **2006**, *14*, 519.

[113] D. Soundara Manickam, H. S. Bisht, L. Wan, G. Mao, D. Oupicky, *J Control Release* **2005**, *102*, 293.

[114] D. Fischer, Y. X. Li, B. Ahlemeyer, J. Krieglstein, T. Kissel, *Biomaterials* **2003**, *24*, 1121.

[115] W. T. Godbey, K. K. Wu, A. G. Mikos, *Biomaterials* **2001**, *22*, 471.

[116] D. Oupicky, A. L. Parker, L. W. Seymour, *J Am Chem Soc* **2002**, *124*, 8.

[117] M. L. Read, S. Singh, Z. Ahmed, M. Stevenson, S. S. Briggs, D. Oupicky, L. B. Barrett, R. Spice, M. Kendall, M. Berry, J. A. Preece, A. Logan, L. W. Seymour, *Nucleic Acids Res* **2005**, *33*.

[118] M. A. Gosselin, W. J. Guo, R. J. Lee, *Bioconjugate Chemistry* **2001**, *12*, 989.

[119] C. Lin, Z. Y. Zhong, M. C. Lok, X. L. Jiang, W. E. Hennink, J. Feijen, J. F. J. Engbersen, *Bioconjugate Chemistry* **2007**, *18*, 138.

[120] Y. B. Lim, S. M. Kim, H. Suh, J. S. Park, *Bioconjugate Chemistry* **2002**, *13*, 952.

[121] D. Fischer, T. Bieber, Y. Li, H. P. Elsasser, T. Kissel, *Pharm Res* **1999**, *16*, 1273.

[122] C. Lin, Z. Zhong, M. C. Lok, X. Jiang, W. E. Hennink, J. Feijen, J. F. Engbersen, *Bioconjugate chemistry* **2007**, *18*, 138.

[123] Z. Zhong, J. Feijen, M. C. Lok, W. E. Hennink, L. V. Christensen, J. W. Yockman, Y. H. Kim, S. W. Kim, *Biomacromolecules* **2005**, *6*, 3440.

[124] O. Boussif, F. Lezoualc'h, M. A. Zanta, M. D. Mergny, D. Scherman, B. Demeneix, J. P. Behr, *Proceedings of the National Academy of Sciences of the United States of America* **1995**, *92*, 7297.

[125] V. A. Bloomfield, *Biopolymers* **1997**, *44*, 269.

[126] J. Chen, C. Wu, D. Oupicky, *Biomacromolecules* **2009**, *10*, 2921.

[127] D. Fischer, T. Bieber, Y. Li, H.-P. Elsässer, T. Kissel, *Pharmaceutical research* **1999**, *16*, 1273.

[128] D. M. Lynn, R. Langer, *Journal of the American Chemical Society* **2000**, *122*, 10761.

[129] D. M. Lynn, D. G. Anderson, D. Putnam, R. Langer, *Journal of the American Chemical Society* **2001**, *123*, 8155.

[130] N. D. Sonawane, F. C. Szoka, Jr., A. S. Verkman, *The Journal of biological chemistry* **2003**, *278*, 44826.

[131] N. D. Sonawane, F. C. Szoka, A. Verkman, *Journal of Biological Chemistry* **2003**, *278*, 44826.

[132] N. D. Sonawane, F. C. Szoka, A. S. Verkman, *Journal of Biological Chemistry* **2003**, *278*, 44826.

[133] M. X. Tang, F. C. Szoka, *Gene Ther* **1997**, *4*, 823.

[134] A. von Harpe, H. Petersen, Y. X. Li, T. Kissel, *J Control Release* **2000**, *69*, 309.

[135] U. Lachelt, P. Kos, F. M. Mickler, A. Herrmann, E. E. Salcher, W. Rodl, N. Badgujar, C. Brauchle, E. Wagner, *Nanomed-Nanotechnol* **2014**, *10*, 35.

[136] Z. Y. Zhong, Y. Song, J. F. J. Engbersen, M. C. Lok, W. E. Hennink, J. Feijen, *J Control Release* **2005**, *109*, 317.

[137] C. Lin, C. J. Blaauboer, M. M. Timoneda, M. C. Lok, M. van Steenbergen, W. E. Hennink, Z. Y. Zhong, J. Feijen, J. F. J. Engbersen, *J Control Release* **2008**, *126*, 166.

[138] Z. Y. Zhong, J. Feijen, M. C. Lok, W. E. Hennink, L. V. Christensen, J. W. Yockman, Y. H. Kim, S. W. Kim, *Biomacromolecules* **2005**, *6*, 3440.

[139] C. W. Pouton, L. W. Seymour, *Adv Drug Deliv Rev* **1998**, *34*, 3.

[140] L. Wan, Y. You, Y. Zou, D. Oupický, G. Mao, *The Journal of Physical Chemistry B* **2009**, *113*, 13735.

[141] M. L. Forrest, J. T. Koerber, D. W. Pack, *Bioconjug Chem* **2003**, *14*, 934.

[142] I. D. Vilfan, C. C. Conwell, T. Sarkar, N. V. Hud, *Biochemistry-Us* **2006**, *45*, 8174.

[143] N. K. Reitan, G. Maurstad, C. D. Davies, S. P. Strand, *Biomacromolecules* **2009**, *10*, 1508.

[144] S. P. Strand, S. Lelu, N. K. Reitan, C. D. Davies, P. Artursson, K. M. Varum, *Biomaterials* **2010**, *31*, 975.

[145] L. Aravindan, K. A. Bicknell, G. Brooks, V. V. Khutoryanskiy, A. C. Williams, *Int J Pharm* **2009**, *378*, 201.

[146] C. Lin, J. F. J. Engbersen, *J Control Release* **2008**, *132*, 267.

[147] L. Parhamifar, A. K. Larsen, A. C. Hunter, T. L. Andresen, S. M. Moghimi, *Soft Matter* **2010**, *6*, 4001.

[148] T. Kirkegaard, M. Jaattela, *Bba-Mol Cell Res* **2009**, *1793*, 746.

[149] K. F. Ferri, G. Kroemer, *Nat Cell Biol* **2001**, *3*, E255.

[150] M. Breunig, U. Lungwitz, R. Liebl, A. Goepferich, *P Natl Acad Sci USA* **2007**, *104*, 14454.

[151] S. Srinivasachari, Y. M. Liu, L. E. Prevette, T. M. Reineke, *Biomaterials* **2007**, *28*, 2885.

[152] T. Boudou, T. Crouzier, K. Ren, G. Blin, C. Picart, *Advanced Materials* **2010**, *22*, 441.

[153] S. Werner, O. Huck, B. Frisch, D. Vautier, R. Elkaim, J.-C. Voegel, G. Brunel, H. Tenenbaum, *Biomaterials* **2009**, *30*, 2291.

[154] P. C. DeMuth, Y. Min, B. Huang, J. A. Kramer, A. D. Miller, D. H. Barouch, P. T. Hammond, D. J. Irvine, *Nature materials* **2013**, *12*, 367.

[155] A. J. Friedenstein, K. V. Petrakova, A. I. Kurolesova, G. P. Frolova, *Transplantation* **1968**, *6*, 230.

[156] D. Benayahu, Y. Kletter, D. Zipori, S. Wientroub, *J Cell Physiol* **1989**, *140*, 1.

[157] J. M. Wozney, V. Rosen, A. J. Celeste, L. M. Mitsock, M. J. Whitters, R. W. Kriz, R. M. Hewick, E. A. Wang, *Science* **1988**, *242*, 1528.

[158] D. M. Kingsley, *Gene Dev* **1994**, *8*, 133.

[159] A. Yamaguchi, *Semin Cell Biol* **1995**, *6*, 165.

[160] Y. Hiraki, H. Inoue, C. Shigeno, Y. Sanma, H. Bentz, D. M. Rosen, A. Asada, F. Suzuki, *J Bone Miner Res* **1991**, *6*, 1373.

[161] Y. Zou, L. Xie, S. Carroll, M. Muniz, H. Gibson, W. Z. Wei, H. Liu, G. Mao, *Biomacromolecules* **2014**, *15*, 3965.

[162] J. Blacklock, H. Handa, D. S. Manickam, G. Z. Mao, A. Mukhopadhyay, D. Oupicky, *Biomaterials* **2007**, *28*, 117.

[163] K. C. Wood, H. F. Chuang, R. D. Batten, D. M. Lynn, P. T. Hammond, *Proc Natl Acad Sci U S A* **2006**, *103*, 10207.

[164] C. Picart, J. Mutterer, L. Richert, Y. Luo, G. D. Prestwich, P. Schaaf, J. C. Voegel, P. Lavalle, *Proc Natl Acad Sci U S A* **2002**, *99*, 12531.

[165] K. C. Wood, J. Q. Boedicker, D. M. Lynn, P. T. Hammond, *Langmuir* **2005**, *21*, 1603.

[166] P. Lavalle, C. Picart, J. Mutterer, C. Gergely, H. Reiss, J. C. Voegel, B. Senger, P. Schaaf, *Journal of Physical Chemistry B* **2004**, *108*, 635.

[167] M. Macdonald, N. M. Rodriguez, R. Smith, P. T. Hammond, *J Control Release* **2008**, *131*, 228.

[168] E. Engvall, E. Ruoslahti, *International Journal of Cancer* **1977**, *20*, 1.

[169] D. J. Rickard, T. A. Sullivan, B. J. Shenker, P. S. Leboy, I. Kazhdan, *Dev Biol* **1994**, *161*, 218.

[170] A. Holmgren, *Journal of Biological Chemistry* **1989**, *264*, 13963.

[171] A. Meister, M. E. Anderson, *Annu Rev Biochem* **1983**, *52*, 711.

[172] A. Holmgren, M. Bjornstedt, *Methods Enzymol* **1995**, *252*, 199.

[173] N. J. Darby, R. B. Freedman, T. E. Creighton, *Biochemistry-Us* **1994**, *33*, 7937.

[174] A. Meister, *Pharmacol Therapeut* **1991**, *51*, 155.

[175] X. M. Jiang, M. Fitzgerald, C. M. Grant, P. J. Hogg, *Journal of Biological Chemistry* **1999**, *274*, 2416.

[176] M. Tager, H. Kroning, U. Thiel, S. Ansorge, *Exp Hematol* **1997**, *25*, 601.

[177] J. Lahav, N. Gofer-Dadosh, J. Luboshitz, O. Hess, M. Shaklai, *Febs Letters* **2000**, *475*, 89.

[178] K. Terada, P. Manchikalapudi, R. Noiva, H. O. Jauregui, R. J. Stockert, M. L. Schilsky, *Journal of Biological Chemistry* **1995**, *270*, 20410.

[179] S. Akagi, A. Yamamoto, T. Yoshimori, R. Masaki, R. Ogawa, Y. Tashiro, *J Histochem Cytochem* **1988**, *36*, 1069.

[180] F. Q. Schafer, G. R. Buettner, *Free Radical Bio Med* **2001**, *30*, 1191.

[181] N. Li, T. D. Oberley, *J Cell Physiol* **1998**, *177*, 148.

[182] L. D. Quarles, D. A. Yohay, L. W. Lever, R. Caton, R. J. Wenstrup, *J Bone Miner Res* **1992**, *7*, 683.

[183] A. Brownlie, I. F. Uchegbu, A. G. Schatzlein, *Int J Pharm* **2004**, *274*, 41.

[184] K. Kunath, T. Merdan, O. Hegener, H. Häberlein, T. Kissel, *The journal of gene medicine* **2003**, *5*, 588.

[185] E. Ruoslahti, M. D. Pierschbacher, *Science* **1987**, *238*, 491.

[186] D. Zhou, L. Cutlar, Y. Gao, W. Wang, J. O'Keeffe-Ahern, S. McMahon, B. Duarte, F. Larcher, B. J. Rodriguez, U. Greiser, W. Wang, *Sci Adv* **2016**, *2*, e1600102.

[187] D. Zhou, Y. Gao, A. Aied, L. Cutlar, O. Igoucheva, B. Newland, V. Alexeeve, U. Greiser, J. Uitto, W. Wang, *J Control Release* **2016**, *244*, 336.

[188] Y. Gao, J. Y. Huang, J. O'Keeffe Ahern, L. Cutlar, D. Zhou, F. H. Lin, W. Wang, *Biomacromolecules* **2016**, *17*, 3640.

[189] A. Meister, *Pharmacol Therapeut* **1991**, *51*, 155.

[190] M. Täger, H. Kröning, U. Thiel, S. Ansorge, *Exp Hematol* **1997**, *25*, 601.

[191] J. Lahav, N. Gofer-Dadosh, J. Luboshitz, O. Hess, M. Shaklai, *FEBS letters* **2000**, *475*, 89.

[192] K. Terada, P. Manchikalapudi, R. Noiva, H. O. Jauregui, R. J. Stockert, M. L. Schilsky, *Journal of Biological Chemistry* **1995**, *270*, 20410.

[193] S. Akagi, A. Yamamoto, T. Yoshimori, R. Masaki, R. Ogawa, Y. Tashiro, *J Histochem Cytochem* **1988**, *36*, 1069.

[194] D. J. Morré, D. M. Morré, *Journal of bioenergetics and biomembranes* **1995**, *27*, 137.

[195] B. Sahaf, A. Söderberg, G. Spyrou, A. M. Barral, K. Pekkari, A. Holmgren, A. Rosén, *Experimental cell research* **1997**, *236*, 181.

ABSTRACT

BIOREDUCIBLE LAYER-BY-LAYER FILMS FOR GENE DELIVERY

by

LINGXIAO XIE

December 2017

Advisor: Dr. Guangzhao Mao

Major: Materials Science and Engineering

Degree: Doctor of Philosophy

Layer-by-Layer (LbL) gene delivery system is fabricated by polycation and plasmid DNA alternative deposition based on electrostatic force between each other. This dissertation explored the relationship between LbL film assembly and disassembly. Demonstrated that the film disassemble process is closely related to film interior structure. LbL interlayer diffusion, which is caused by the polyelectrolytes own properties, such as polymer chain length, molecular weight, and charge density, can influence film growth mode. The interlayer diffusion is the main reason to lead fast and bulk DNA releasing of bioreducible LbL film. Preventing interlayer diffusion by inserting small diffusion coefficient polymer, such as Polyethylenimine (PEI), can effectively achieve sustained and sequential DNA releasing. This dissertation also developed a series of poly(amido amine)s (PAAs) with high transfection efficiency and biocompatibility for LbL film design. Through polycation/DNA polyplex experiment, we obtained a type of PAA, pAPOL-1, with high buffer capacity, reasonable degradation rate, and low cytotoxicity. This pAPOL-1 can be incorporated into LbL film to build next generation localized delivery vehicle. The novel LbL film, LbL film 1, largely improved LbL film transfection efficiency and maintained low toxicity

to HEK 293 and MC 3T3 cell lines. Small amount of PEI inserted into LbL film acting as barrier layer successfully screened the residue charge, stabilized film interior layer structure, and slowed down the degradation rate. The LbL film 1 provides a promising method for multiple therapeutic gene delivering in desired order. Study of introducing therapeutic gene *in vivo* described in this dissertation also make contributions to the development of gene therapy. In conclusion, bioreducible LbL films with high efficiency and low toxicity developed in this dissertation provides a sustained and sequential delivery method which can contribute to localized gene delivery application.

AUTOBIOGRAPHICAL STATEMENT

LINGXIAO XIE

EDUCATION

- 2012 – 2017, Ph.D., Materials Science and Engineering, Wayne State University, Detroit, Michigan, US.
- 2008 – 2012, B.S., Polymer Materials and Engineering, Xiangtan University, Xiangtan, Hunan, China.

EXPERIENCE

- 2013 – 2017, Graduate Teaching Assistant; Graduate Research Assistant, Wayne State University, US.
- 2011 Summer, Intern, Epoxy Resin Division of Baling Petrochemical Corporation Ltd, Hunan, China.

PUBLICATION

1. Zou, Y.; **Xie, L**.; Carroll, S.; Muniz, M.; Gibson, H.; Wei, W.-Z.; Liu, H.; Mao, G. Layer-by-layer Films with Bioreducible and Non-bioreducible Polycations for Sequential DNA Release, Biomacromolecules, 15, 3965-3975, 2014.
2. Kesharwani, P.; **Xie, L**.; Mao, G.; Padhye, S.; Iyer, A. K. Hyaluronic Acid-conjugated Polyamidoamine Dendrimers for Targeted Delivery of 3,4-Difluorobenzylidene Curcumin to CD44 Overexpressing Pancreatic Cancer Cells, Colloids Surf. B: Biointerfaces, 136, 413-423, 2015.
3. Wickramasinghe, L.D.; Mazumder, S.; Gonawala, S.; Perera, M. M.; Baydoun, H.; Thapa, B.; Li, L.; **Xie, L**.; Mao, G.; Zhou, Z.; Schlegel, H. B.; Verani, C. N. Mechanisms of Rectification in Au/molecule/Au Devices Based on Langmuir-Blodgett Films of Iron(III) and Copper(II) Surfactants, Angew. Chem. Int. Ed., 53, 1-7, 2014.